AN ANALYSIS OF CHARGE TRANSPORT AND EQUILIBRIUM IN THE GLOBAL ATMOSPHERE

By

EDWARD LYLE SHREVE

Bachelor of Science
University of Oklahoma
Norman, Oklahoma
1962

Master of Science
New Mexico State University
Las Cruces, New Mexico
1964

Submitted to the faculty of the Graduate College
of the Oklahoma State University
in partial fulfillment of the requirements
for the Degree of
DOCTOR OF PHILOSOPHY
May, 1969

OKLAHOMA
STATE UNIVERSITY
LIBRARY

SEP 29 1969

AN ANALYSIS OF CHARGE TRANSPORT AND EQUILIBRIUM

IN THE GLOBAL ATMOSPHERE

Thesis Approved:

Victor W. Bolie
Thesis Adviser

Kenneth A. McCollom

Charles M. Bacon

E. K. McFarlan

D. D. Durham
Dean of the Graduate College

725080

ACKNOWLEDGEMENTS

I wish to express my sincere thanks to my thesis adviser, Professor V. W. Bolie for his guidance, help and encouragement during my research. For the many hours he devoted on my behalf I am grateful.

I also wish to thank my committee chairman, Professor K. A. McCollom, who guided my doctoral study program. I am also indebted to the remaining two members of my committee, Professor C. M. Bacon for encouragement and instruction during my doctoral studies, and Professor T. L. Demen for his encouragement and time spent on my behalf.

The privilege of holding a National Defense Graduate Fellowship provided financial support during my doctoral studies. Financial support by the Themis Environmental Conditions Project is also gratefully acknowledged.

To my wife, Peggy, I express my warmest appreciation for her encouragement and sacrifice during my undergraduate and graduate programs. She is also thanked for typing the draft of this thesis.

TABLE OF CONTENTS

Chapter Page

Chapter Page

LIST OF TABLES

LIST OF ILLUSTRATIONS

CHAPTER I

INTRODUCTION AND LITERATURE SURVEY

1.1 Statement of the Problem and Outline of Solution Methods. The subject of atmospheric electricity has been investigated from both the experimental and theoretical points of view for more than two hundred years. Present attempts to correlate measured data with more modern theoretical concepts indicate that substantially more extensive investigations need to be done on this subject. For example, the most widely accepted theory of atmospheric electricity, that on a global average there is from 1400-1800 amperes of current flowing to the earth in fair weather areas, and a like amount of current leaving the earth in thunderstorm areas would not necessarily be an accurate description if appreciable diffusion currents were present in the atmosphere. Consequently, this thesis is a report of a study of charge transport and equilibrium in the global atmosphere which was conducted in order to develop a more rigorous theoretical approach to the distributions of ion densities, electric field, space charge density and drift and diffusion currents in the fair weather atmosphere. These distributions will hopefully provide some additional insight into the subject of atmospheric electricity.

The general approach to the study was to develop a comprehensive mathematical model based on the generalized continuity equations and the Poisson equation. Known geophysical data and physical laws were used to evaluate the functional form of the parameters and coefficients appearing

in the atmospheric model.

Solutions to the model were then obtained under the three simplifying assumptions: 1) steady state conditions exist, 2) large ion content is negligible, and 3) horizontal variations in electrical properties are small. Even under these assumptions the model is quite complex and consists of three simultaneous, non-linear differential equations with variable coefficients. Initial conditions were taken from the best available experimental results presented in the literature.

Finally, a thunderstorm model for an electrical current generator was developed and analyzed to compare electrical properties in fair weather and thunderstorm areas.

The remainder of this chapter is devoted to a survey of the present state of knowledge of atmospheric electricity.

1.2 Summary of Air-Earth Current Flow and Earth's Surface Change. The present theory of air-earth current flow and maintenance of the earth's negative surface charge density is that positive charge is carried to the earth in fair weather areas, and away from the earth in thunderstorm areas, (Wilson, 1920).

On the basis of data and theoretical calculations there is considered to be a current of 1800 amperes flowing to the earth in fair weather areas, a potential difference of 360kv between the earth and the ionosphere, and a total earth-ionosphere resistance of 200 ohms.

The average value of electric field at the earth's surface is usually taken as being approximately -130v/m (Chalmers, 1957). Thus the $\bar{E}$ vector points toward the earth's center. On the basis of electromagnetic boundary conditions, the earth's surface charge density, ω, is

$$\omega = \varepsilon_0 E = (8.854 \times 10^{-12} \text{ farads/m}) (-130 \text{v/m})$$

$$= -1.15 \times 10^{-9} \text{ coulombs/m}^2.$$

Then, if the current flow to earth (Chalmers, 1957) is taken as 2.4×10^{-12} amperes/m^2 or 2.4×10^{-12} coulombs/sec-m^2, the earth charge would be neutralized after

$$t = 1.15 \times 10^{-9} \text{ coulombs/m}^2 \div 2.4 \times 10^{-12} \text{ coulombs/sec-m}^2$$

$$= 480 \text{ sec.} = 8 \text{ minutes.}$$

The continuity equation for electrical charge requires that if 1800 amperes flows to the earth, and if the earth maintains its given charge, then there exists a circuit by which this current can flow away from the earth. The accepted theory is that through lightning and point discharge, the charge which arrives at the earth in fair weather areas by precipitation and conduction current is removed from the earth. The circuit can then be envisioned as shown in Figure 1.

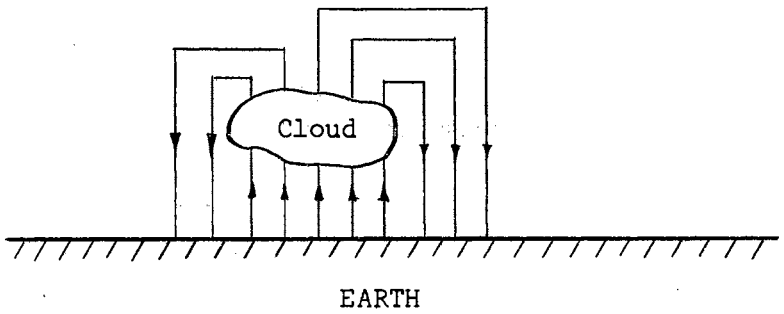

Figure 1. Air-Earth Conduction Current Circuit

Table I gives a balance sheet of charge transfer by different investigators, (Chalmers, 1957).

TABLE I

CHARGE TRANSFER BALANCE SHEET

Place	Author	Fair Weather Conduction	Point Discharge	Precipitation	Lightning	Total
Cambridge	Wormell(1930)	+ 60 c/km^2-yr	-100	+20	-20	- 40
Cambridge	Wormell(1953)	+ 60	-170	+20	- 5.6	- 96
Durham	Chalmers(1947)	+ 60	- 90	+40	-35	- 25
Durham	Revised	+ 60	-180	+40	- 5	- 85
Kew	Chalmers(1949)	+ 35	-125	+22	-45	-113
Kew	Revised	+ 35	-300	+22	- 6	-249
World	Wait(1950)	+100	- 30	+20	-20	- 70
World	Israël(1953)	+ 90	-100	+30	-20	0

All results for England show an excess of negative charge. Chalmers speculates the answer lies in Polar or desert regions, because in areas of considerable thunderstorm activity (England for example) an excess of negative charge is transferred to the earth. Hence, he concludes regions of low thunderstorm activity (deserts and polar regions) will have an excess of positive charge, resulting in an overall balance.

1.3 Summary of Atmospheric Electricity Definitions and Experimental Results.

a) Columnar Resistance - The resistance of a vertical column of air of one square-meter cross-sectional area, which reaches from the earth to

the ionosphere, is called the columnar resistance of the atmosphere. Israël (1953) arrives at a figure of 7.4×10^{16} ohm/m^2, or approximately 10^{17} ohm/m^2. The columnar conductance would then be 10^{-17} mho/m^2. Considering the earth's surface area to be $5 \times 10^{14} m^2$, the total earth-ionosphere conductance is:

$$G_{E-I} = (5 \times 10^{14} m^2)(10^{-17} \text{mho}/m^2) = 5 \times 10^{-3} \text{mho}.$$

Then

$$R_{E-I} = 1/G_{E-I} = 10^3/_5 = 200 \text{ ohms}$$

is the total resistance between earth and ionosphere.

b) Ionospheric Potential - Gish (1951) has estimated the total current flowing to the earth from the ionosphere to be 1800 amperes - Kraakevik (1958) maintains 1400 amperes. Then the potential of the ionosphere is calculated to be

$$V = IR = (1800)\ (200) = 360\text{kv}.$$

Based on observations of I and R, there is a diurnal variation of ionospheric potential of $\pm$ 20% about its mean. Clark (1958) arrives at a mean of 290 kv on the basis of measurements made from aircraft, while Gish and Sherman (1936) quote 400 kv as the potential of the ionosphere.

c) Ions in the Atmosphere - Important in atmospheric electricity phenomena are four types of ions, generally classified as large and small, where each size ion may be positively or negatively charged. Also important are the Aitken or condensation nucleii, neutral particles on which water condenses when air is saturated with moisture. The importance of these nucleii is that the small ions may become attached to these neutral particles to form large ions.

The mobility, μ_+, (average drift velocity per unit of electric field) for the positive small ions is given by Bricard (1965) as 1.4 cm^2/v-sec, and μ_- for the negative small ions is given as 1.9 cm^2/v-sec at standard temperature and pressure (STP). The mobilities U_+ and U_- for the large ions are given by Schonland (1953) as being of the order of 0.0004 cm^2/v-sec.

Measurements show that the concentrations n_+, n_-, N_+, N_- (ions/cc) of the four types of ions varies with time and location depending on many factors (Chalmers, 1957, Sagalyn and Faucher, 1954) such as air pollution, climatic conditions, extent of the austauch or exchange region, and whether over land or sea regions. Chalmers (1957) states that at land stations n_+ is 750/cc, n_- is 680/cc, $N_{\pm}$ is 4000/cc, and over oceans n_+ is 640/cc, n_- is 575/cc, and $N_{\pm}$ is 4500/cc.

Ions in the atmosphere are primarily produced by different means depending on location and altitude. At low altitudes, the main source of ionization is radiation from radioactive substances in the air and in the earth's crust. While as altitude increases, the ionization due to cosmic radiation becomes predominant (Schonland, 1953). These processes (radioactive substance radiation and cosmic radiation) produce small ions. The large ions are produced by combination of nucleii and small ions. Small ions are lost by combination with: 1) oppositely charged small ions, 2) oppositely charged large ions or 3) uncharged nucleii. Large ions are lost by combination with: 1) oppositely charged large ions or 2) oppositely charged small ions.

d) Atmospheric conductivity - The conductivity of the atmosphere will be denoted by σ. Conductivity, σ, in general is defined by ohm's law,

$$\overline{J} = \sigma\overline{E},$$

where $\overline{J}$ is the current density vector (amperes/m^2) and $\overline{E}$ is the electric field vector (volts/m). Conductivity of the atmosphere is due to the presence of the ions discussed in the previous paragraph.

Atmospheric conductivity, σ, can be considered as the sum of two polar conductivities σ_+ and σ_-, where σ_+ is the conductivity from positively charged ions, and σ_- from negative ions. Assuming ions are singly charged, i.e., possess a charge of $\pm$ 1.602 x 10^{-19} coulombs, the expressions for the polar conductivities are:

$$\sigma_+ = (e)\ (\mu_+ n_+ + U_+ N_+),$$

$$\sigma_- = (e)\ (\mu_- n_- + U_- N_-),$$

where e is the electronic charge. Then the total conductivity is

$$\sigma = \sigma_+ + \sigma_-.$$

Conductivity at the earth's surface, over land, is usually taken as 2 x 10^{-14} mho/meter (Chalmers, 1957).

Because the mobility of the large ions is much less than that of the small ions, the conductivity is usually considered to be accomplished by the small ions. This assumption is valid unless the concentration of large ions becomes very large, as for example, where the air is highly polluted. Qualitatively, for regions of high pollution, condensation nucleii will be densely concentrated, hence, the concentration of small ions will decrease because of increased combination with nucleii, and therefore, the concentration of less mobile large ions will increase. As a result, atmospheric conductivity in polluted air will

be less than for "clear air" areas.

Using the defined polar conductivities, the vertical current density is

$$J = (\sigma_+ + \sigma_-)E \text{ amperes/m}^2.$$

Independent measurements by Sagalyn (1958) and Curtis and Hyland (1958) show that the mean value of σ_-/σ_+ is 1.05. The following Figure shows the variation of conductivity with altitude at Payerne, Switzerland (Mühleisen, 1965).

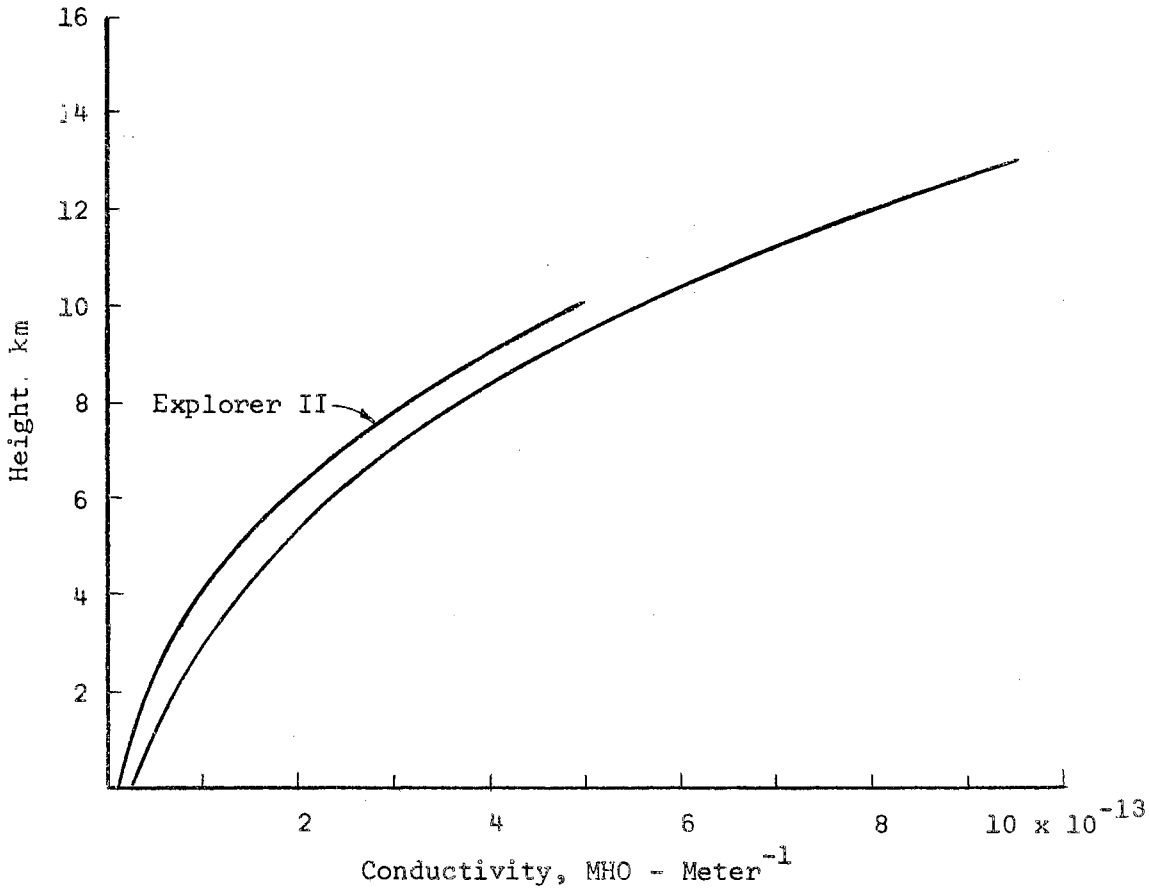

Figure 2. Atmospheric Conductivity

Although in the original data, only σ_+ was given, the relationship that σ_- is $1.05\sigma_+$ was used to obtain

$$\sigma = \sigma_+ + 1.05\sigma_+ = 2.05\sigma_+ .$$

Explorer II data from Bricard (1965) is also shown on this figure. Two factors considered responsible for the increase of conductivity with altitude are: 1) Increased cosmic ray ionization with altitude, and 2) fewer condensation nucleii at higher altitudes, (Chalmers, 1957).

Although the theory of atmospheric conductivity considered four types of ions, if more types are present, with different mobilities and different magnitudes of charge, the expression for conductivity would be

$$\sigma = \sigma_+ + \sigma_- = \sum_i \mu_i (n_+)_i q_i + \sum_j \mu_j (n_-)_j q_j$$

where μ is mobility, n is concentration, and q is the magnitude of charge possessed by a given type of ion. Gish (1944) has experimentally arrived at the expression

$$\frac{1}{\sigma} = 2.94 \exp(-4.52h) + 1.39 \exp(-.375h) + 0.369 \exp(-.121h),$$

where h is in meters and $1/\sigma$ is in 10^{13} ohm-meters.

e) Atmospheric Electric Field - In fair weather, the electric field is negative, with an average surface value of -130v/m. Measurements by Clark (1958) show that the field intensity decreases approximately exponentially with altitude. Chalmers (1957) asserts that the increase of conductivity with altitude is fundamental, and the electric field decrease is a consequence of this since the current density is the same at all altitudes (Kraakevik, 1958 and Law, 1963 maintain this assumption is suspect). For example, if V is the potential of the ionosphere,

and R is the Columnar resistance, then I, the conduction current density is given by

$$I = V/R.$$

If r is the resistance of the lowest one meter of the $1m^2$ column, then

$$E = Ir = \frac{Vr}{R} = \frac{V}{\sigma R}$$

is the average potential drop across this one meter, so that changes in conductivity are reflected in changes in potential gradient.

As expected from the preceding paragraph, the electric field and conductivity experience similar diurnal and secular variations. The two following figures show experimental values of measurements of atmospheric electric field intensity and its diurnal variation.

1.4 Thunderstorm Electricity. The existing theories regarding the role of thunderstorms in atmospheric electricity have been mentioned. Salient features of thunderstorm electricity will be presented.

a) Thunderstorm Cells - An individual thunderstorm may consist of several cells, where a cell is defined as a individual chimney of convection in a storm (Boudreaux, 1959). This convection updraft carries moisture-laden air to elevations where ice crystals are formed. The charge distribution in a typical cell is positive charge at the top of the cell, negative charge at the bottom of the cell. The charge in this thundercloud will induce charges on the earth's surface with a resulting change in the electric field. Electric field intensity may become high enough so that point discharges occur. Lightning flashes to the ground may occur, transporting charge to or from earth, and precipitation may also transport charge to earth. These three manifestations of a

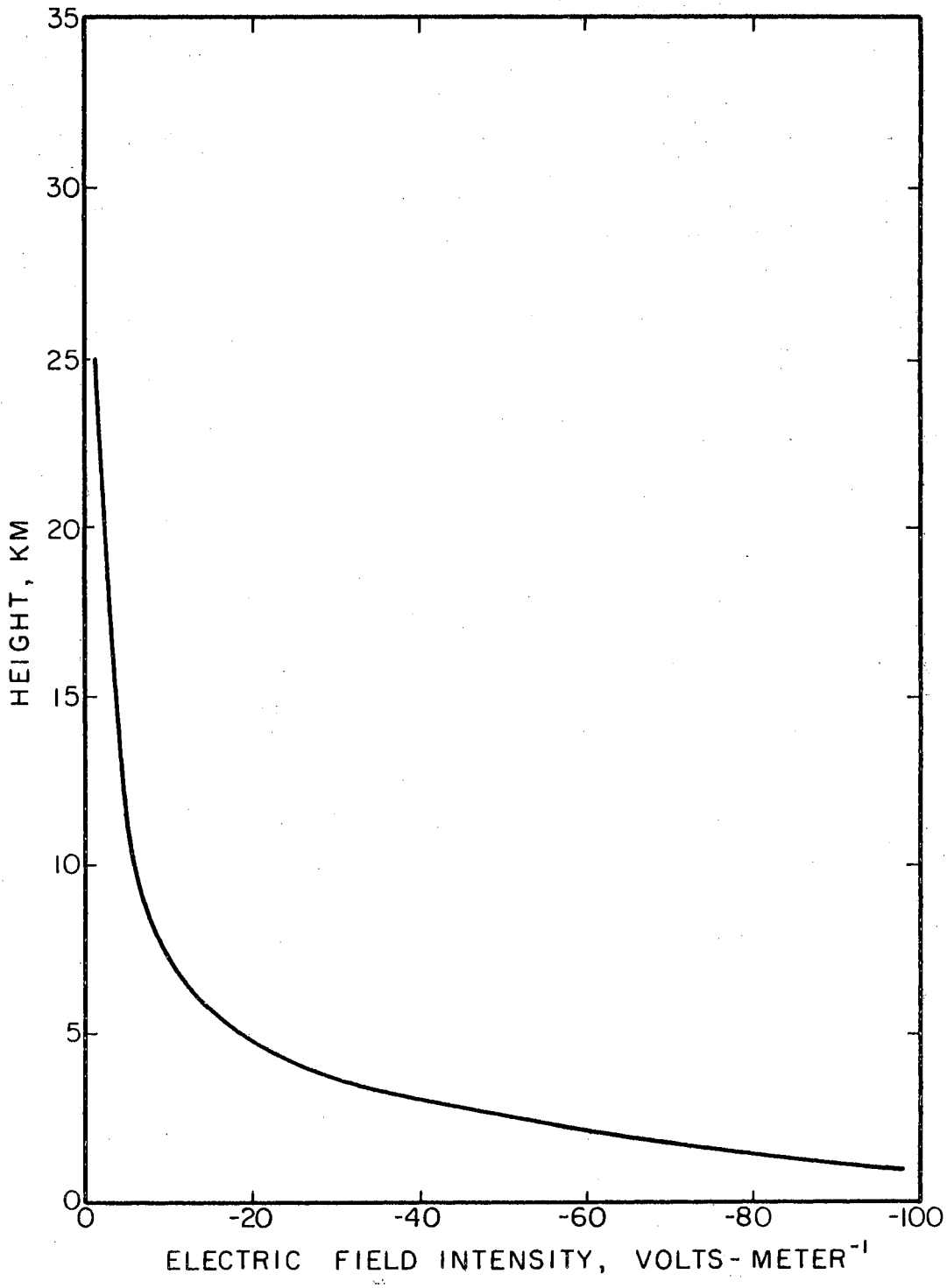

Figure 3. Altitude Variation of Electric Field

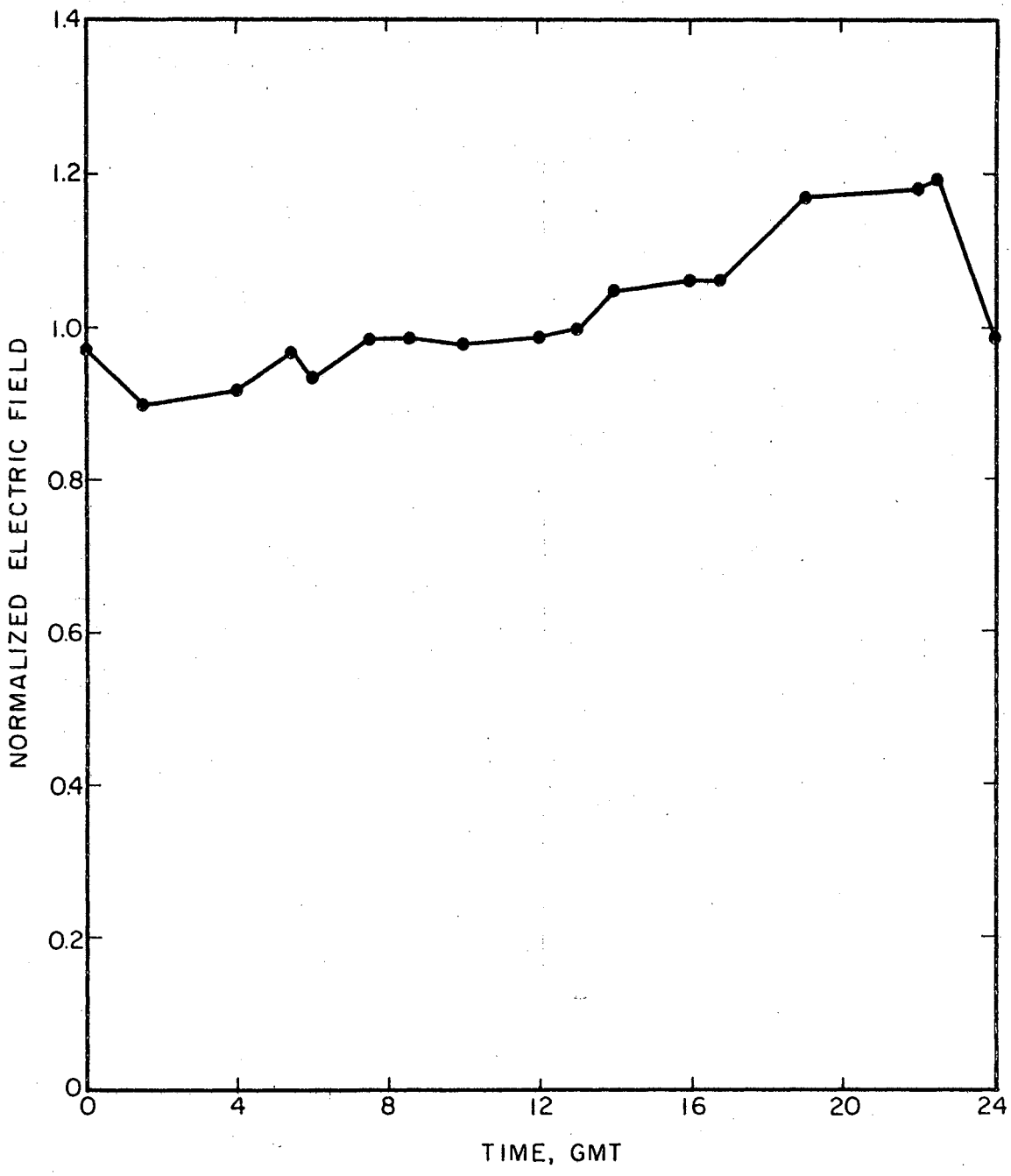

Figure 4. Diurnal Variation of Atmospheric Electric Field

thunderstorm; point discharge, lightning, and precipitation are considered to be the most important in maintaining the earth's charge distribution.

b) Charge Separation in Thunderstorms - Numerous theories have been formulated regarding the mechanism or mechanisms whereby thunderstorms attain their observed charge distributions (Chalmers, 1957). It is possible that several of these theories are correct in that charge separation may be due to more than one process. In general, the theories fall into two categories: 1) ions produced by cosmic rays, etc., in the cloud somehow become separated, positive ions to the top of the cell and negative ions to the bottom, 2) neutral bodies in the cloud become divided, the heavier part having one polarity, the lighter part the opposite polarity. The second category is given more credence by workers in the area.

Workman and Reynolds theory (Workman and Reynolds, 1949) which is in the second category is most widely accepted. This theory is based on laboratory results which show that when water freezes, there is a potential difference between the ice and water phases during the freezing process, and similarly during melting. Now if, during freezing, the water is blown off a freezing water drop, then the water and ice will be charged oppositely and are separated. So, in a thunderstorm, if water being carried aloft by the updraft freezes, and the water and ice blown apart, then the ice which is usually negative falls toward the bottom of the cell, and the water which is positive is carried on toward the top of the cell. Magnitudes of charge separated by this process are given by Stott and Hutchinson (1965). Such a charge separation process would lead to the charge distribution in a typical thunderstorm cell.

c) Electric Field Variations Due to Thunderclouds - Schonland (1928) in South Africa measured the electric field as thirteen different thunderstorms passed over. On each of these, the field reversed polarity and became positive. This would indicate that the polarity of these storms was as discussed earlier. The magnitude of the field varied depending on factors such as cloud size and altitude.

d) Point Discharge Currents - The measurement of the amount of charge transferred to or from the earth by point discharge currents has proved quite difficult (Wormell, 1927, Schonland, 1928, Chalmers, 1957). Results indicate variations of current through trees depending on such factors as whether the tree is in leaf or not, and wind direction.

Point discharge currents occur when the electric field near an object raised above its surroundings becomes large enough so that atmospheric ions are accelerated to the point where they can produce ionization by collision. Ions of polarity opposite to the electric field move to the object and comprise a current to earth. Generally, only in the presence of thunderstorms does the electric field become large enough to cause this breakdown. Schonland's (1928) experiments with trees indicate a minimum of 600 to 1000 v/m is required to cause point discharge for objects the size of trees.

e) The Role of Lightning in Charge Transfer - During the period when the lightning stroke provides an ionized conducting path between cloud and earth, charge can be transported from the earth. The total effect must depend on the number of discharges and the charge transported by each flash. Wormell (1939) concluded 0.4 flashes to earth per km^2 with 0.28 flashes per km^2 bringing negative charge to earth. He estimated the average charge transferred per flash is 20 coulombs so that

-5.6 coulombs/km^2-year are brought to earth. Results of other investigators range up to -45 coulombs/km^2- year (Chalmers, 1957).

f) Precipitation Currents - Investigators have measured the charge in precipitation (rain, hail, snow) to try to determine charge brought to earth by precipitation. Single drop charges and average effect of large numbers of drops have been measured, with emphasis on single drop measurements. Banerji and Lele (1952) found an average of 10^{-11} coulombs per drop of rain, although this value was substantially greater than other investigators have found. Estimates of total charge brought to earth have been given earlier.

1.5 Summary. The salient theories of atmospheric electricity, for both fair and disturbed weather conditions have been presented, along with quoted numerical values of some of the variables of atmospheric electricity. Among the investigators in atmospheric electricity is the consensus that many of the theories are unsatisfactory, that many problems in the area are still unsolved and those that have been "solved" still require further work. Two statements made at the third international conference on atmospheric electricity - Montreux, Switzerland, May 5 - 10, 1963 are illustrative: "The continued existence of these problems reminds us again of their complexity. They appear to defy solution." - Dr. S. C. Coroniti, and "Moreover, the results in this field are so complex and so contradictory that it seems senseless to continue!" - Hans Israël. The data presented in Table I indeed shows that much work needs to be done to answer the questions of atmospheric electricity. However, investigations in the field of atmospheric electricity are constantly being carried out, with improved success brought about by improved instrumentation and measuring techniques and improved theories

CHAPTER II

AN ELECTRICAL MODEL OF THE FAIR WEATHER ATMOSPHERE

2.1 Introduction. An examination of the existing theories of atmospheric electricity as presented in Chapter I yields the following salient features: 1) in fair weather areas, there is a conduction current of 1400-1800 amperes flowing to the earth, 2) a like amount of current leaves the earth in thunderstorm areas, 3) the ionosphere is at a potential of approximately +360kv with respect to the earth, 4) there exists in the atmosphere an electric field which decreases with altitude from a ground level value of the order of -130 volts/meter, and 5) the conductivity of the atmosphere increases monotonically with altitude from a ground level value of the order of 2×10^{-14} mhos/meter, this conductivity being attributable to the presence of ions.

The earth-atmosphere-ionosphere system is sometimes compared to a spherical capacitor; the earth and ionosphere being the plates of this capacitor, and the atmosphere acting as a "leaky" dielectric. Thunderstorms are thought to be the generators which keep the system in equilibrium.

Measurements of conduction current in the atmosphere are accomplished by two methods, direct and indirect. The direct method involves measuring the charge per unit time collected by the measuring equipment, while in the indirect method, conductivity and electric field are measured, and conduction current is calculated using Ohm's law.

Conductivity, on the other hand, can be measured directly or can be determined on the basis of ionic concentration measurements using the relationship discussed in Chapter I. Ionic concentrations and conductivity are usually measured using Gerdien condensers carried by balloons (Stergis, et al., 1955), aircraft (Kraakevik, 1957) or rockets (Boudreau, et al., 1959).

In this chapter, an electrical model of the global atmosphere is developed from fundamental considerations of transport theory applied to electrically charged particles. This model, being somewhat more comprehensive than previously proposed mechanisms, is expected to yield a more valid theory governing distributions of ionic concentrations and electric field within the atmosphere. From these distributions can be calculated atmospheric conductivity, drift currents, diffusion currents and space charge density.

2.2 Atmospheric Model Description. Consideration may initially be given to an ion of charge q and mass m situated in the earth's atmosphere. Neglecting relativistic effects, the forces acting on the ion will consist of the Lorentz force $\overline{f}_L$, and the force of gravity $\overline{f}_g$. Newton's law of motion for the ion can then be written as

$$\overline{f} = m \frac{d\overline{v}}{dt} = \overline{f}_L + \overline{f}_g$$

where $\overline{v}$ is the ion's velocity vector. If $\overline{g}$ is the acceleration due to the earth's gravitational field, $\overline{E}$ the atmospheric electric field, and $\overline{B}$ the total magnetic field comprised of the earth's magnetic field plus any self generated field due to the charged particle's velocity, then Newton's law becomes:

$$\bar{f} = \frac{m d\bar{v}}{dt} = \bar{f}_L + \bar{f}_g = q[\bar{E} + \bar{v} \times \bar{B}] + m\bar{g}.$$

In the atmosphere, both the $\bar{E}$ and $\bar{g}$ vectors are directed radially inward toward the center of the earth. Consequently, the first and third terms in the right hand side of the preceeding expression can be combined algebraically. The magnitudes of the terms $q\bar{E}$ and $m\bar{g}$ can be compared using known geophysical data.

The principal atmospheric ion is considered to be 0_2^+ with a mass of 5.31×10^{-26} kilograms (Whipple, 1965). The gravitation constant is approximately 9.8 meters/sec^2, q is 1.6×10^{-19} coulombs and $\bar{E}$ varies within the atmosphere from 1.0 volt/meter up to approximately 100 volts/meter. Then the ratio of $\left|\frac{m\bar{g}}{q\bar{E}}\right|$ satisfies the inequality

$$10^{-8} \leq \left|\frac{m\bar{g}}{q\bar{E}}\right| \leq 10^{-6}.$$

Consequently,

$$q\bar{E} + m\bar{g} \tilde{=} q\bar{E}.$$

Thus Newton's law of motion is, to a good approximation

$$\bar{f} = q[\bar{E} + \bar{v} \times \bar{B}].$$

Ion viscosity, ν, may be defined as the ratio of the force acting on an ion to its resulting velocity. Thus

$$\nu = \left|\frac{\bar{f}}{\bar{v}}\right| = \frac{q|\bar{E} + \bar{v} \times \bar{B}|}{|\bar{v}|},$$

which implies

$$\bar{v} = \frac{\bar{f}}{\nu} = \frac{q[\bar{E} + \bar{v} \times \bar{B}]}{\nu} = \mu[\bar{E} + \bar{v} \times \bar{B}],$$

where the ratio of ion charge to ion viscosity is the ionic mobility, μ. The current density associated with charged particles moving with velocity, $\overline{v}$, is given by

$$\overline{J} = q\, n\, \overline{v}$$

where n is the particle concentration. Thus the magnitude of the cross product $\overline{v} \times \overline{B}$ satisfies the inequality

$$|\overline{v} \times \overline{B}| \leq |\overline{v}| \cdot |\overline{B}| = \left|\frac{\overline{J}}{qn}\right| \cdot |\overline{B}|.$$

As discussed in Chapter I, $\overline{J}$ is of the order of 10^{-12} amperes/m^2, and n is of the order of 10^9 ions/m^3. Thus, $\left|\frac{\overline{J}}{qn}\right|$ is of the order of 10^{-2} m/sec. The earth's magnetic field is known to be of the order of 10^{-4} webers/m^2 or less, so that

$$|\overline{v} \times \overline{B}| \leq \left|\frac{\overline{J}}{qn}\right| \cdot |\overline{B}| \lesssim 10^{-6} \text{ volts/m.}$$

The upper limit is negligible compared to the magnitude of the electric field. Over many years of experimental measurements and observations by previous investigators, no evidence has been found to indicate the existence of any appreciable self-generated magnetic fields due to possible plasma characteristics of ions in motion in the atmosphere. Thus, the resulting expression for ion velocity is approximately

$$\overline{v} = \mu\overline{E}.$$

If this equation is multiplied by the ion concentration, n, there results

$$n\overline{v} = \mu n\overline{E}.$$

But $n\overline{v}$ is simply the ion flux in ions-m^{-2}-sec^{-1}. Thus, magnetic field and gravitational forces can be neglected in determining ion flux in the atmosphere.

Since it is known from electrostatics that a particle of negative polarity is accelerated opposite to the direction of the electric field, and a positive particle accelerated in the direction of the electric field, then

$$\overline{F}_c = \pm \mu n \overline{E}$$

where the plus sign obtains if the ion is positive.

From the kinetic theory of gases, it is known that if there is a difference in concentration of molecules within the gas, i.e., a concentration gradient, there will be a net diffusion of molecules away from regions of higher concentration toward regions of lower concentration, such that there is a net particle flux given by

$$\overline{F}_D = -D\overline{\nabla}n$$

where $\overline{F}_D$ is the particle diffusion flux, D is the diffusion coefficient, and $\overline{\nabla}n$ denotes the gradient of the particle concentration, n.

The total flux $\overline{F}$, for a given type of ion in the atmosphere is then the sum of the fluxes attributable to diffusion and the electric field, or

$$\overline{F} = \overline{F}_c + \overline{F}_D = -D\overline{\nabla}n \pm \mu n\overline{E}.$$

The current density, $\overline{j}$ (amperes/m^2) due to the ion flux is given by the product of ionic charge times ionic flux. Therefore,

$$\overline{j} = q[-D\overline{\nabla}n \pm \mu n\overline{E}].$$

a) Generalized Continuity Equation and Poisson's Equation. - The generalized continuity equation states that the time rate of change of concentration of a given type of particle (assumed here to possess an electrical charge) equals the divergence of the negative flux of that particle, plus the particle generation rate per unit volume, less the rate of particle loss per unit volume. Poisson's equation states that the divergence of the electric displacement vector equals the net charge density present. Stated mathematically, assuming only one type of charged particle,

$$\frac{\partial n}{\partial t} = \overline{\nabla} \cdot [-\overline{F}] + G - L$$

and

$$\overline{\nabla} \cdot \overline{D} = \overline{\nabla} \cdot \varepsilon\overline{E} = \rho = qn$$

where

n = particle concentration

t = time

G = particle generation rate per unit volume

L = particle loss rate per unit volume

$\overline{F}$ = particle flux

$\overline{D}$ = electric displacement

$\overline{E}$ = electric field intensity

ε = permittivity of medium

q = particle charge.

For the case of charged particles (ions) in the atmosphere, using

the flux expression derived in the preceding section, the continuity equation becomes

$$\frac{\partial n}{\partial t} = \overline{\nabla} \cdot [D\overline{\nabla}n \mp \mu nE] + G - R$$

where the loss term is symbolized by R, since the primary mechanism of ion loss in the atmosphere is due to recombination (Schonland, 1953).

Considering the four types of ions discussed in Chapter I, a flux term will exist for each type of ion. The symbols which will be used in describing these fluxes are summarized in the following table, where upper case symbols apply to large ions, and lower case symbols apply to small ions.

TABLE II

SYMBOLS AND DIMENSIONS OF PARAMETERS

Parameter	Symbol	Dimensions
Concentration	n , N	ions/m^3
Diffusion Coefficient	d , D	m^2/sec
Mobility	μ , U	m^2-volt^{-1}-sec^{-1}
Electric Field	$\overline{E}$	volt/m
Generation Rate	g , G	ions-m^{-3}-sec^{-1}
Recombination Rate	r , R	ions-m^{-3}-sec^{-1}
Flux	$\overline{f}$, $\overline{F}$	ions-m^{-2}-sec^{-1}

The four flux terms, where the subscript indicates ion polarity; are:

$$\overline{F}_+ = -D_+\overline{\nabla}N_+ + U_+N_+\overline{E}$$

$$\overline{F}_- = -D_-\overline{\nabla}N_- - U_-N_-\overline{E}$$

$$\overline{f}_+ = -d_+\overline{\nabla}n_+ + \mu_+n_+\overline{E}$$

$$\overline{f}_- = -d_-\overline{\nabla}n_- - \mu_-n_-\overline{E}.$$

If the total positive ion and negative ion fluxes are denoted by $\overline{F}_{+_T}$ and $\overline{F}_{-_T}$ respectively, then

$$\overline{F}_{+_T} = \overline{F}_+ + \overline{f}_+ = [(u_+n_+ + U_+N_+)\overline{E} - (d_+\overline{\nabla}n_+ + D_+\overline{\nabla}N_+)]$$

$$\overline{F}_{-_T} = \overline{F}_- + \overline{f}_- = -[(u_-n_- + U_-N_-)\overline{E} + (d_-\overline{\nabla}n_- + D_-\overline{\nabla}N_-)].$$

In accord with the available experimental evidence, it is assumed that only a single positive or negative increment of electronic charge q exists on each large or small ion. Thus, the positive and negative ion current densities $\overline{j}_+$ and $\overline{j}_-$ are given by the product of the appropriately signed ionic charge $\pm q$ and these polar flux expressions, that is:

$$\overline{j}_+ = q_+\overline{F}_{+_T}$$

$$\overline{j}_- = q_-\overline{F}_{-_T}$$

In each of these expressions, the current density is the superposition of a drift or conduction current and a diffusion current, e.g.,

$$(\overline{j}_+)_D = -q[d_+\overline{\nabla}n_+ + D_+\overline{\nabla}N_+]$$

$$(\overline{j}_+)_C = \sigma_+\overline{E} = q[\mu_+n_+ + U_+N_+]\overline{E}$$

$$(\bar{j}_-)_D = q[d_-\bar{\nabla}n_- + D_-\bar{\nabla}N_-]$$

$$(\bar{j}_-)_C = \sigma_-\bar{E} = q[\mu_- n_- + U_- N_-]\bar{E},$$

where the subscripts D and C indicate diffusion and conduction respectively.

From this discussion it is seen that if the four concentrations n_+, n_-, N_+, and N_-, and the electric field $\bar{E}$ can be determined, both diffusion and conduction current densities can be calculated in terms of the ionic mobilities, diffusivities, and charges.

b) Atmospheric Model - Thus, the electrical model of the atmosphere which will be explored in detail consists of the four generalized continuity equations, coupled with the Poisson equation, i.e., the model is:

$$\frac{\partial n_-}{\partial t} = \bar{\nabla} \cdot [d_-\bar{\nabla}n_- + \mu_- n_-\bar{E}] + g_- - r_- \qquad (2.1)$$

$$\frac{\partial n_+}{\partial t} = \bar{\nabla} \cdot [d_+\bar{\nabla}n_+ - \mu_+ n_+\bar{E}] + g_+ - r_+ \qquad (2.2)$$

$$\frac{\partial N_-}{\partial t} = \bar{\nabla} \cdot [D_-\bar{\nabla}N_- + U_- N_-\bar{E}] + G_- - R_- \qquad (2.3)$$

$$\frac{\partial N_+}{\partial t} = \bar{\nabla} \cdot [D_+\bar{\nabla}N_+ - U_+ N_+\bar{E}] + G_+ - R_+ \qquad (2.4)$$

$$\bar{\nabla} \cdot \varepsilon\bar{E} = q[(n_+ + N_+) - (n_- + N_-)] \qquad (2.5)$$

The atmospheric model thus represented consists of five simultaneous partial differential equations in the five unknowns N_+, N_-, n_-, n_+, and $\bar{E}$. The general solutions of these five equations provide the theoretical ion distributions and electric field in the atmosphere. From these

quantities, the drift and diffusion currents, conductivity, and space charge density can be calculated, for further comparison with the available experimental evidence.

To summarize, the problem is to examine in detail the theoretical adequacy of a five-equation model of the electrical properties of the fair-weather atmosphere. The theoretical ionic concentrations and the electric field distribution in the atmosphere are made available through numerical and analytical solutions of the equations. Implicit in the model are the assumptions that the magnetic field and gravitational forces are negligible.

CHAPTER III

CHARACTERISTICS AND MEASURED ELECTRICAL PROPERTIES OF THE ATMOSPHERE

3.1 Introduction. Before determining atmospheric model parameters such as the ionic mobilities, diffusion coefficients, recombination coefficients and generation rates; atmospheric temperature, pressure and density distributions must be obtained. Atmospheric characteristics such as extent, chemical composition and chemical processes will also be examined in this chapter.

3.2 Atmospheric Nomenclature. The atmosphere is considered to be composed of spherical layers having indistinct boundaries. The name of each layer consists of a word with the suffix "sphere", and the upper boundary of the layer is denoted by the same word with the suffix "pause". For example, the upper boundary of the troposphere is the tropopause. The International Union of Geodesy and Geophysics (IUGG) has adopted the notation that the atmospheric shells be denoted by (named in order of increasing altitude): troposphere, stratosphere, mesosphere, and thermosphere where each shell is characterized by a definite temperature distribution. Figure 5 and Table III from the "U. S. Air Force Handbook of Geophysics" illustrate the adopted nomenclature.

The atmospheric model will be examined in detail for the lower three regions; the troposphere, stratosphere, and mesosphere; with primary interest in the troposphere and stratosphere.

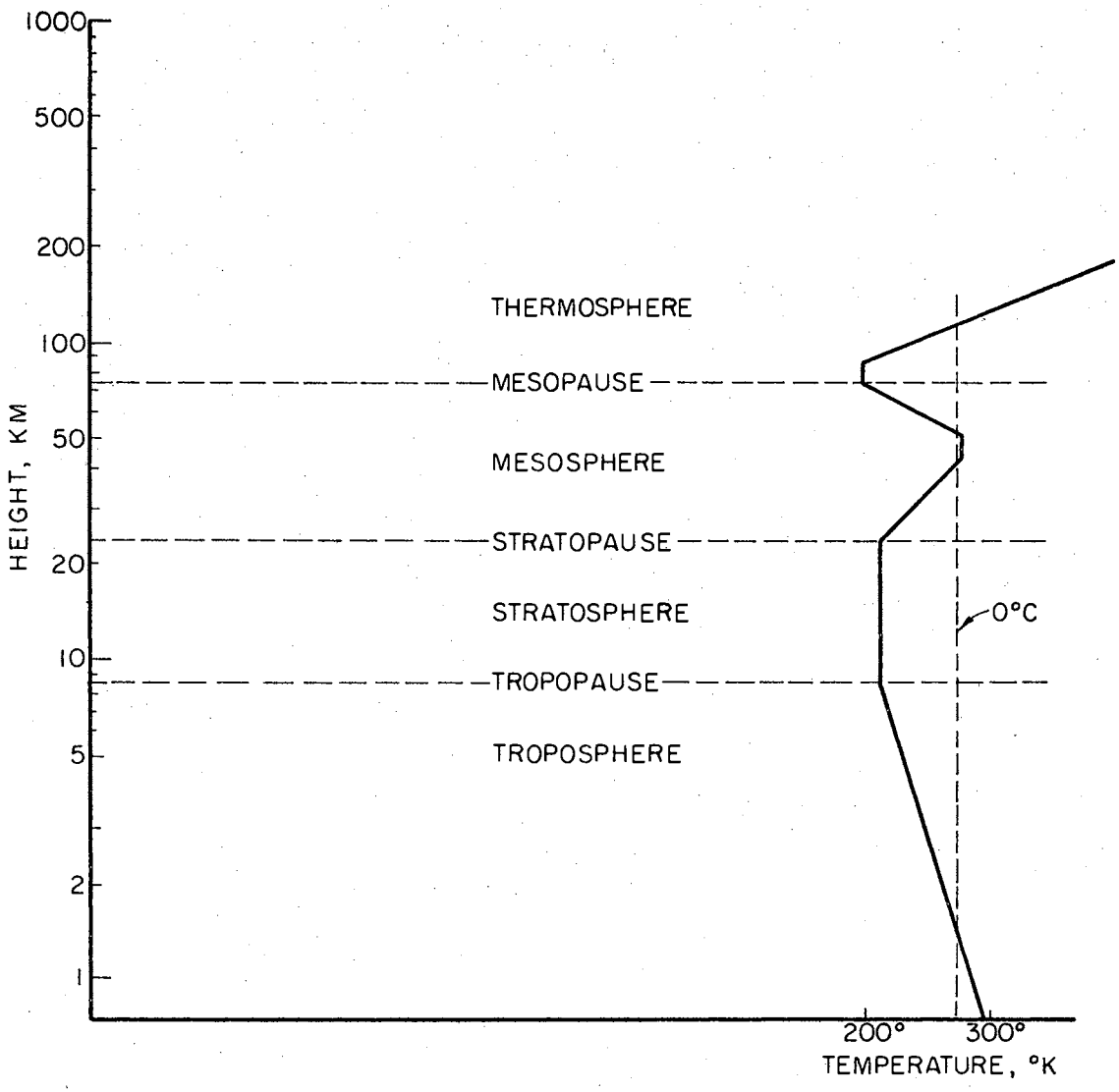

Figure 5. Atmospheric Regions

TABLE III

ATMOSPHERIC REGIONS

Region	Temperature Distribution
Troposphere	Characterized by uniform temperature decrease of nominal value 6.5°K/km.
Stratosphere	Nominally constant temperature.
Mesosphere	Region of the first temperature maximum. The major temperature minimum occurs at the mesopause.
Thermosphere	Region of rising temperature above the mesopause. No upper altitude limit.

3.3 Atmospheric Composition and Primary Chemical Reactions. The principal atmospheric gases are nitrogen, oxygen, argon and carbon dioxide. For altitudes below the mesopause, the proportions of these gases are thought to be invariant. Table IV lists the characteristics of these constituents.

On the basis of the relative weights of the atmospheric constituents, the molecular weight of air is calculated to be 28.966.

Within the troposphere and stratosphere, electron and positive ion ion-pairs are formed primarily by cosmic radiation, and by radiation from radioactive matter in the air and in the earth's crust. However, ionozation due to the presence of radioactive matter is negligible above the bottom two kilometers of the troposphere. Negative small ions are formed by the attachment of electrons to neutral molecules, the most predominate reaction according to Whipple (1965) is

$$O_2 + e^- \rightarrow O_2^-.$$

TABLE IV

PRINCIPAL ATMOSPHERIC CONSTITUENTS (FROM "U. S. AIR FORCE HANDBOOK OF GEOPHYSICS")

Constituent	% by Volume	Molecular or Atomic Weight	Molecular or Atomic Weight (gms)
Nitrogen (N_2)	78.088	28.016	48.50880×10^{-24}
Oxygen (O_2)	20.949	32.000	53.12256×10^{-24}
Argon (A)	0.93	39.944	66.31024×10^{-24}
Carbon Dioxide (CO_2)	0.03	44.011	73.06178×10^{-24}

In the upper portion of the stratosphere and in the mesosphere, electrons are produced not only by cosmic radiation, but also by photo-detachment,

$$O_2^- + h\nu \rightarrow O_2 + e^-,$$

and collisional detachment,

$$O_2^- + M \rightarrow O_2 + M + e^-,$$

where M is a neutral molecule. Throughout the troposphere, stratosphere and lower portion of the mesosphere, the electron mean lifetime is so short that the free electron density is negligible (Cole and Pierce,

1965). For altitudes where the electron mean lifetime becomes appreciable, the model would be supplemented by an additional continuity equation describing the concentration of electrons. This would be the case in the upper portion of the mesosphere.

As discussed in Chapter I, the small ions produced by the above processes can become attached to Aitken nuclei to form the highly immobile large ions.

3.4 Atmospheric Temperature, Pressure and Density. Temperature, pressure and density (T, P, ρ) distributions in the atmosphere which will be used in determining parameters in the atmospheric model will be taken from tables in the "U. S. Standard Atmosphere, 1962" and its 1966 supplement. The particular distributions are annual averages at mid-latitude (45°N). Although all three variables P, T, and ρ are given, any one of the three can be calculated from the other two by the hydrostatic equation solution

$$\rho = \frac{PM}{RT} \qquad (3.1)$$

where ρ is density, P is pressure, M is molecular weight (28.966), R is the universal gas constant, and T is temperature. Figures 6, 7, and 8 show respectively the atmospheric temperature, pressure, and density distributions.

In the following chapter, the data represented in these figures will be used to derive ion mobilities, diffusion coefficients, and generation and recombination rates.

3.5 Measured Electrical Properties of the Atmosphere. The atmospheric variables; electric field, conductivity, ionic concentration and drift currents, as measured by various investigators will be presented

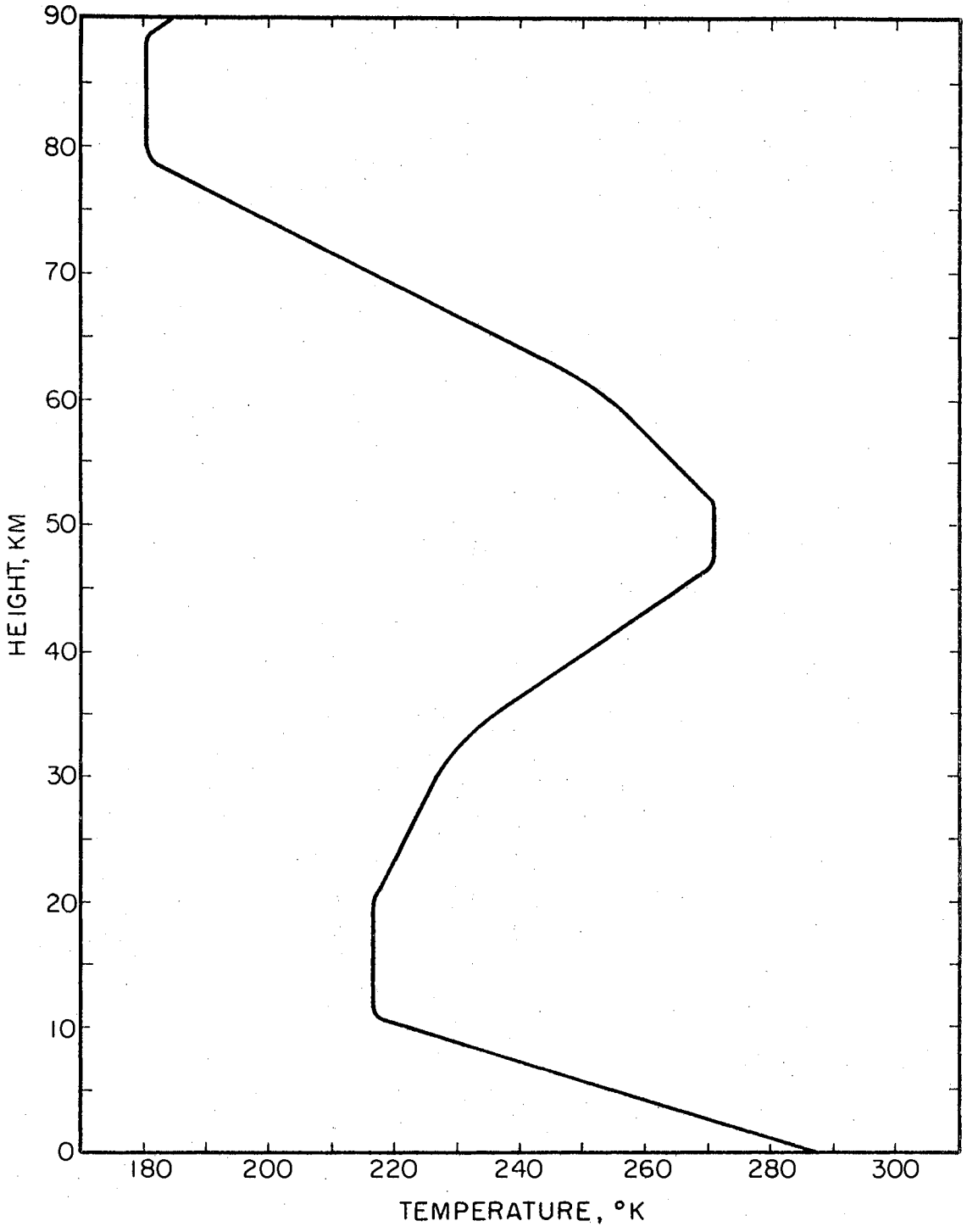

Figure 6. Atmospheric Temperature Profile

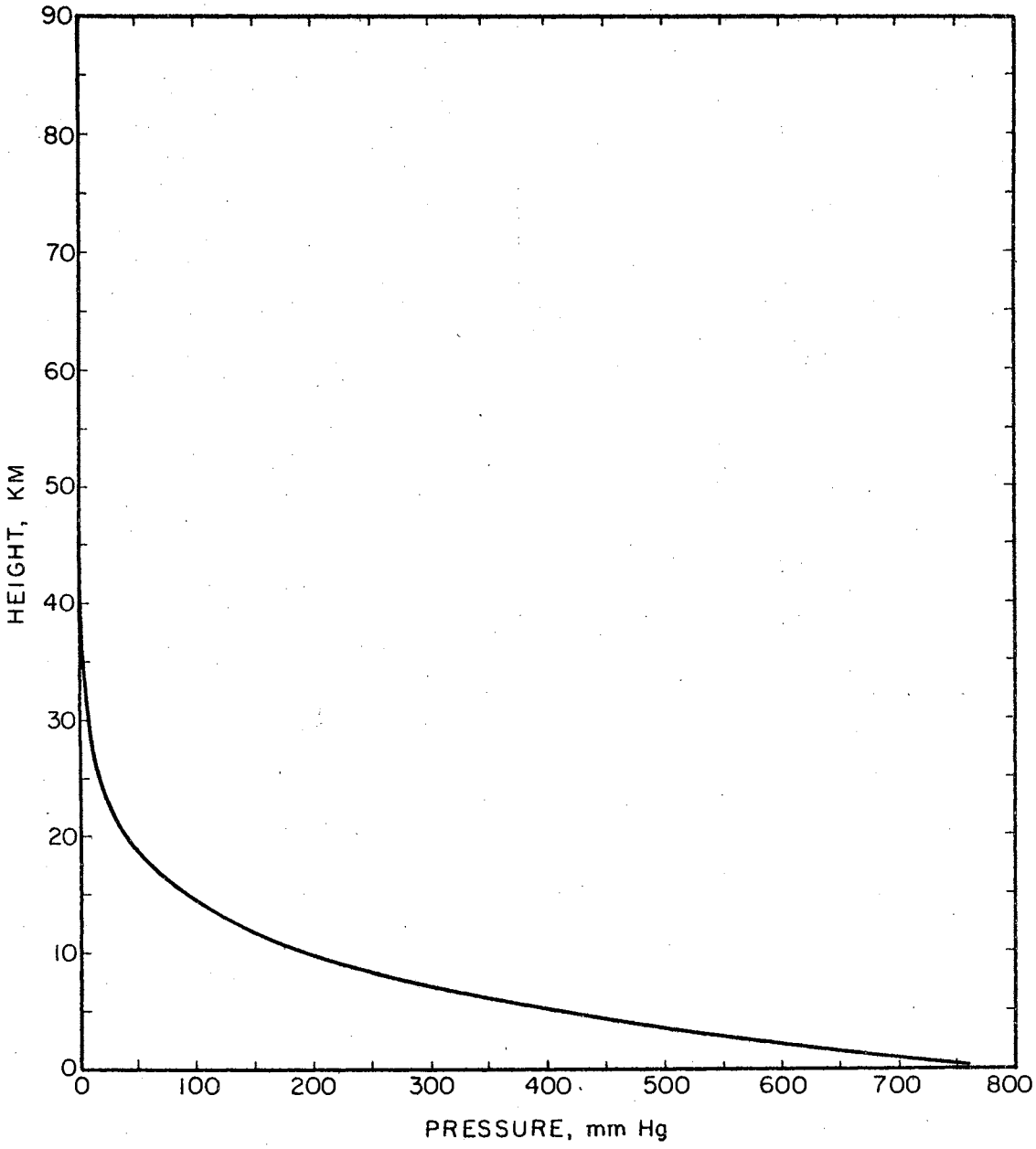

Figure 7. Atmospheric Pressure

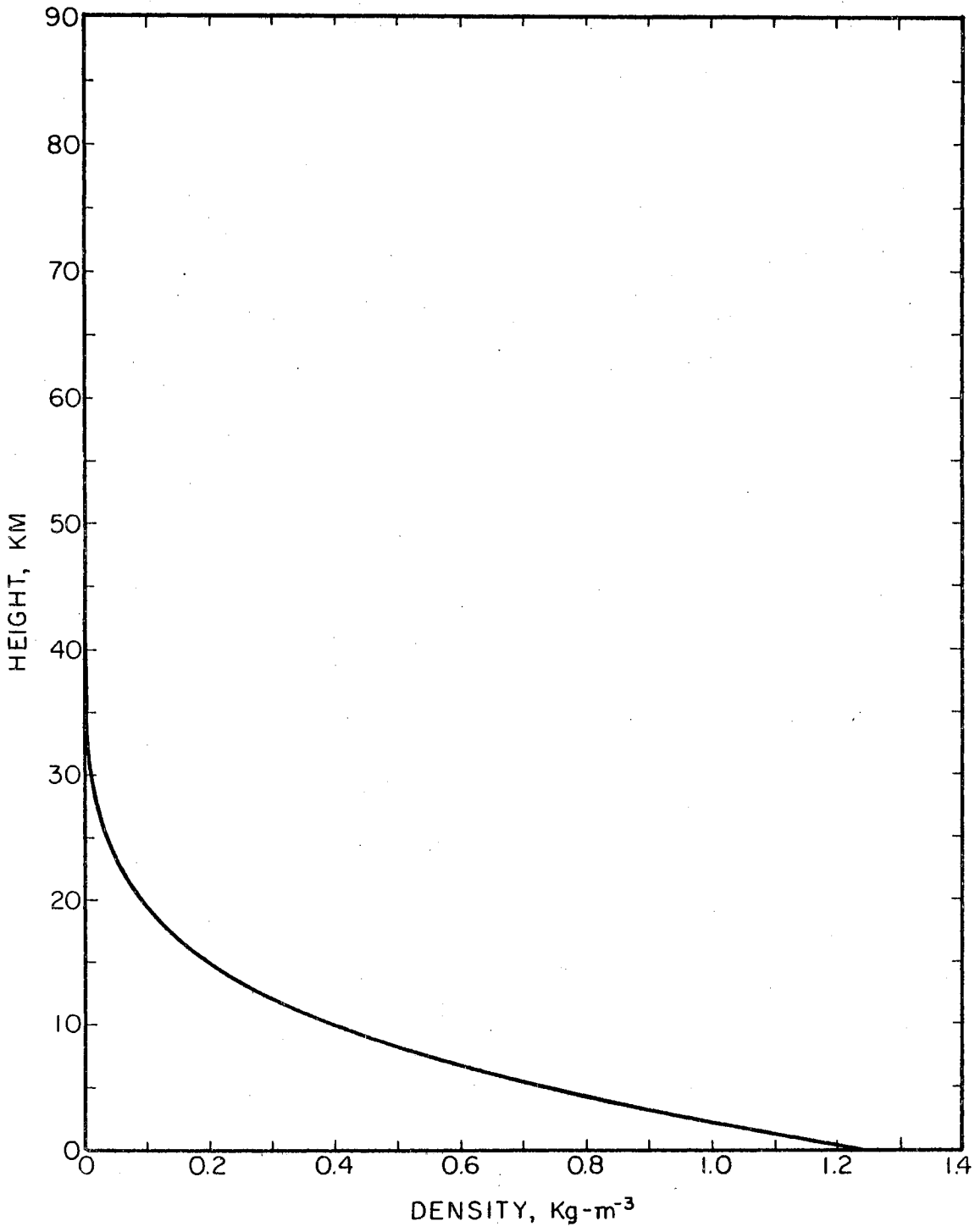

Figure 8. Atmospheric Density

to provide a basis for comparison with the results of analysis of the atmospheric model, and to provide data for use in determining quantities which will aid in the analysis.

a) Electric Field - On the basis of measurements, this variable is assumed to decrease approximately exponentially with altitude. Figure 9 shows measurements by Stergis, et al., (1957) and Hatakeyama (1965), where the measured values are extrapolated above twenty-five kilometers.

Hatakeyama's data is closely approximated by the analytic expressions, where Z is altitude in meters, and E is in volts per meter:

for $0 \leq Z \leq 3000$

$$E = -130 \times e^{-3.0 \times 10^{-4} \times Z} \tag{3.2}$$

for $3000 < Z \leq 18000$

$$E = -81.5 \times e^{-1.63 \times 10^{-4} \times Z} \tag{3.3}$$

and for $Z \leq 18000$

$$E = -37.52 \times e^{-1.243 \times 10^{-4} \times Z} \tag{3.4}$$

and the data of Stergis, et al., is approximated by:

for $0 \leq Z \leq 7500$

$$E = -130 \times e^{-3.175 \times 10^{-4} Z} \tag{3.5}$$

for $7500 < Z \leq 15000$

$$E = -12 \times e^{-1.85 \times 10^{-4} (Z - 7500)} \tag{3.6}$$

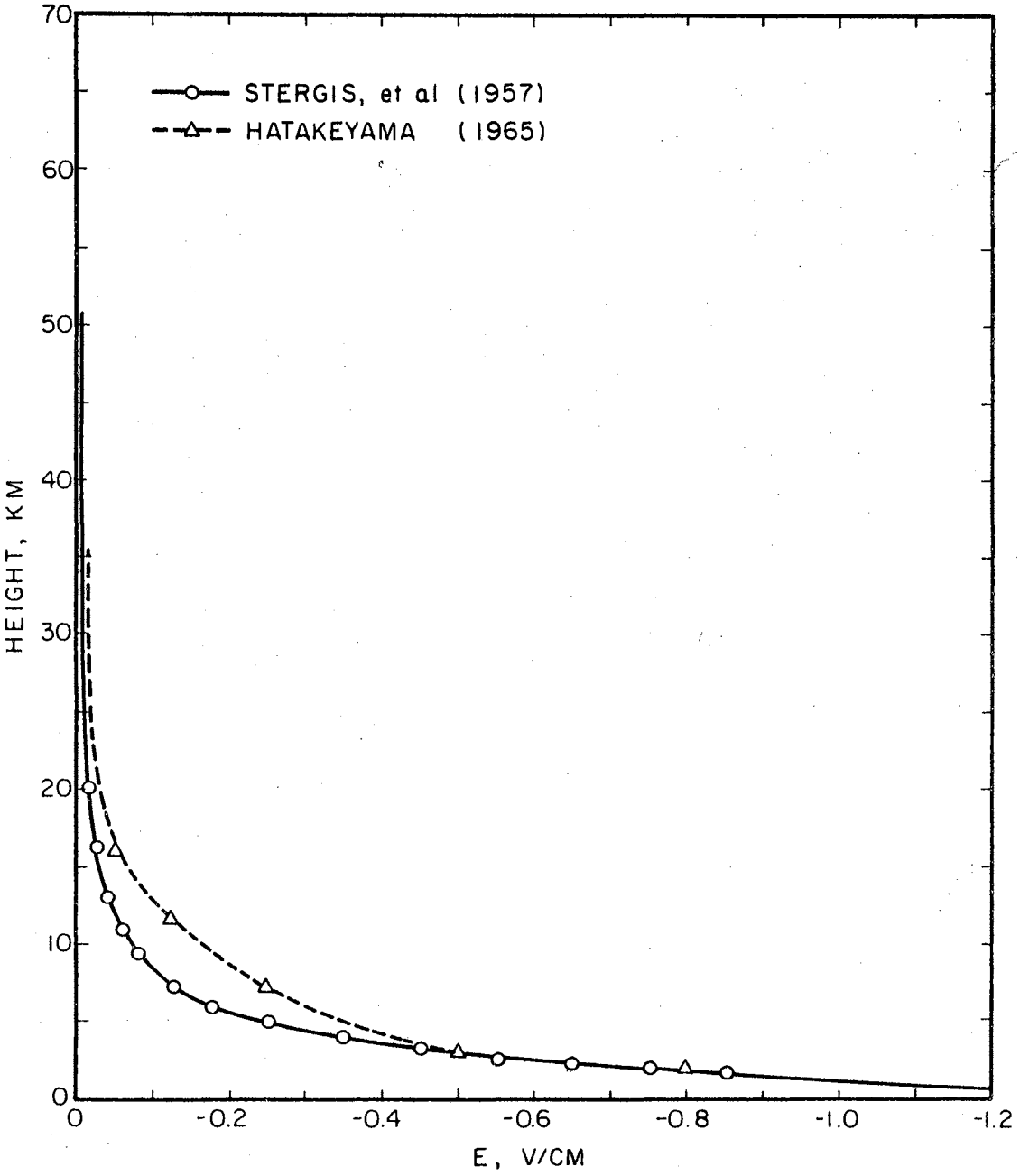

Figure 9. Measured Electric Field

and for Z > 15000

$$E = -3 \times e^{-1.45 \times 10^{-4}(Z - 15000)} \tag{3.7}$$

Von Schweidler (1929), obtained an analytic expression for the electric field on the basis of balloon measurements. His formula is

$$E = -[90e^{-3.5 \times 10^{-3}Z} + 40e^{-2.3 \times 10^{-4}Z}] \tag{3.8}$$

where Z is in meters, and the electric field in volts/meter.

The electric potential difference between the earth and the upper atmosphere can be calculated using these expressions and the definition of potential difference between points A and B,

$$\phi_{A-B} = -\int_{A}^{B} \overline{E} \cdot d\overline{l}.$$

The upper atmosphere will be taken as being at infinity. Then if ϕ_{E-A} is the potential difference between the earth and the top of the atmosphere,

$$\phi_{E-A} = -\int_{0}^{\infty} E(Z)dZ.$$

Using Equations 3.2, 3.3, and 3.4 as the electric field results in

$$\phi_{E-A} = 5 \times 10^{5} \text{volts},$$

while using Equations 3.5, 3.6, and 3.7 gives

$$\phi_{E-A} = 4 \times 10^{5} \text{volts}.$$

These potentials are in fair agreement with the results quoted in Chapter I, where it is pointed out that some disagreement exists as to the exact ionospheric potential. In fact, the exchange layer will have an important bearing on the measured atmospheric electric field, since, being a relatively "high resistance" region there will be a large potential drop across the layer. Thus, if meteorological conditions at the location where the electric field is measured are such that the exchange layer is thin or even nonexistent, the integration of the measured field should indicate a lower ϕ_{E-A} than if the exchange region is of greater extent.

b) Conductivity - Stergis, et al., (1955) measured the polar conductivities using balloon borne instruments at White Sands, New Mexico. In their experiments, σ_- was measured two days prior to σ_+, and the total conductivity shown in Figure 10 is the sum of these polar conductivities, i.e.,

$$\sigma_T = \sigma_+ + \sigma_-.$$

c) Conduction Current Density - Figure 11 shows the results of conduction current density measurements made from an aircraft off the East and West Coasts (Kraakevik, 1958). Above the top of the exchange layer, the current was essentially constant up to the highest altitude at which measurements were made.

d) Ionic Concentrations

1) Large Ion Concentrations - Sagalyn and Faucher (1954) report on the measurements of large ion concentrations made during over forty airplane flights. Figure 12 shows two of the nine concentration profiles reported. These two are typical of the nine measurements in that

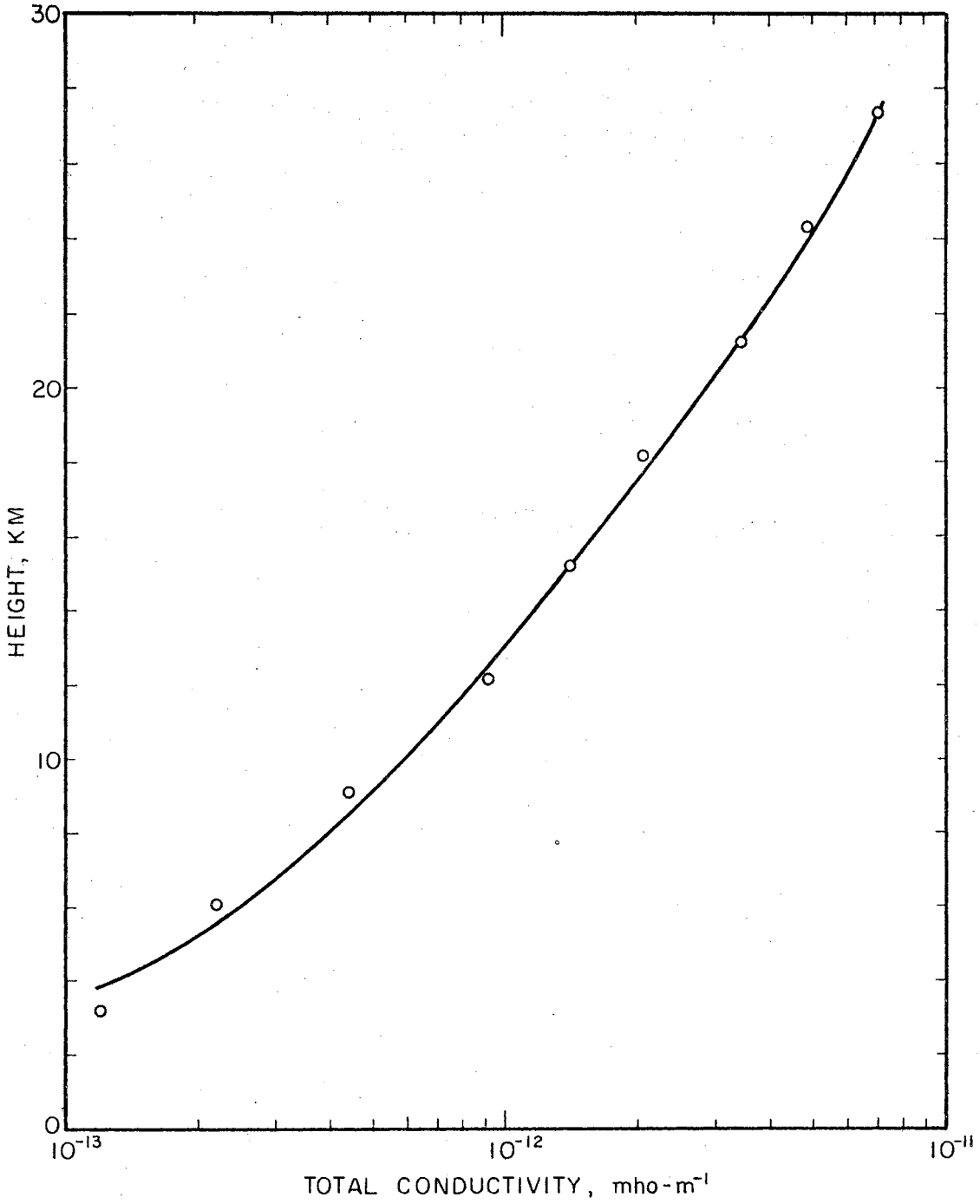

Figure 10. Measured Conductivity

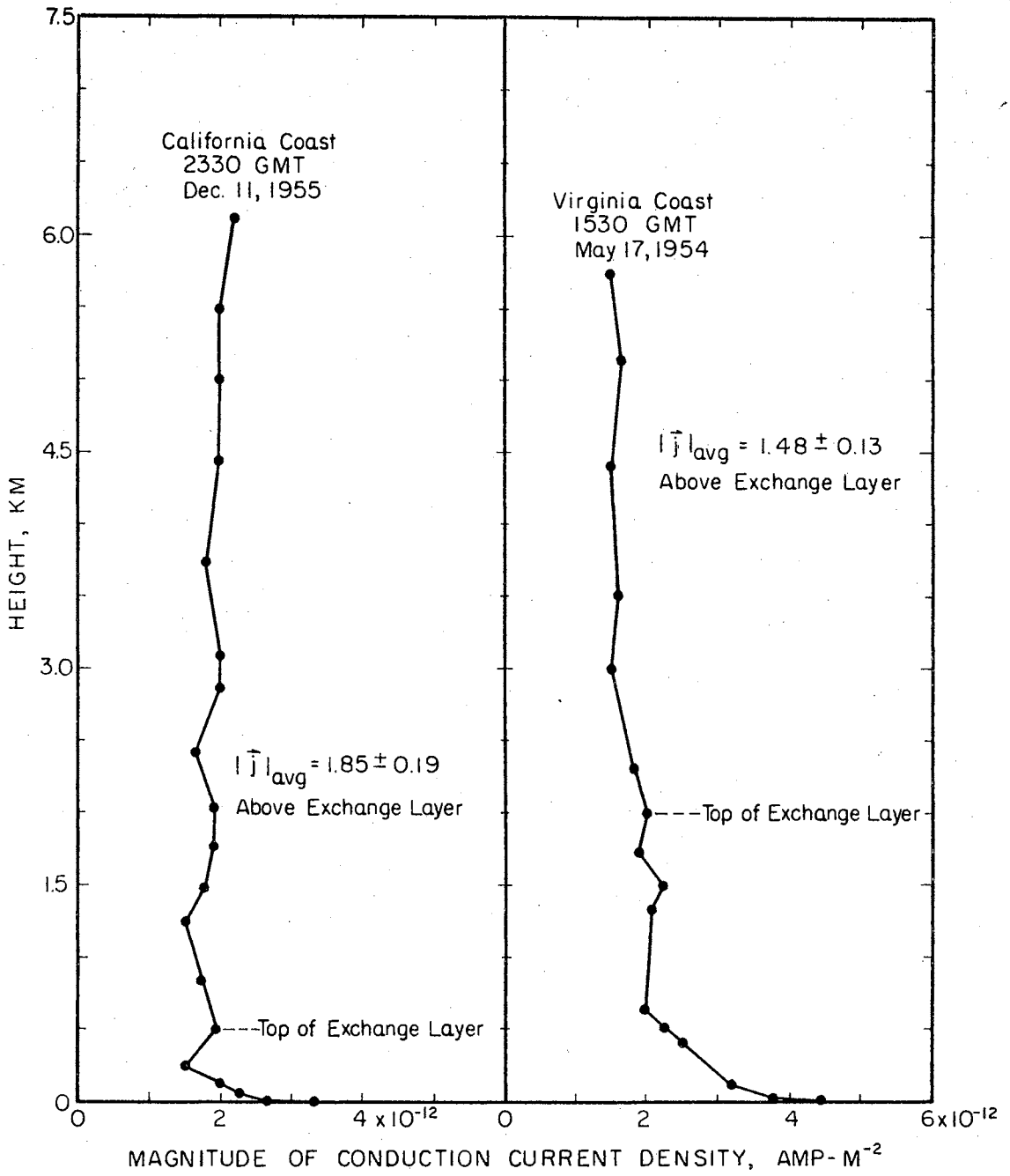

Figure 11. Measured Conduction Current Density

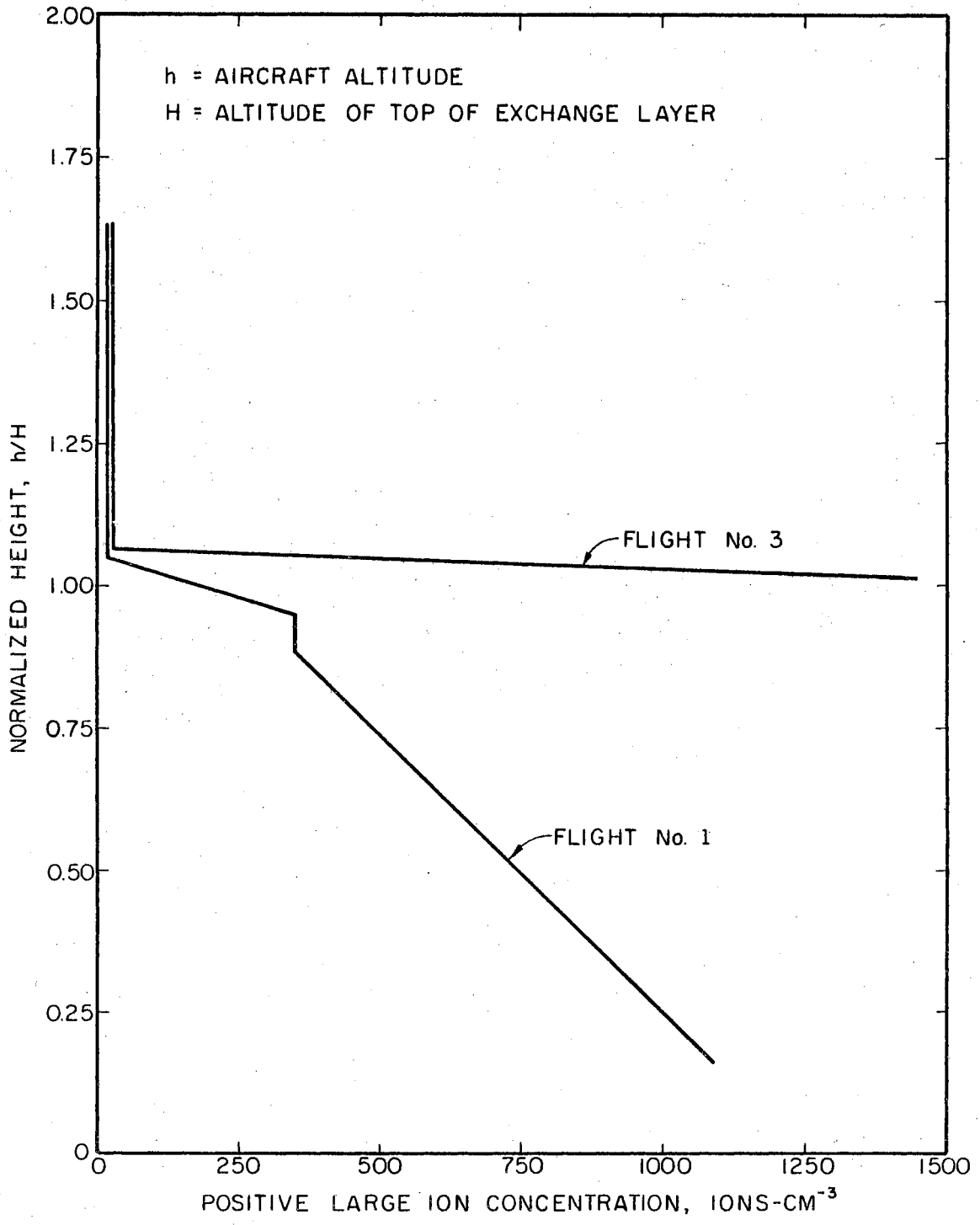

Figure 12. Positive Large Ion Concentration

within the exchange layer the large ion concentration varies widely, depending on meteorological conditions, and then reduces to a small value above the exchange layer. These investigators determined the top of the exchange layer by the altitude at which a sharp decrease in temperature gradient was detected. The average height was six thousand feet, with a standard deviation of two thousand feet. The maximum and minimum values were ninety-four hundred feet and thirty-two hundred feet respectively.

This series of measurements also showed that the large ion concentration was approximately the same for large ions of either polarity, i.e., $N_+ \approx N_-$. This would indicate that the positive small ion density considerably exceeds the negative small ion density within the exchange layer since it is seen from Table VI of Chapter IV that the negative small ions combine with nucleii at nearly twice the rate of the positive small ions. This is the so called "electrode effect" in which there is an excess of positive ions near the earth's negatively charged surface.

2) Small Ion Concentration - Small ion concentrations have not been measured nearly as extensively as atmospheric conductivity. A few investigators have made measurements of small ion densities, however. For example, Kroening (1960) measured negative small ion densities for altitudes up to 35 km. His results are presented in Figure 13.

The decrease in ion density above 15 km was not expected on the basis of Kroening's theoretical predictions. Analysis of the atmospheric model will hopefully provide more satisfactory predictions of ion densities. Also shown in Figure 13 are the results reported by Paltridge (1965). These two curves are the result of smoothing the data reported.

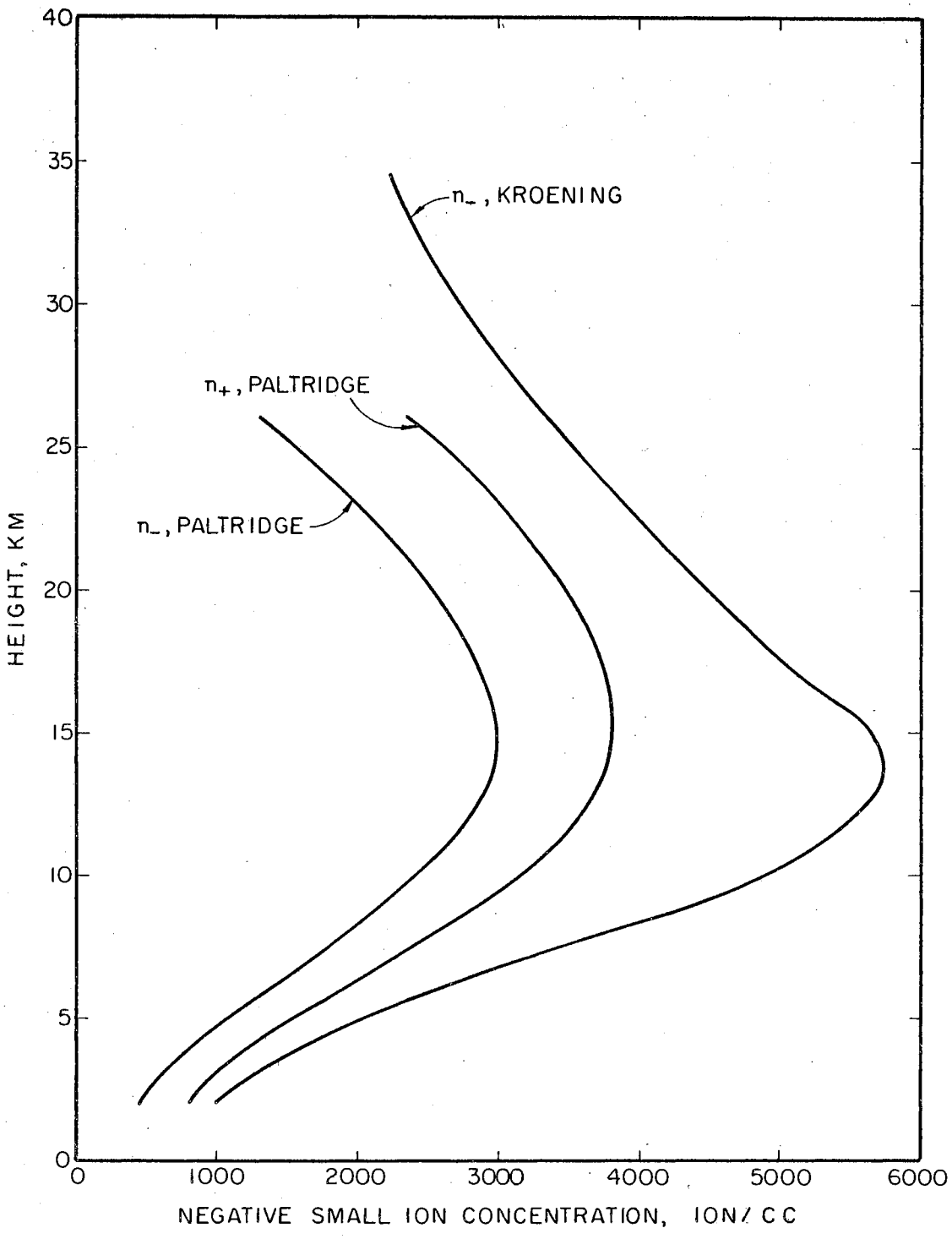

Figure 13. Small Ion Concentrations

3.6 Atmospheric Ionization. In that portion of the atmosphere below two kilometers, ionization is produced by radiation from radioactive material in the earth's crust, radioactive gases in the air, and from cosmic rays. Table V from Hess and O'Donnell (1951) lists the total ionization produced by these sources at altitudes of three centimeters and one meter. In this table, I denotes one ion pair-cm^{-3}-sec^{-1}.

TABLE V

RATE OF IONIZATION IN THE LOWEST ATMOSPHERE

Source of Ionization	3 cm Altitude	100 cm Altitude
γ rays	3.58I	1.76I
α rays	2.18I	0.47I
γ rays	3.76I	3.21I
Cosmic rays	1.96I	1.96I
Total	11.48I	7.40I

The following two figures, after Bricard (1965) show the rates of ionization in the lower atmosphere. Figure 14 showing ionization by radioactive matter in the earth's crust, and Figure 15 ionization by radioactive gases in the air. After examining cosmic ray ionization, it will become apparent that above a few kilometers, the ionization rates presented in these two figures becomes negligible.

Measurements of cosmic ray ionizatior by Bowen, et al. (1938) show that ionization increases with altitude up to approximately 16 km, and

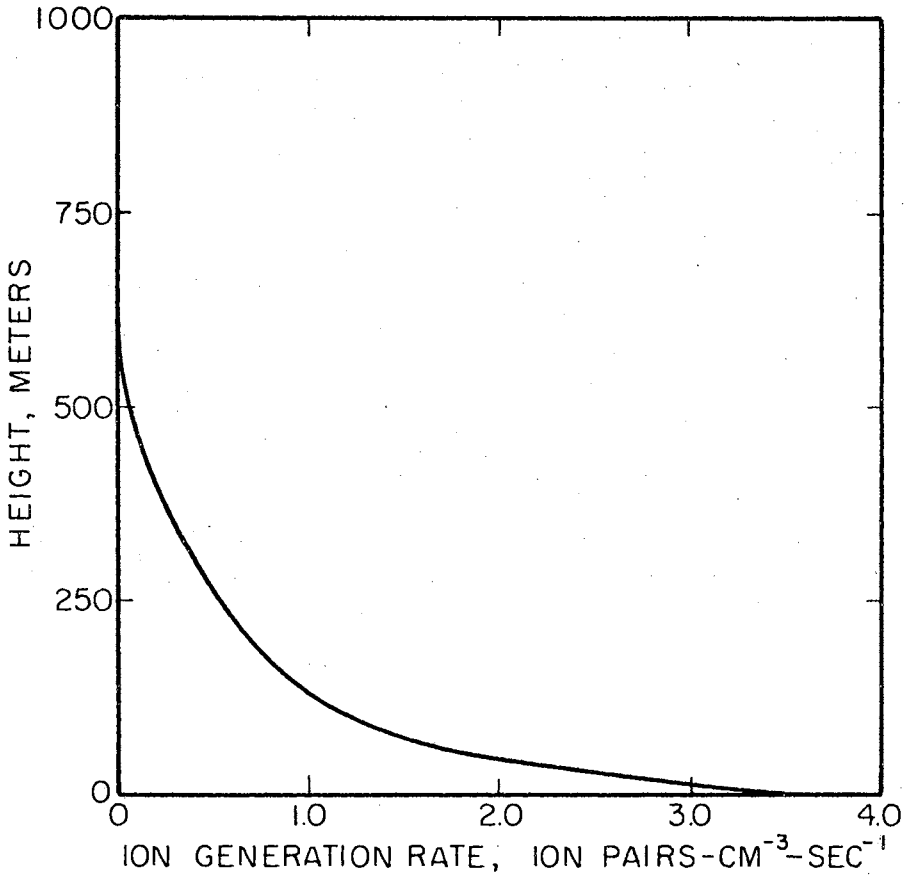

Figure 14. Ionization From Radioactive Matter in Earth's Crust

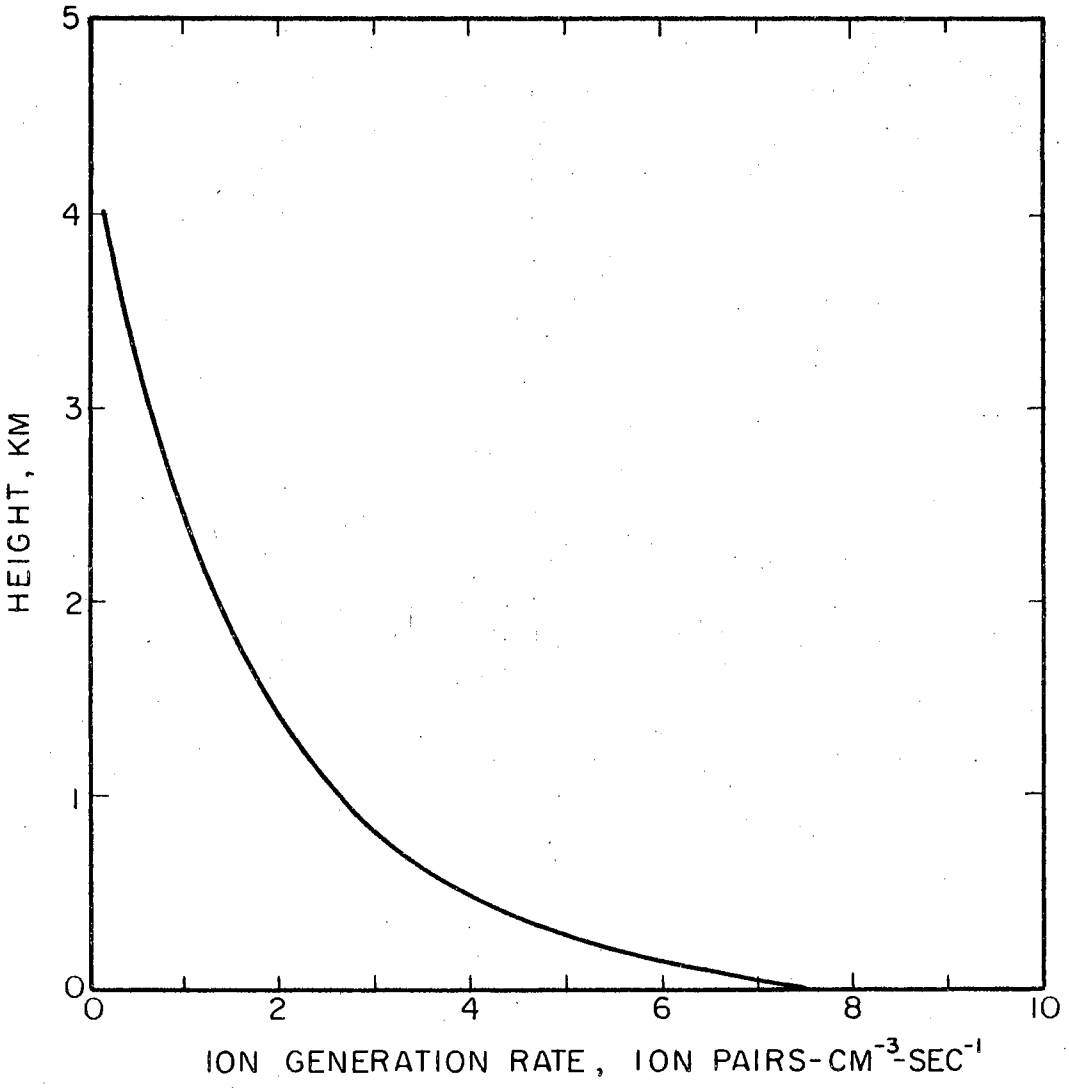

Figure 15. Ionization From Radioactive Matter in Air

then monotonically decreases in the remainder of the atmosphere. Such behavior is probably primarily due to "cosmic showers", where the cosmic primaries initiate secondaries, tertiaries, etc. These descendents ionizing more and more air molecules as they traverse the atmosphere, until they have lost sufficient energy in ionization that their ability to ionize begins to decrease, and continues to decrease. Because of shielding by the earth's magnetic field, cosmic ray intensity is a function of geomagnetic latitude, (GML), having a minimum at the geomagnetic equator and a maximum at the geomagnetic poles. Also, cosmic ray intensity has been shown to be inversely correlated to solar activity (Forbush, 1954). Figure 16 from Bowen, et al, (1938) shows cosmic ionization measured at different geomagnetic latitudes, and Figure 17 from Neher, et al., (1953) shows cosmic ionization variation with GML. Figure 18 from Neher and Anderson (1958) shows the results of cosmic ionization measured at different times at the same GML. The year 1954 corresponded to a period of solar minimum, and 1936 to a solar maximum. It can also be seen from this figure that the "peak" of ionization occurs at higher altitudes as solar activity decreases.

The abscissa of Figure 16 is given in meters of water below the top of the atmosphere, where 10.33 meters of water corresponds to ground level. To convert altitude to meters of water requires using the atmospheric temperature and pressure tables, and tables of mercury density. For example, at a pressure of 760 mm Hg and a temperature of 273°K, the density of mercury is 13.596 gm/cc. Hence

$$0.76\text{m Hg}\left[\frac{13.596\text{gm} - \text{cm}^{-3} - \text{Hg}^{-1}}{1.0\text{gm} - \text{cm}^{-3} - \text{H}_2\text{O}^{-1}}\right] = 10.33\text{m H}_2\text{O}.$$

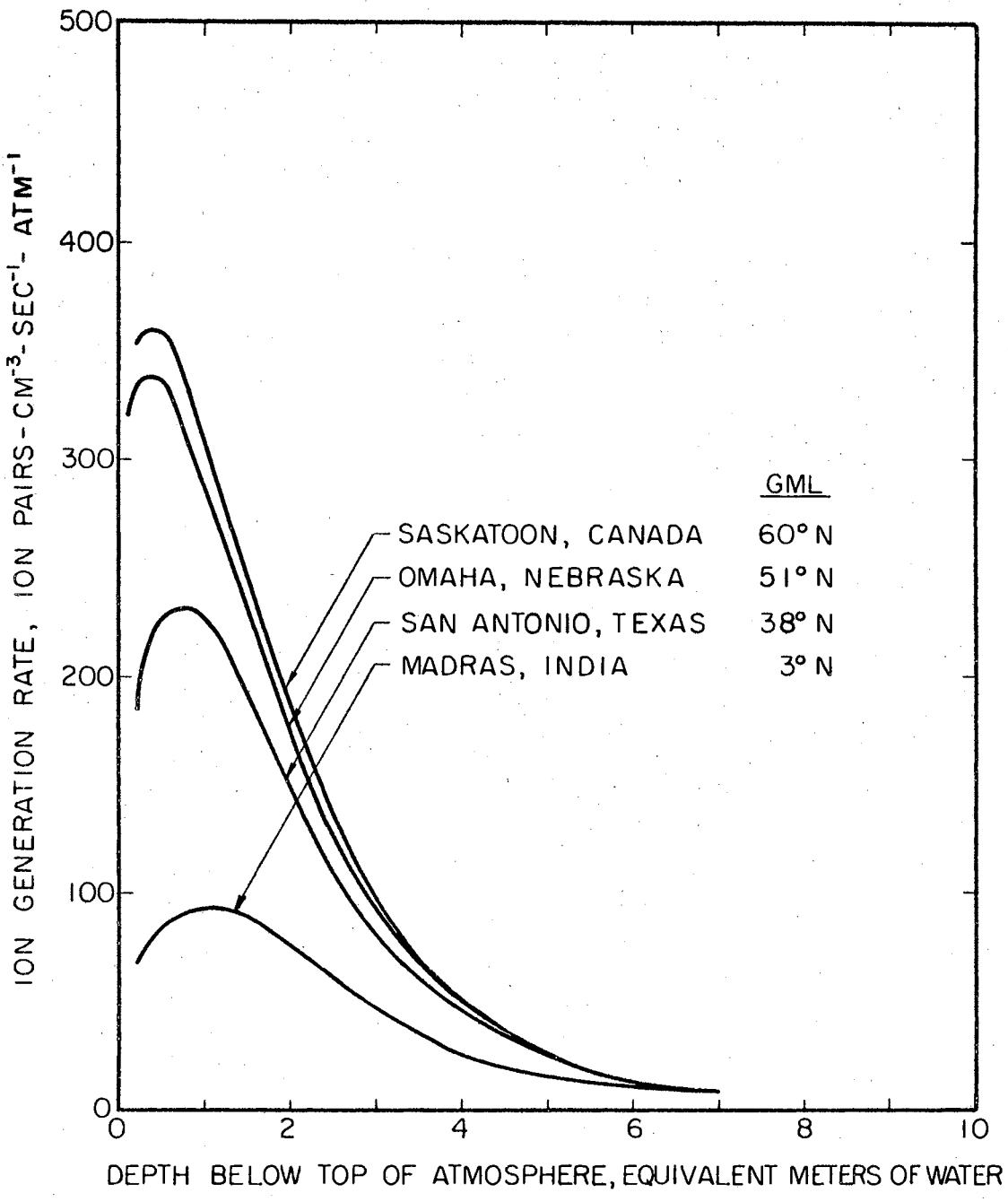

Figure 16. Cosmic Ray Ionization at Different Geomagnetic Latitudes

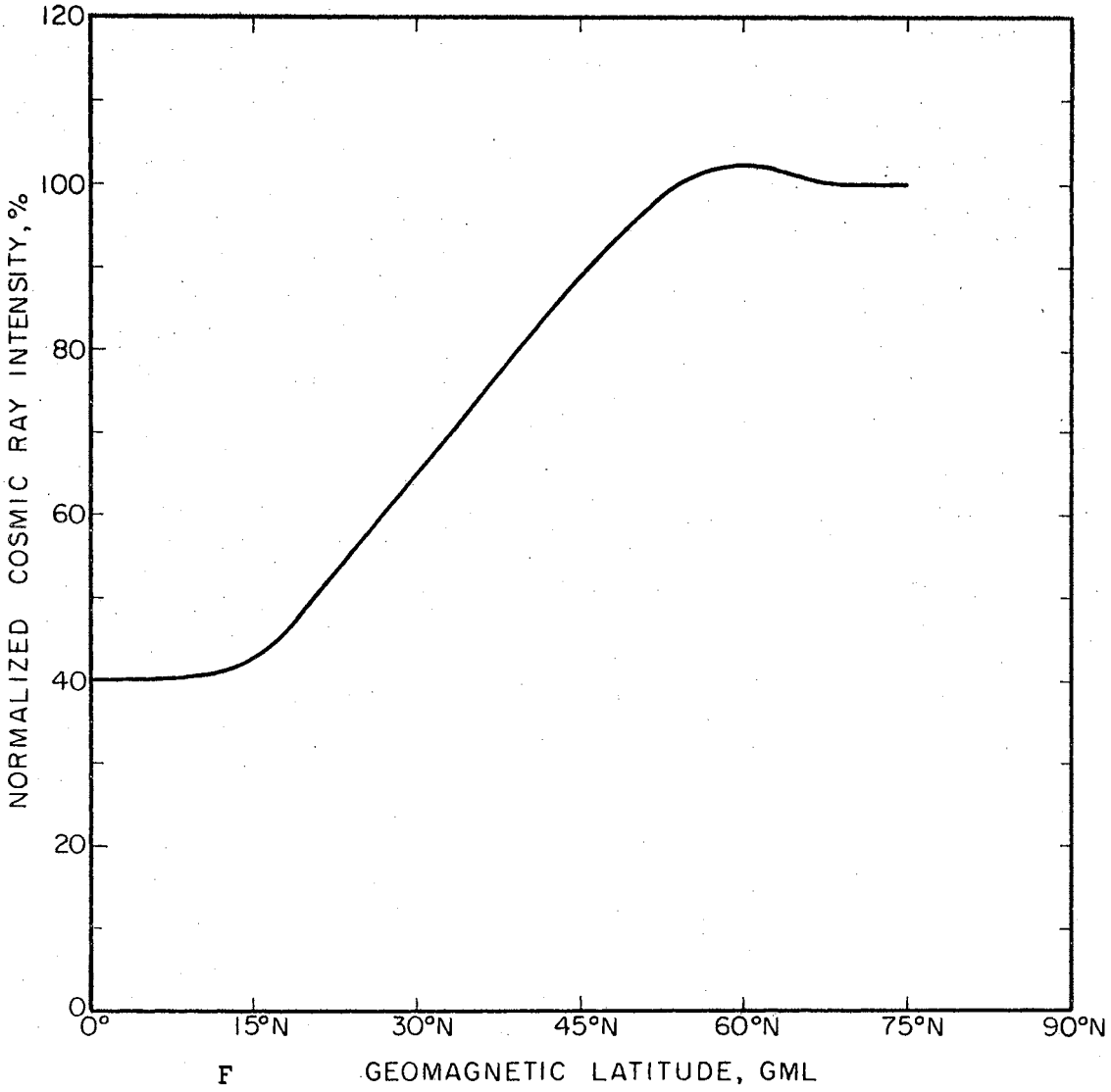

Figure 17. Geomagnetic Latitude Effect on Cosmic Ionization

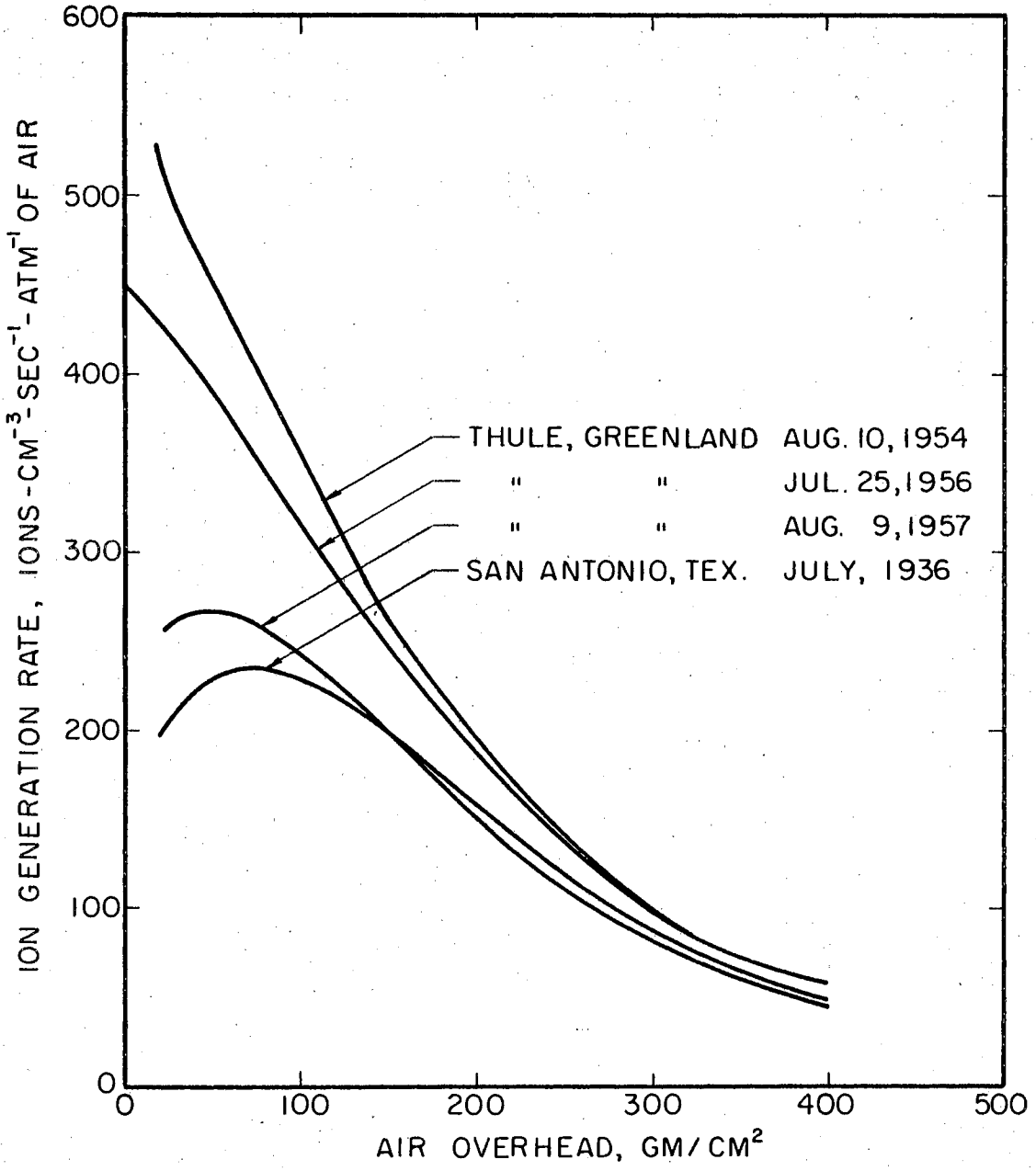

Figure 18. Time Variation of Cosmic Ionization

Any altitude can be obtained from its equivalent in meters of water by the inverse process.

The abscissa of Figure 18 is given in gm/cm^2 of air overhead which can be converted to altitude. For example at STP,

$$(0.76m\ Hg)\left[\frac{13.596\ gm}{cc - Hg}\right] = 1033.0\ gm/cm^2\ of\ air.$$

In illustration, using the pressure, temperature, and mercury density tables gives an atmospheric pressure of 73.6 mm Hg at 16.3 km and density of Hg as 13.6 gm/cc. Then:

$$7.36 \times 13.6 = 100\ gm/cm^2 \qquad \text{air overhead}$$

$$= 1.0\ \text{meters of}\ H_2O.$$

Ordinates of both Figure 16 and 18 give ionization rates referred to one atmosphere. In order to obtain the ionization at a given altitude the ordinate must be multiplied by the ratio of the atmospheric density at the desired altitude to the standard air density at 760 mm Hg and 273°K.

Using the conversion process outlined above, the ionization at 51°N GML from Figure 16 was converted to ionization rate as a function of altitude in kilometers. The result is shown in Figure 19. Figure 20 from Cole and Pierce (1965) is a similar derivation for periods of intermediate solar activity.

The geophysical data represented in this chapter will be used in determining the behavior of the atmospheric model parameters, and will also aid in interpreting results of analysis of the model.

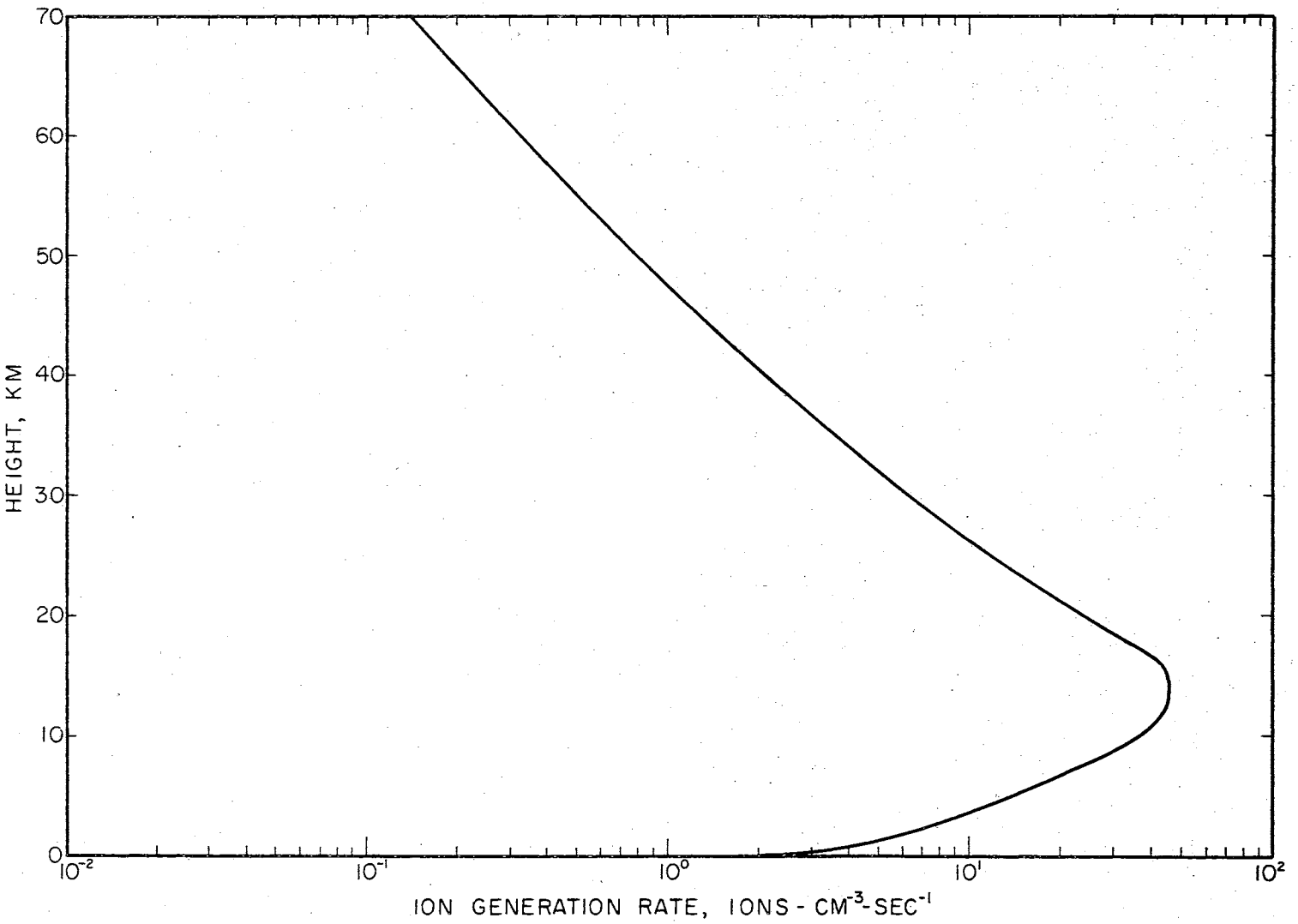

Figure 19. Cosmic Ionization at 51°N GML

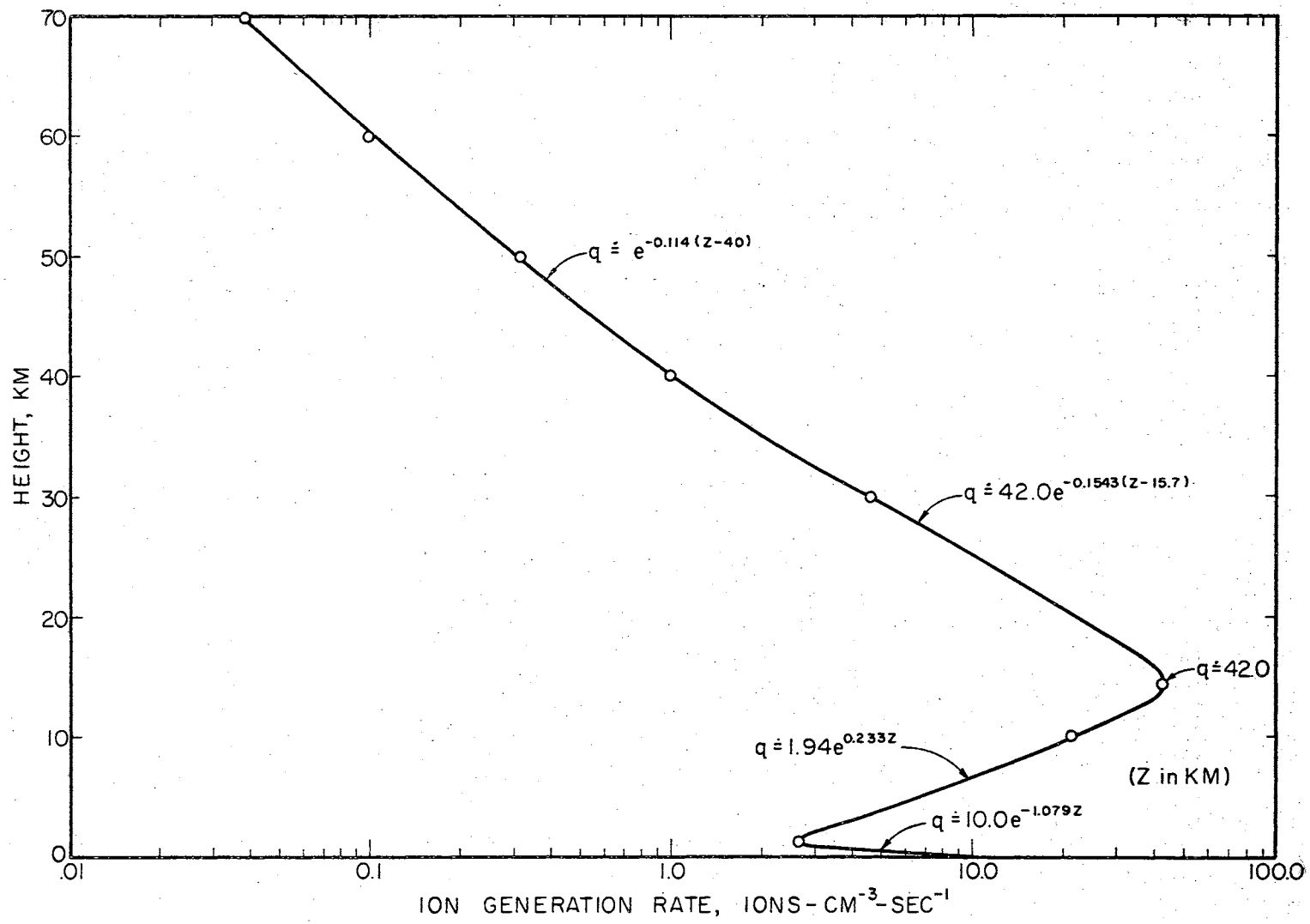

Figure 20. Cosmic Ionization for Intermediate Solar Activity

CHAPTER IV

DERIVATION OF ATMOSPHERIC MODEL FOR ALTITUDES ABOVE THE EXCHANGE LAYER

4.1 Introduction. Prior to analysis of the atmospheric model defined by Equations 2.1 through 2.5, the altitude dependence of the mobility, diffusivity, generation rate and recombination rate terms appearing in the model must be known. This dependence will be determined using known relations from semiconductor theory, the theory of ionized gases, and the data given in Chapter III.

The data represented in Figures 12 and 13 indicate that above the exchange layer (average height of 1.8 km), the large ion content becomes negligible compared to the small ion density. Attention will initially be directed toward the form of the atmospheric model above the exchange layer.

4.2 Small Ion Mobilities. The average mobility of the positive small ion at STP is of the order of 1.4 cm^2-$volt^{-1}$-sec^{-1}, and that of the negative small ion is of the order of 1.9 cm^2-$volt^{-1}$-sec^{-1} (Bricard, 1965). According to Loeb (1955), the mobility of ions in a gas is inversely proportional to the density of the gas. Then if μ_0 is the mobility measured at density ρ_0,

$$\mu(\rho) = \frac{\rho_0}{\rho} \mu_0 .$$

Using Equation 3.1, the mobility can be expressed as a function of pressure and temperature,

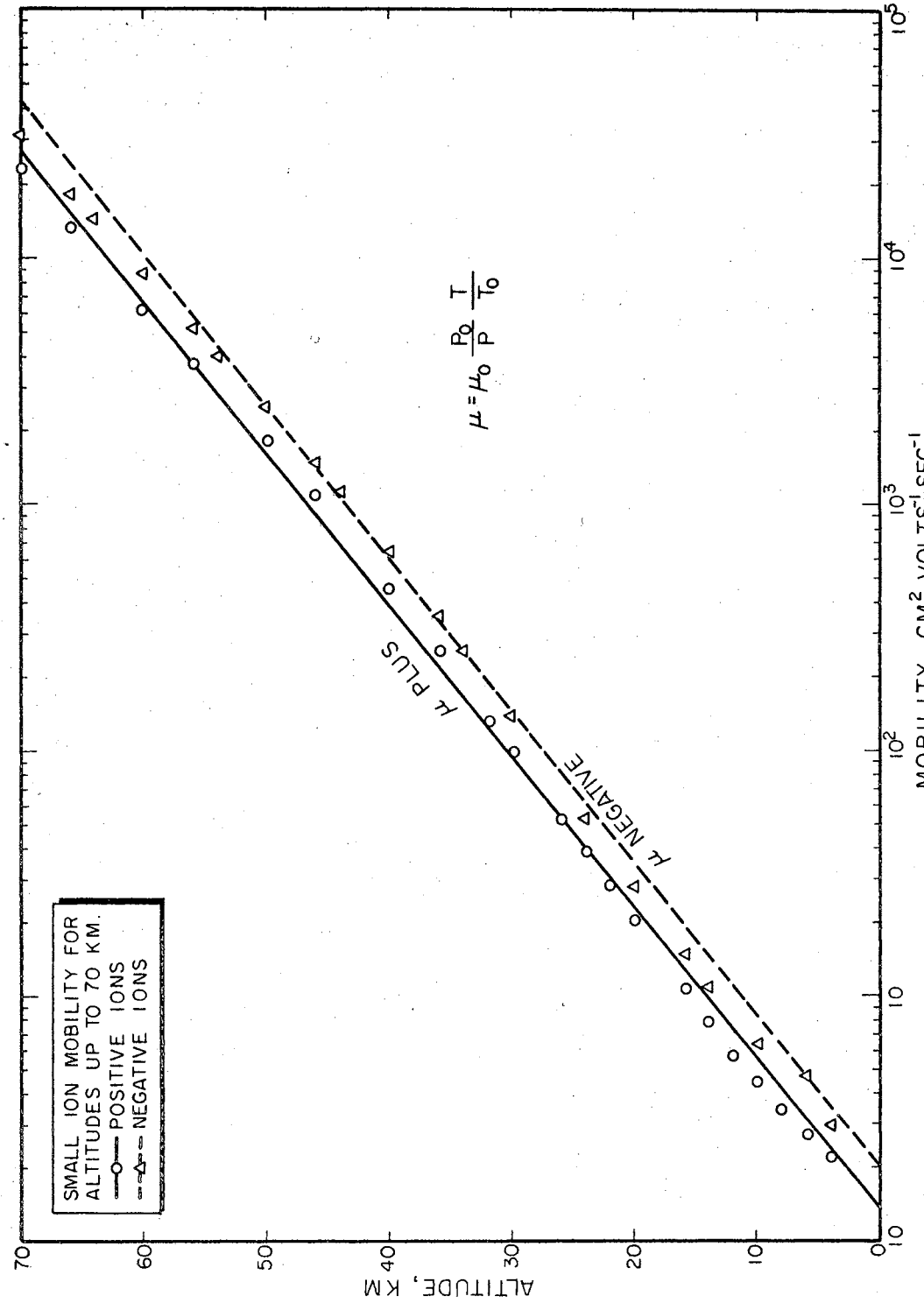

Figure 21. Small Ion Mobilities

$$\mu\,(P,T) = \frac{P_o M}{RT_o}\,\frac{RT}{RM}\,\mu_o = \frac{P_o T}{PT_o}\,\mu_o,$$

or as a function of altitude,

$$\mu\,(Z) = \frac{P_o T(Z)}{P(Z)T_o}\,\mu_o. \tag{4.1}$$

Equation 4.1 holds for ions of either polarity.

The ionic mobilities are known to also be functionally dependent on humidity, although little is known as to the exact form of this dependence. Further experimental work needs to be done to define the effect humidity has on the small ion mobilities. Consequently, the dry air laboratory values will be used for the model analysis, and only temperature and pressures effects will be considered.

Using the data given in the temperature and pressure tables, small ion mobilities as a function of altitude were determined from Equation 4.1. The results are shown in Figure 21. Analytic expressions for the mobilities can be derived form the calculated data. The results are, where Z is expressed in km,

$$\mu_+\,(Z) = 1.4e^{0.14Z}\ \text{cm}^2\text{-volt}^{-1}\text{-sec}^{-1} \tag{4.2}$$

$$\mu_-\,(Z) = 1.9e^{0.14Z}\ \text{cm}^2\text{-volt}^{-1}\text{-sec}^{-1} \tag{4.3}$$

Small ion drift velocities in the vertical direction, given by the product of mobility times electric field, can be determined on the basis of the measured electric field intensity and the theoretical mobility expressions. Equations 3.2, 3.3, and 3.4 give the electric field as measured by Hatakeyama, and Equations 4.2 and 4.3 the ion mobilities. The dimensions of the electric field were converted to volts/cm so that

the velocities are in cm/sec. Figure 22 shows these velocities, where a positive velocity is in the direction of increasing altitude.

4.3 Small Ion Diffusivities. From the ionic mobility expressions and the temperature data, diffusion coefficients can be determined using Einstein's relation

$$d = \frac{kT}{q}\,\mu. \tag{4.4}$$

In this expression, k is Boltzman's constant, and singly charged ions are assumed, i.e., q is the electronic charge. Substituting Equation 4.1 into 4.4 gives

$$d(Z) = \frac{k}{q}\,\frac{T^2(Z)}{T_o}\,\frac{P_o}{P(Z)}\,\mu_o.$$

The results of this calculation for small ions of both polarity and for Z up to seventy km are shown in Figure 23.

Analytic expressions can be derived to represent the diffusion coefficients in the atmosphere.

For $Z \leq 10$ km,

$$d_+(Z) = 0.036e^{0.0916Z} \tag{4.5a}$$

$$d_-(Z) = 0.0488e^{0.0916Z} \tag{4.5b}$$

For $10 < Z \leq 50$ km,

$$d_+(Z) = 0.090e^{0.1543(Z - 10)} \tag{4.6a}$$

$$d_-(Z) = 0.122e^{0.1543(Z - 10)} \tag{4.6b}$$

and for $Z \leq 50$ km,

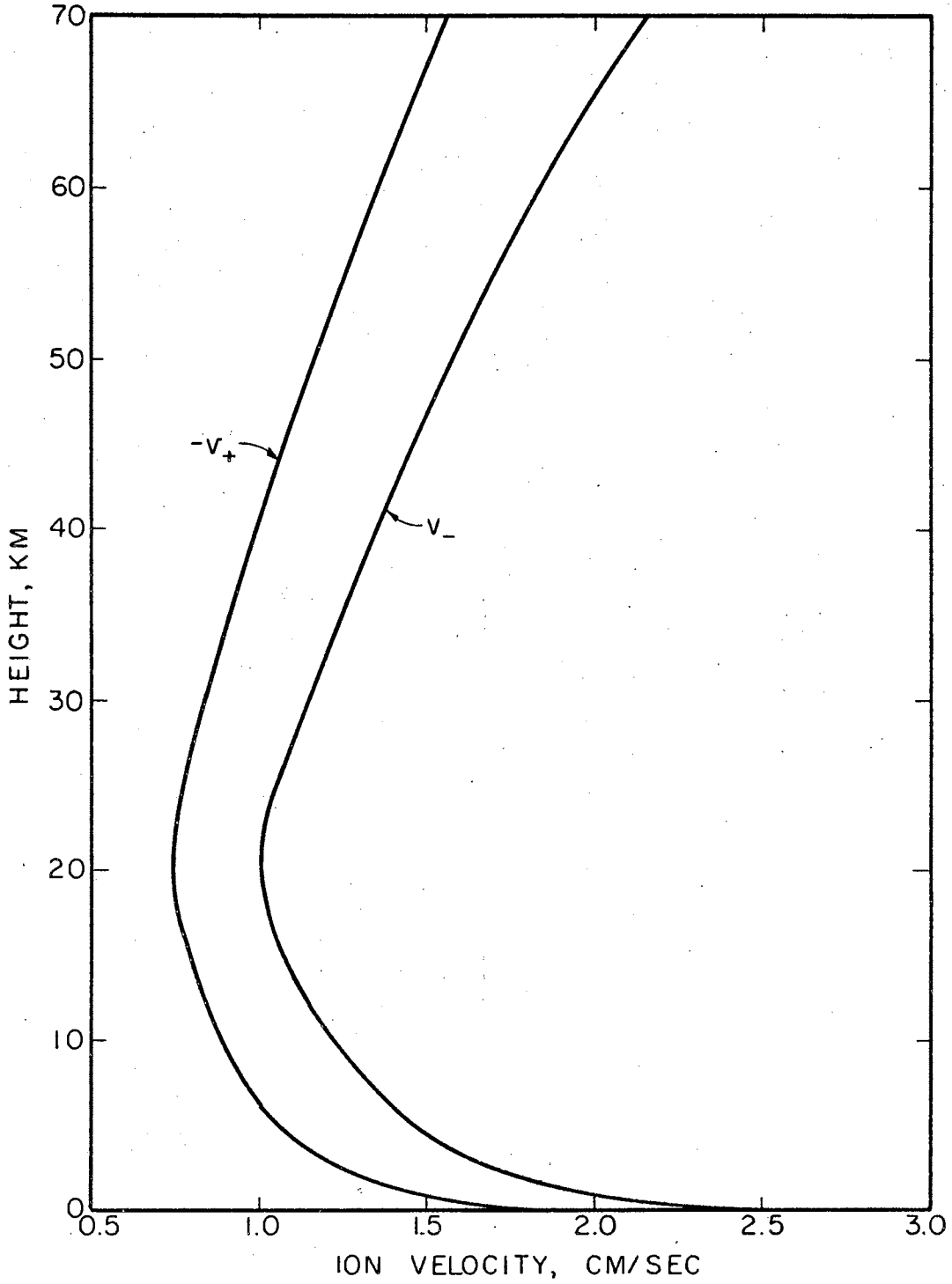

Figure 22. Small Ion Velocities

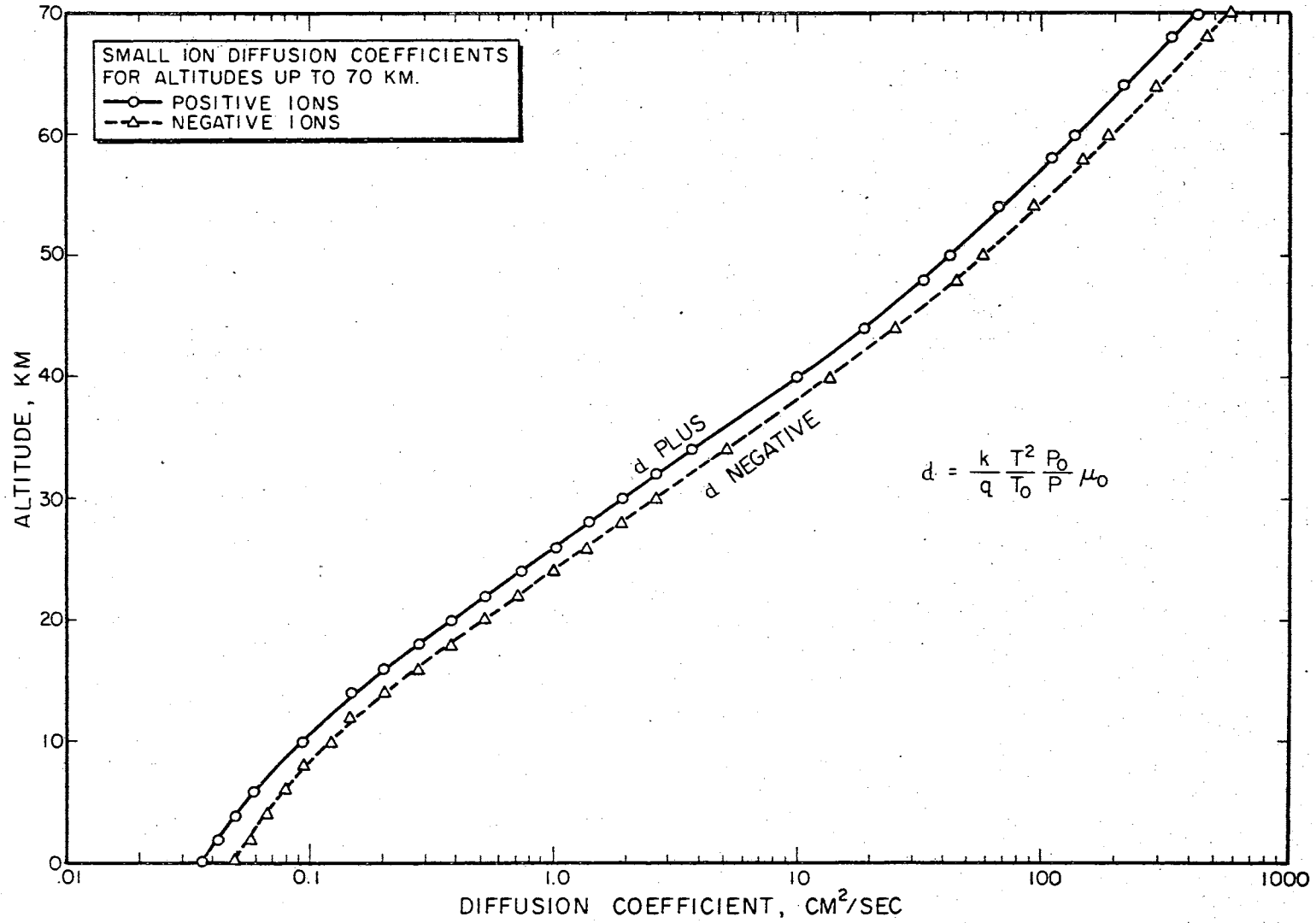

Figure 23. Small Ion Diffusivities

$$d_+(Z) = 41.4e^{0.117(Z - 50)} \qquad (4.7a)$$

$$d_-(Z) = 56.1e^{0.117(Z - 50)} \qquad (4.7b)$$

In these expressions, d is in $cm^2/sec.$, and Z is in km.

4.4 Small Ion Recombination Rate. For altitudes where large ion concentration is negligible, the primary mechanism of loss will be small ion-small ion recombinations. Thus, the rate of recombination will be proportional to the small ion concentrations, i.e., the more ions present, the faster recombination will occur. Furthermore, the two recombination terms, r_- and r_+, will be the same (if the free electron lifetime is negligible) since for this type recombination, for every negative small ion lost, a positive small ion is also lost. Consequently, the recombination model is

$$r_- = r_+ = \alpha n_+ n_-,$$

where α is a constant of proportionality (dependent on temperature and pressure), known as the recombination coefficient and has dimensions of $volume\text{-}ion^{-1}\text{-}sec^{-1}$.

Of the theories regarding ion recombination, Thomson's three-body theory has been shown to most accurately describe such recombinations in air. In fact, Sayers (1938) experimentally verified that this theory is valid in air for pressures from 10^{-2} mm Hg up to 760 mm Hg. A detailed derivation of Thomson's theory is given in Appendix A. Only its most outstanding features and the resulting expression for α will be discussed here.

In essence, Thomson's theory concludes that even though two oppositely charged ions come within that distance, d, of one another where

average kinetic energy and Coulombic potential energy are equal, i.e., when

$$\frac{3}{2} kT = \frac{q^2}{4\pi\varepsilon_o d}$$

recombination is not certain. However, if during this period of orbital encounter, either or both of the ions experience a collision with at least one neutral air molecule, sufficient ionic kinetic energy will be lost, and ion-ion recombination will occur. Such collisions are to be expected if the ion mean free path L is such that $L < d$. Since mean free path is dependent on density, or equivalently pressure and temperature, this at least intuitively indicates that Thomson's recombination coefficient α will depend on these atmospheric variables.

The conclusion of Thomson's theory is that the recombination coefficient is given by the expression

$$\alpha_T = 1.73 \times 10^{-5} \left(\frac{273}{T}\right)^{\frac{3}{2}} \left(\frac{1}{M}\right) f(x) \qquad \text{cc-ion}^{-1}\text{-sec}^{-1},$$

where M is the molecular weight of the ions relative to hydrogen and f(x) is a function accounting for the probability of ion-molecule collisions. The argument x is a temperature and pressure dependent variable determined from the expression

$$x = 0.81\left(\frac{273}{T}\right)^2 \left(\frac{P}{760}\right) \left(\frac{L_A}{L}\right),$$

where L_A/L is the ratio of mean free path of a molecule at STP to that of the ion, and is approximately 3 for air. Therefore,

$$x = 2.43\left(\frac{273}{T}\right)^2 \left(\frac{P}{760}\right).$$

The probability function of x is of the form

$$f(x) = 1 - \frac{4}{x^4}\left[1 - e^{-x}(x + 1)\right]^2.$$

From experimental data taken at 293°K and 760 mm Hg, α has been determined to be 1.6×10^{-5} cc/ion-sec. Calculating x, and f(x) at this temperature and pressure, then $(1/M)^{1/2}$ can be determined from the recombination coefficient expression. The final expression is:

$$\alpha_T = 1.93 \times 10^{-6} \left(\frac{273}{T}\right)^{\frac{3}{2}} f(x).$$

Results of this calculation using the temperature and pressure distributions in the atmosphere are shown in Figure 24. The Thomson recombination coefficient can be expressed as a function of altitude as follows:

for $0 \leq Z \leq 15$,

$$\alpha_T = 1.75 \times 10^{-6}$$

for $15 \leq Z < 50$,

$$\alpha_T = 1.5 \times 10^{-6}\, e^{-0.16(Z - 15)}$$

and for $50 \leq Z \leq 70$,

$$\alpha_T = 5.5 \times 10^{-9}\, e^{-0.118(Z - 50)},$$

where Z is in kilometers and α_T is in cm^{-3}-ion^{-1}-sec^{-1}.

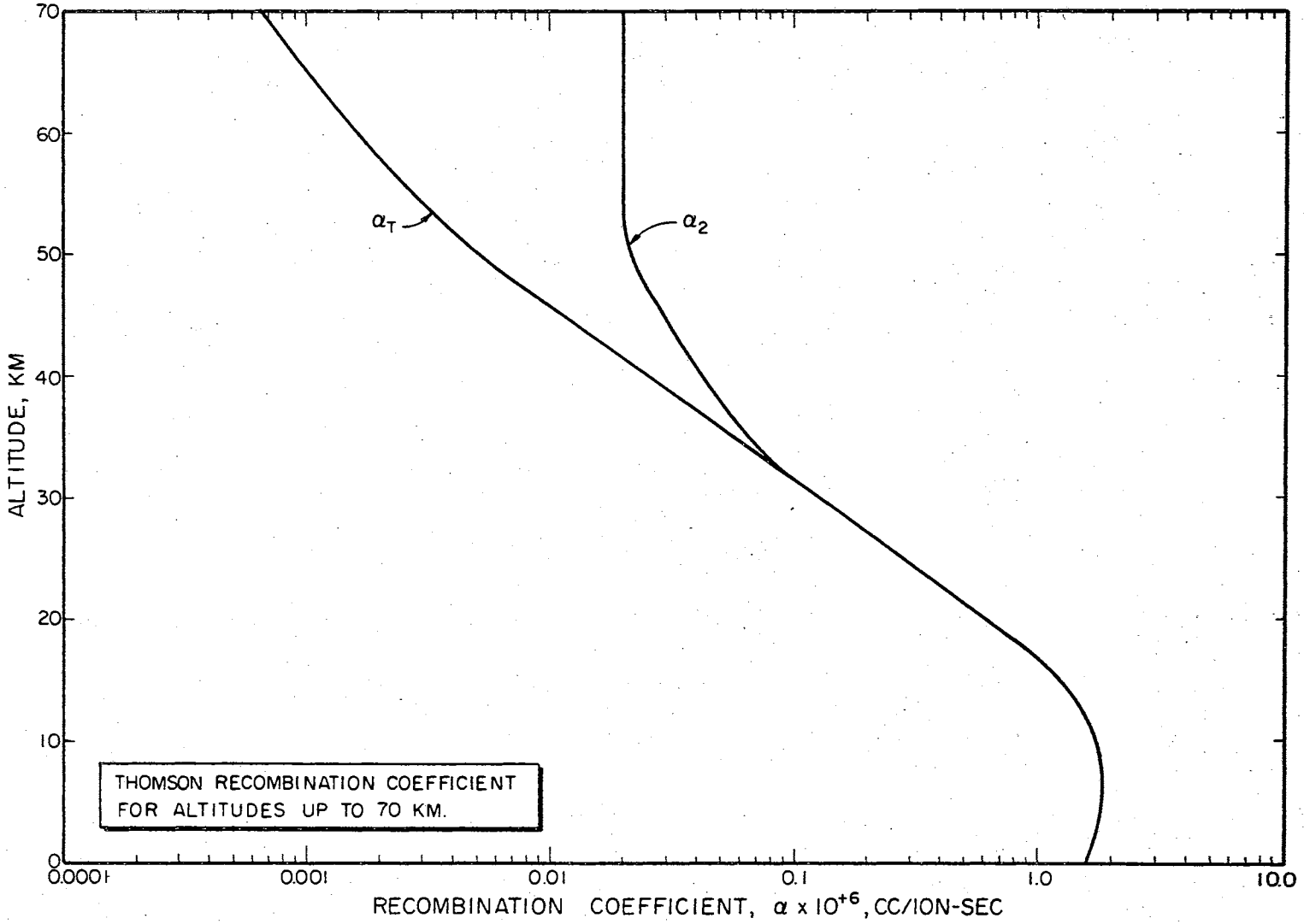

Figure 24. Small Ion Recombination Coefficients

More recent theoretical evidence from Cole and Pierce (1965) indicates that the Thomson three-body reaction is valid for altitudes below thirty-five km, but that a two-body reaction is possibly dominant at greater altitudes. The result of using this newer recombination data is also shown in Figure 24. Analytic expressions for this function are:

For $0 \leq Z < 15$,

$$\alpha_2 = 1.75 \times 10^{-6} \tag{4.8}$$

for $15 \leq Z < 34$,

$$\alpha_2 = 1.5 \times 10^{-6} \, e^{-0.16(Z - 15)} \tag{4.9}$$

for $34 \leq Z < 50$,

$$\alpha_2 = 6.7 \times 10^{-8} \, e^{-.073(Z - 34)} \tag{4.10}$$

and for $Z \geq 50$,

$$\alpha_2 = 2.0 \times 10^{-8} \tag{4.11}$$

4.5 Small Ion Generation Rate. Initial considerations of ion generation will be based on the assumption that electron mean lifetime is negligible. Under this assumption, positive and negative small ions are generated at exactly the same rate, i.e., in Equations 2.1 and 2.2,

$$g_- = g_+ .$$

The generation of ions will be assumed to follow the curve shown in Figure 20 of Chapter III. This curve can be analytically represented by the following functions:

for $0 \leq Z \leq 1.25$,

$$g = 10.0\, e^{-1.079Z} \tag{4.12}$$

for $1.25 < Z \leq 13$,

$$g = 1.94\, e^{0.233Z} \tag{4.13}$$

for $13 < Z \leq 15.7$,

$$g = 42.0 \tag{4.13}$$

for $15.7 < Z \leq 40$,

$$g = 42.0\, e^{-0.1543(Z - 15.7)} \tag{4.15}$$

and for $Z > 40$,

$$g = e^{-0.114(Z - 40)} \tag{4.16},$$

where Z is in km and g is in ions-cm^{-3}-sec^{-1}. The behavior of this function for altitudes less than 1.25 km is accounted for by the ionization due to radioactive substances in the earth and in the air, above this altitude, cosmic ray ionization becomes dominant. Equations 4.12 through 4.16 will be used as the generation model for small ions of either polarity.

4.6 Generation and Recombination in Regions Where Large Ion Content is Not Negligible. For altitudes above the exchange layer, the various coefficients, $\mu_{\pm}$, $d_{\pm}$, and the forcing functions, $g_{\pm} - r_{\pm}$, are now considered known, and analysis of the reduced model can proceed in this altitude regime. As stated earlier, initial emphasis will be placed on analysis of the model above the exchange layer. However, within the

exchange layer, the generation and recombination terms are of a different form. In this region,

$$G_- - R_- = \eta_{20} n_- N_0 - \eta_{12} n_+ N_- - \eta_{00} N_+ N_-$$

$$G_+ - R_+ = \eta_{10} n_+ N_0 - \eta_{12} n_- N_+ - r_{00} N_+ N_-$$

$$g_- - r_- = g - \alpha n_+ n_- - \eta_{21} n_- N_+ - \eta_{20} n_- N_0$$

$$g_+ - r_+ = g - \alpha n_+ n_- - \eta_{12} n_+ N_- - \eta_{10} n_+ N_0,$$

where N_0 denotes a neutral nucleii. Mean values of the combination coefficients at STP are given in Table VI where the entry dimensions are $cm^{+3}\text{-ion}^{-1}\text{-sec}^{-1}$.

TABLE VI

RECOMBINATION COEFFICIENTS

α	η_{10}	η_{20}	η_{12}	η_{21}	η_{00}
1.65×10^{-6}	0.6×10^{-6}	1.1×10^{-6}	2.4×10^{-6}	4.5×10^{-6}	0.001×10^{-6}

It is seen from the preceding set of equations that the model is greatly simplified if the concentrations N_0, N_+, and N_- can be neglected.

4.7 Form of Model Above Exchange Layer. The form of the model which obtains above the austauch region is thus reduced to the three equations:

$$\frac{\partial n_-}{\partial t} = \overline{\nabla} \cdot [d_- \overline{\nabla} n_- + \mu_- n_- \overline{E}] + g - \alpha n_+ n_- \qquad (4.17)$$

$$\frac{\partial n_+}{\partial t} = \overline{\nabla} \cdot [d_+ \overline{\nabla} n_+ - \mu_+ n_+ \overline{E}] + g - \alpha n_+ n_- \qquad (4.18)$$

$$\overline{\nabla} \cdot \varepsilon_0 \overline{E} = q(n_+ - n_-) \qquad (4.19).$$

This reduced model will be explored analytically by use of various mathematical techniques incorporating the foregoing experimentally based data and derivations.

CHAPTER V

SIGNIFICANCE OF UNCERTAINTIES IN MEASURED ELECTRICAL PROPERTIES

5.1 Introduction. The last consideration prior to analysis of the atmospheric model will be to examine uncertainties in measurements of electrical properties of the atmosphere and to note the effect these uncertainties will have on the analysis.

5.2 Atmospheric Electric Field. Figure 9 shows the results of electric field measurements by two different investigators. Both results shown are smoothed curves fit to the measured data, and indicate that the derivative of the electric field is always positive, i.e.,

$$\frac{dE}{dZ} > 0$$

for all Z. From the Poisson equation, Equation 4.19, this implies that

$$n_+ > n_- \tag{5.1}$$

for all Z. However, an examination of Figure 25, also reported by Hatakeyama (1965) shows that Equation 5.1 is not necessarily true for all altitudes. In fact, Figure 26 shows the results of numerically differentiating the curve in Figure 25, and then using Equation 4.19 to solve for the difference in small ion concentrations. Thus,

$$n_+ - n_- = \frac{\varepsilon_0}{q} \frac{dE}{dZ},$$

where dE/dZ is obtained as indicated. Figure 26 then gives an

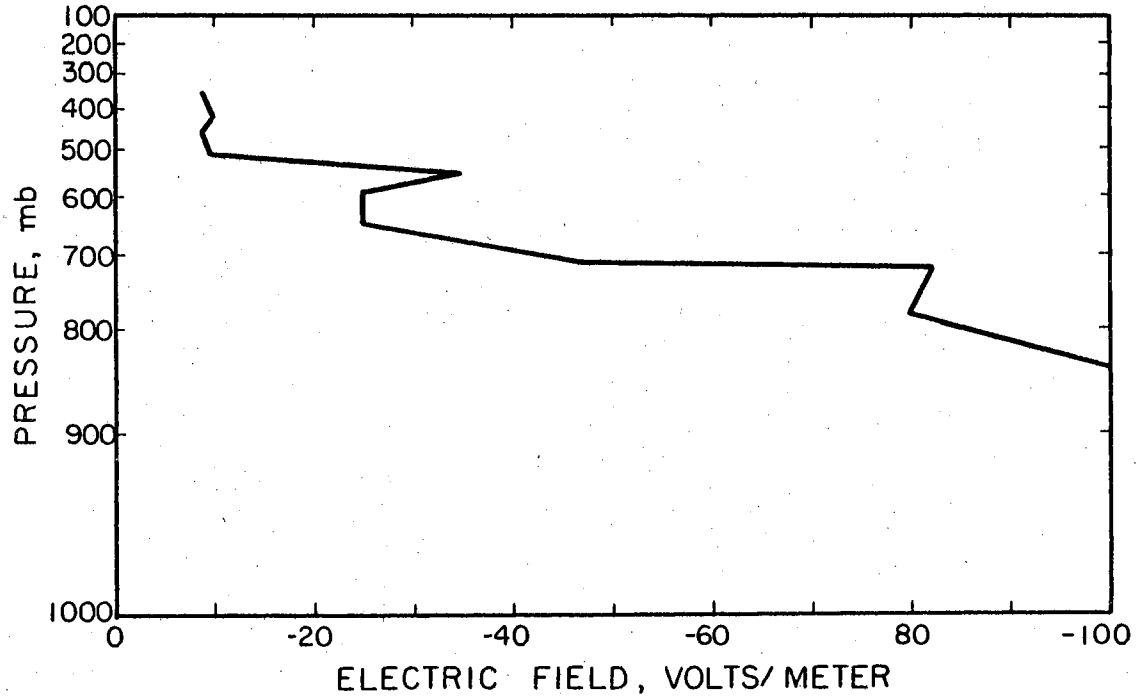

Figure 25. Atmospheric Electric Field

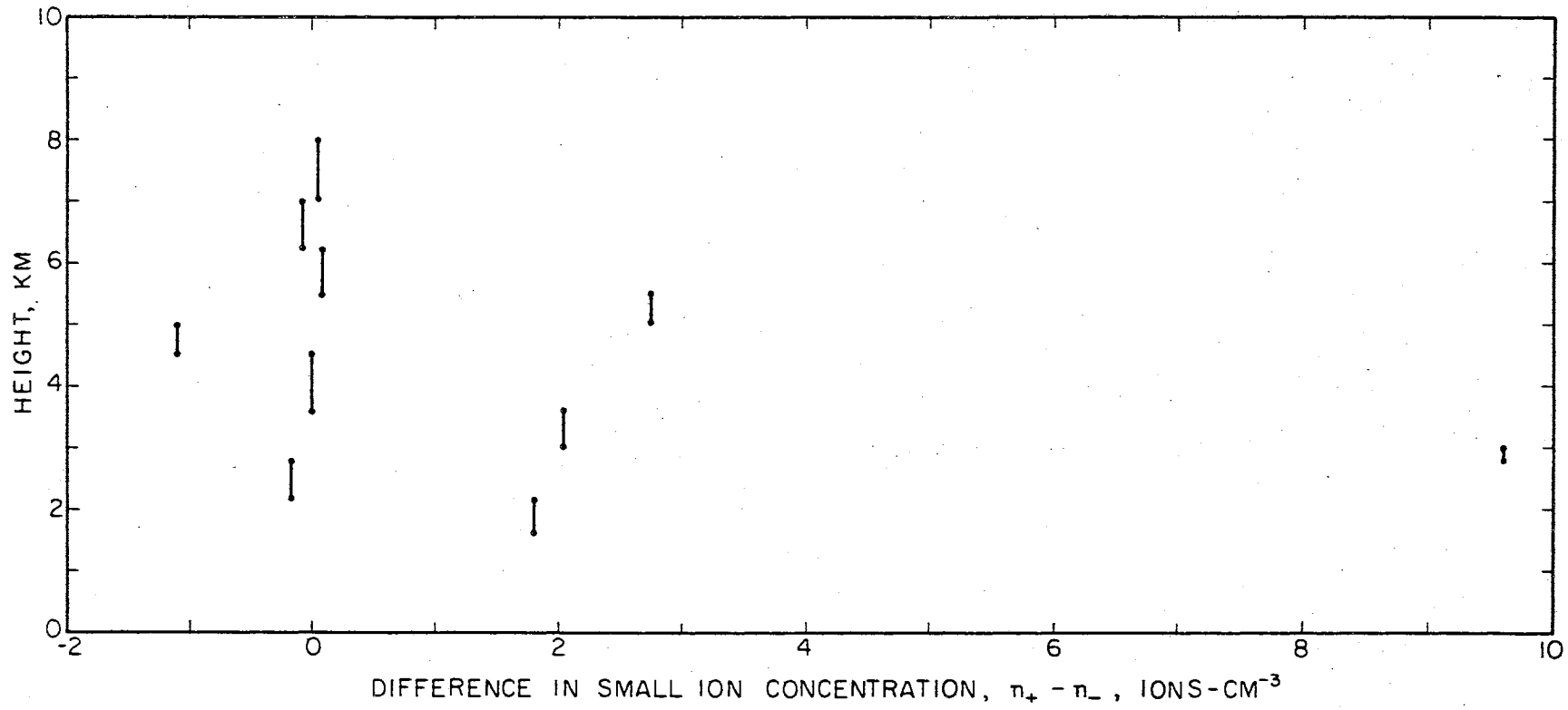

Figure 26. Difference in Small Ion Concentrations

approximate indication of $n_+ - n_-$ which will be used to compare with small ion density measurements in Section 5.4.

A possible answer to this reversal in the sign of the electric field derivative might be that if Aitken nucleii or condensation particles were present at the altitudes of these sign reversals, then according to the data in Table VI, the positive small ions could combine with the nucleii at a higher rate than the negative small ions, and a condition reached at which

$$n_- > n_+.$$

Other investigators, for example Koenigsfeld (1953), report on balloonsonde electric field measurements, and find that at an altitude within the troposphere, the electric field reduces to approximately -10 v/m and remains constant for all higher altitudes. The results of Koenigsfeld are shown in Figure 27.

This data would indicate that above approximately ten kilometers, the small ion densities were equal. Figure 9 data indicates that under average conditions, n_+ is slightly greater than n_-, but their difference becomes smaller as altitude increases. In fact, an examination of Equations 3.2 through 3.7 implies the small ion difference decreases exponentially with altitude.

With regard to the atmospheric electric field, typical measurements conclude that the field behaves approximately as shown in Figure 9, that is, decreases nearly exponentially with altitude to some small limiting value, and from this can be deduced that the difference of ions is small, and also decreases with altitude.

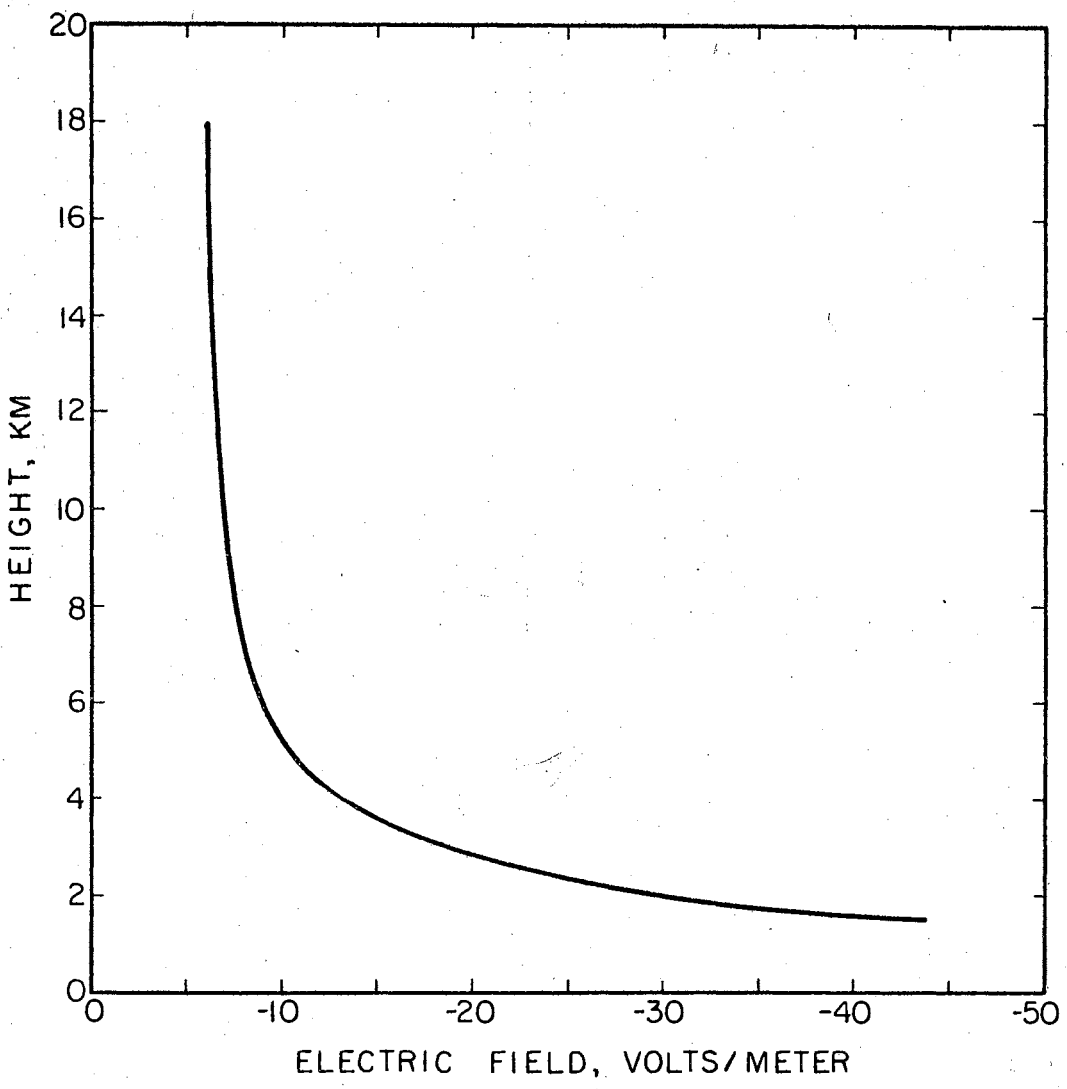

Figure 27. Atmospheric Electric Field

5.3 Conductivity, Polar Conductivity Ratio, and Ionic Mobilities.

Atmospheric polar conductivities or the ratio of the polar conductivities has received nearly as much consideration as the electric field in the number of measurements made. However, with the exception of a few measurements, e.g. Woessner et al. (1958), investigators have been content with measuring either σ_+ or σ_-, or if both were measured, measurements were made at different times and not simultaneously. Nevertheless, there is general agreement that the conductivity increases with altitude in an exponential manner and is due to the presence of small ions. The measurements of Gish and Sherman (1936), however, showed a decrease in conductivity at higher altitudes not detected by most investigators.

Where some disagreement arises is in measurements of the polar conductivity ratio,

$$\frac{\sigma_-}{\sigma_+} = \frac{\mu_- n_-}{\mu_+ n_+}. \tag{5.2}$$

Sagalyn (1958), Kraakevik (1955) and Curtis and Hyland (1958) all report an average ratio of approximately 1.05 $\pm$ 0.1 on the basis of measurements made from aircraft. Woessner, et al. (1958) obtains a ratio of near unity above the exchange layer. Now Phillips (1955), has shown in the laboratory that as air pollution is decreased, the conductivity ratio approaches the mobility ratio, which laboratory measurements indicate is approximately 1.3 to 1.4. Woessner et al. (1958) conclude that pollution is small above the exchange layer because σ_-/σ_+ approaches unity, but they also agree with the above mobility ratio. Their conclusion seems to be in contradiction with laboratory measurements of σ_-/σ_+ and μ_-/μ_+. Sagalyn (1958) concludes that since the small ions of

either polarity are generated and recombine at nearly the same rate, then

$$\frac{n_-}{n_+} \approx 1,$$

so that the mobility ratio must also be near unity. There is apparently a difference in laboratory and field measurements. A possible reason for the difference could well be the effect of humidity on small ion mobility. Limited investigations in this regard do show a reduction of the mobility ratio as humidity is increased. However, direct measurements of small ion mobility as a function of altitude have not been carried out to the extent that laboratory measurements can be contradicted. Such measurements certainly need to be made in order to determine any correlation (or further lack of correlation) with laboratory results. In this light, the model analysis will assume that laboratory measurements of the mobility ratio are the most reliable, and that the mobility ratio μ_-/μ_+ may have an average constant value, the value depending on pollution content.

5.4 Small Ion Concentration Measurements. Small ion concentration measurements are the least extensive of any of the fair weather atmospheric electricity quantities. Figure 13 shows the results of two of these measurements. The data of Paltridge (1965) gave the result that over the entire altitude regime measured

$$\frac{n_+}{n_-} = 1.43 \pm 0.14.$$

Looking at this result in conjunction with electric field measurements

and Poisson's equation,

$$\frac{dE}{dZ} = \frac{q}{\varepsilon_0}(n_+ - n_-) \approx \frac{q}{\varepsilon_0}(0.43)\, n_-,$$

or

$$n_- = \frac{\varepsilon_0}{0.43q}\frac{dE}{dZ}.$$

Now Hatakeyama's electric field data gives that within the troposphere,

$$\frac{dE}{dZ} = +130(3 \times 10^{-4})\, e^{-(3 \times 10^{-4})Z},$$

where Z is in meters, and dE/dZ in volts $-m^{-2}$. Then

$$n_- = \frac{8.854 \times 10^{-12}}{(0.43)(1.602 \times 10^{-19})}(-130)(-3 \times 10^{-4})\, e^{-(3 \times 10^{-4})Z},$$

$$= (5 \times 10^{5})\, e^{-3 \times 10^{-4}Z} \quad \text{ions/m}^3$$

$$= 0.5\, e^{-3 \times 10^{-4}Z} \quad \text{ions/cc.}$$

This figure is at least three orders of magnitude less than measurements of ionic concentration indicate. Admittedly, Hatakeyama's and Paltridge's measurements were made at different times and at different geographic locations, but this great discrepancy is not to be expected. Since electric field is more easily measured and has received more extensive investigation, the most acceptable conclusion seems to be that the small ion densities are nearly equal, i.e.,

$$n_+ \tilde{\sim} n_-.$$

It can also be noted from Figure 13 that the small ion density decreases at higher altitudes. This condition was not detected in the conductivity measurements of most investigators. As pointed out earlier, the conductivity increases exponentially at a rate at least as great as the rate of mobility increase. This suggests that the ion concentrations also continued to increase. One theory put forth to explain the noted decrease in small ion density is the possibility of "bunches" of pollution at higher altitudes. However, no satisfactory explanation of how these pollutants arrived at such high altitudes has been made. Also suspect is the operation of the measuring apparatus itself at extreme altitudes.

5.5 Conclusions. The discussion in this chapter has pointed out discrepancies in measurements of atmospheric electricity variables. One point all investigators agree on is that improvements in instrumentation and measuring techniques are required. This point seems to be extremely well taken.

Analysis of the atmospheric model will proceed using the conclusions that seem to be most concrete. These include a mobility ratio of 1.3 to 1.4, nearly equal ion densities, a monotonically decreasing electric field, monotonically increasing conductivities, and a nearly constant conductivity ratio in "clean" air.

CHAPTER VI

STEADY STATE AND ONE DIMENSIONAL ANALYSIS OF THE ATMOSPHERIC MODEL

6.1 Introduction. Equations 4.17, 4.18 and 4.19 form the atmospheric model for regions where the large ion content is negligible. This chapter will describe the analysis of this three equation model.

6.2 Steady State and One-Dimensional Form of the Atmospheric Model. Sagalyn and Faucher (1954), and Gish and Wait (1950) have made measurements of the horizontal variation of electrical properties of the atmosphere. Both investigators report that variations of these properties in the horizontal direction were small, at most ten per cent of the mean value measured at constant altitude. Assuming this to be the case, the model is considerably simpler in that spatial derivatives in only the vertical direction require consideration. For if v denotes any atmospheric electrical quantity, then the gradient of v is given by

$$\bar{\nabla} v = \frac{\partial v}{\partial x} \bar{i} + \frac{\partial v}{\partial y} \bar{j} + \frac{\partial v}{\partial Z} \bar{k} \quad .$$

Since horizontal variations are assumed to be much smaller than vertical variations,

$$\bar{\nabla} v \approx \frac{\partial v}{\partial Z} \bar{k} \quad .$$

Incorporating this result into the model gives

$$\frac{\partial n_-}{\partial t} = \frac{\partial}{\partial Z} \left[d_- \frac{\partial n_-}{\partial Z} + \mu_- n_- E \right] + g - \alpha n_+ n_- = 0$$

$$\frac{\partial n_+}{\partial t} = \frac{\partial}{\partial Z}\left[d \frac{\partial n_+}{+\partial Z} - \mu_+ n_+ E\right] + g - \alpha n_+ n_- = 0$$

and

$$\frac{\partial E}{\partial Z} = \frac{q}{\varepsilon_0}(n_+ - n_-) \quad .$$

One further known property of the atmosphere will be considered - that steady state or at least "quasi-static" equilibrium obtains. This assumption is valid if time variations of temperature, pressure, and cosmic ray intensity are small. Cosmic ray intensity is known to maintain a nearly constant value during a given period of the solar cycle, while the time derivatives of temperature and pressure are also small in areas of fair weather. Assuming this to also be the case, the model simplifies to,

$$\frac{d}{dZ}\left[d_-(Z) \frac{dn_-(Z)}{dZ} + \mu_-(Z) n_-(Z) E(Z)\right] + g(Z) - \alpha(Z) n_+(Z) n_-(Z) = 0 \qquad (6.1)$$

$$\frac{d}{dZ}\left[d_+(Z) \frac{dn_+(Z)}{dZ} - \mu_+(Z) n_+(Z) E(Z)\right] + g(Z) - \alpha(Z) n_+(Z) n_-(Z) = 0 \qquad (6.2)$$

$$\frac{dE}{dZ} = \frac{q}{\varepsilon_0}[n_+(Z) - n_-(Z)] \quad , \qquad (6.3)$$

which consists of three ordinary, second order, simultaneous, nonlinear differential equations with variable coefficients. This is the model which will be analyzed with as much rigor as possible.

The assumptions which have been made in the model transition from Equations 2.1 through 2.5 to Equations 6.1, 6.2 and 6.3 are: 1) large ion content is negligible, 2) horizontal variations of electrical quantities are much smaller than vertical variations, and 3) steady state conditions obtain.

6.3 Attempts at Numerical Integration. The three preceding equations can be put into a form more amenable to numerical study. Performing the differentiation indicated in Equations 6.1 and 6.2, where a prime indicates differentiation with respect to Z,

$$d_-n_-'' + (d_-' + \mu_-E)n_-' + (\mu_-E' + E\mu_-')n_- + g - \alpha n_+n_- = 0$$

$$d_+n_+'' + (d_+' - \mu_+E)n_+' - (\mu_+E' + E\mu_+')n_+ + g - \alpha n_+n_- = 0 \quad .$$

Substituting Equation 6.3 into these two equations gives

$$d_-n_-'' + (d_-' + \mu_-E)n_-' + [\frac{\mu_-q}{\varepsilon_0}(n_+ - n) + E\mu_-']n_- + g - \alpha n_+n_- = 0$$

$$d_+n_+'' + (d_+' - \mu_+E)n_+' - [\frac{\mu_+q}{\varepsilon_0}(n_+ - n_-) + E\mu_+']n_+ + g - \alpha n_+n_- = 0 \quad .$$

Making the substitutions

$$x = n_-'$$

$$y = n_+' \quad ,$$

and solving for x' and y' results in the set of five, first order differential equations

$$x' = n_-'' = \frac{[\frac{q}{\varepsilon_0}(n_- - n_+)\mu_- - \mu_-'E]n_- - [d_-' + \mu_-E]x - [g - \alpha n_+n_-]}{d_-}$$

$$y' = n_+'' = \frac{[\frac{q}{\varepsilon_0}(n_+ - n_-)\mu_+ + \mu_+'E]n_+ - [d_+' - \mu_+E]y - [g - \alpha n_+n_-]}{d_+}$$

$$n' = x$$

$$n_+' = y$$

$$E' = \frac{q}{\varepsilon_0}(n_+ - n_-) \quad .$$

These five equations are in a form suitable for numerical integration techniques. Both Runge-Kutta and predictor-corrector methods were tried for integration of this set of equations. However, because of the repeated subtraction of nearly equal numbers which occurs in these equations, extremely small integration step sizes were required in order to maintain truncation and round-off errors at a small value, with the result that the amount of computer time on the Oklahoma State University IBM 7040 which would be necessary to integrate the three equation model was impractical. Consequently, attempts at a complete numerical solution were abandoned in favor of analytic and limited numerical methods.

6.4 Pre-Solution Conclusions From the Atmospheric Model. Several conclusions regarding behavior of atmospheric electrical quantities can be inferred from the model prior to its solution. For convenience, these conclusions will be presented as a set of theorems and corollaries. For proof of these theorems, the model, Equations 6.1 through 6.3, will be rewritten as,

$$\frac{d}{dZ}[d_- n_-'] + \frac{d}{dZ}[\mu_- n_- E] + g - \alpha n_+ n_- = 0 \qquad (6.4)$$

$$\frac{d}{dZ}[d_+ n_+'] - \frac{d}{dZ}[\mu_+ n_+ E] + g - \alpha n_+ n_- = 0 \qquad (6.5)$$

$$\frac{dE}{dZ} = \frac{q}{\varepsilon_0}(n_+ - n_-) \quad . \qquad (6.6)$$

Theorem 1: Hypothesis -- Diffusion current density independent of altitude implies conduction current density is also independent of altitude.

Proof -- From the hypothesis,

$$\frac{d}{dZ}[j_d] = \frac{d}{dZ}[q(d_- n_-' - d_+ n_+')] = 0 \quad ,$$

or

$$\frac{d}{dZ}[d_- n_-'] = \frac{d}{dZ}[d_+ n_+'] \quad .$$

Now subtracting Equation 6.5 from 6.4, and using the preceding result gives

$$\frac{d}{dZ}[(\mu_- n_- + \mu_+ n_+)E] = 0 \quad ,$$

or

$$\frac{d}{dZ}[q(\mu_- n_- + \mu_+ n_+)E] = \frac{d}{dZ}[j_c] = 0 \quad ,$$

and the theorem is proved.

Corollary 1.1: Hypothesis -- Polar diffusion fluxes independent of altitude implies conduction current density is independent of altitude.

Proof -- From the hypothesis

$$\frac{d}{dZ}[d_- n_-'] = \frac{d}{dZ}[d_+ n_+'] = 0 \quad ,$$

and the result follows from Theorem 1.

Theorem 2: Hypothesis -- Conduction current density independent of altitutde implies that the diffusion current density is independent of altitude.

Proof -- From the hypothesis,

$$\frac{d}{dZ}[j_c] = \frac{d}{dZ}[q(\mu_+ n_+ + \mu_- n_-)E] = 0 \quad ,$$

or

$$\frac{d}{dZ}(\mu_- n_- E) = -\frac{d}{dZ}(\mu_+ n_+ E) \quad .$$

Subtracting Equation 6.5 from 6.4, and incorporating this result gives

$$\frac{d}{dZ}[d_- n_-' - d_+ n_+'] = \frac{d}{dZ}\left[\frac{j_d}{q}\right] = 0 \quad ,$$

and the theorem is proved.

Corollary 2.1: Hypothesis -- Polar conduction fluxes independent of altitude implies that the diffusion current density is independent of altitude.

Proof -- From the hypothesis,

$$\frac{d}{dZ}(\mu_- n_- E) = \frac{d}{dZ}(-\mu_+ n_+ E) = 0 \quad ,$$

and the result then follows from Theorem 2.

Theorem 3: Hypothesis -- Altitude independent conduction current density, and a constant positive polar conductivity ratio implies the polar conduction fluxes are independent of altitude, and hence the diffusion current density is independent of altitude.

Proof -- From the hypothesis,

$$\frac{d}{dZ}[q(\mu_- n_- + \mu_+ n_+ E) = 0 \quad ,$$

or

$$\frac{d}{dZ}(\mu_- n_- E) = -\frac{d}{dZ}(\mu_+ n_+ E) \quad .$$

Also from the hypothesis,

$$\mu_- n_- = C\,\mu_+ n_+ \quad , \qquad C > 0 \quad .$$

Then

$$\frac{d}{dZ}(\mu_- n_- E) = -C\frac{d}{dZ}(\mu_- n_- E) \quad .$$

Suppose

$$\frac{d}{dZ}(\mu_- n_- E) \neq 0 \quad ,$$

then

$$C = -1 \quad ,$$

which is a contradiction. Thus

$$\frac{d}{dZ}(\mu_- n_- E) = C \frac{d}{dZ}(\mu_+ n_+ E) = 0 \quad , \qquad C > 0 \quad ,$$

and the first statement is proved. The second assertion follows from Corollary 2.1.

Theorem 4: Hypothesis -- Either conduction current density or diffusion current density being independent of altitude implies the total current density is independent of altitude.

Proof -- The proof follows by combining Theorems 1 and 2, for if either of the current densities is altitude invariant, so is the other, and hence their sum, the total current density, is altitude invariant. These theorems and corollaries will be used in the following analysis.

6.5 Altitude Independent Conduction Current Density Solution to the Atmospheric Model. As discussed in Section 3.5(c), measurements indicate that a constant vertical conduction current density flows above the exchange layer in fair weather areas. Then from Theorem 2, a constant diffusion current density must also obtain in this region. If this latter current is denoted as J_{D_0}, then from the definition of diffusion current density,

$$q\left(d_- \frac{dn_-}{dZ} - d_+ \frac{dn_+}{dZ}\right) = J_{D_0} \quad . \tag{6.7}$$

Using results given in Chapters IV and V, namely that

$$d_- = 1.357 d_+ \quad ,$$

and

$$n_+ \approx n_- = n \quad ,$$

Equation 6.7 becomes

$$0.357 d_+ q \frac{dn}{dZ} = J_{D_0} \quad , \tag{6.8}$$

or

$$\frac{dn}{dZ} = \frac{J_{D_0}}{0.375 q d_+} \quad . \tag{6.9}$$

Integrating Equation 6.9 from Z_0 to Z, where p is a variable of integration,

$$\int_{Z_0}^{Z} \frac{dn}{dp}\, dp = \frac{J_{D_0}}{0.357q} \int_{Z_0}^{Z} \frac{dp}{d_+(p)} \quad ,$$

yields

$$n(Z) = n_0 + \frac{J_{D_0}}{0.357q} \int_{Z_0}^{Z} \frac{dp}{d_+(p)} \quad . \tag{6.10}$$

Analytic expressions for the positive small ion diffusivity are given in Equations 4.5a, 4.6a and 4.7a. Using these expressions, Equation 6.10 can be integrated analytically. The IBM 7040 was used to evaluate the resulting expressions for n(Z). The results for two different sets of initial conditions are shown in Figure 28.

Initial conditions necessary for this solution are the initial small ion concentration and the initial derivative of the small ion concentration. The diffusion current density was determined using this initial derivative and diffusivity in Equation 6.8. One set of initial conditions was determined from Kroening's data in Figure 13, and the second set obtained from a theoretical curve of n, derived by assuming the generation rates and recombination rates are equal. In this latter case,

$$n = \left[\frac{g}{\alpha}\right]^{\frac{1}{2}} \quad ,$$

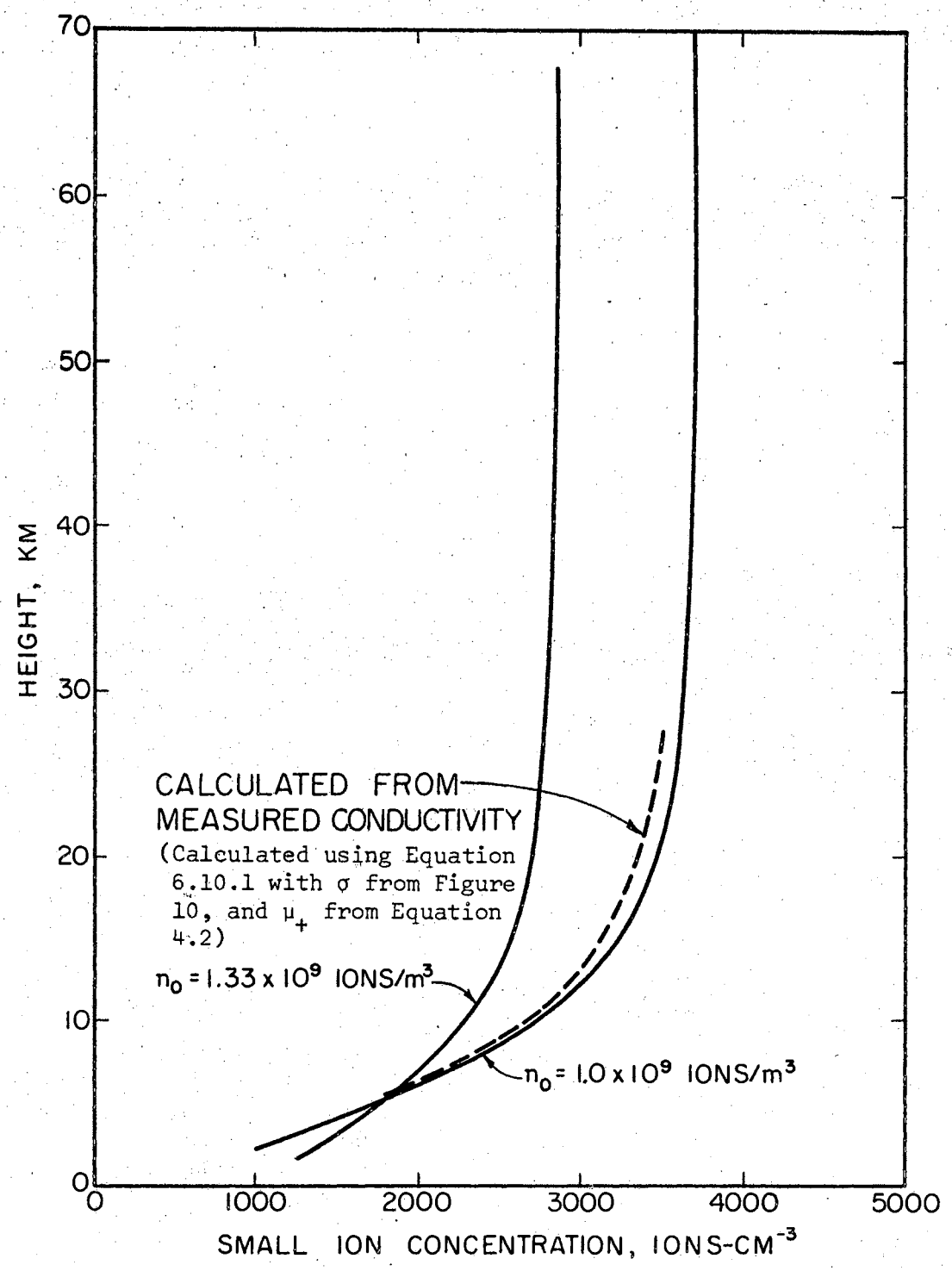

Figure 28. Theoretical Small Ion Concentrations

which is shown in Figure 29 for comparison purposes. Both α_T and α_2 were used in the calculation. The first set of initial conditions used was,

$$(n)_0 = 1.0 \times 10^9 \text{ ions} - m^{-3}$$

$$(\frac{dn}{dZ})_0 = 3.0 \times 10^5 \text{ ions} - m^{-4} \quad ,$$

and the second set was

$$(n)_0 = 1.33 \times 10^9 \text{ ions} - m^{-3}$$

$$(\frac{dn}{dZ})_0 = 1.7 \times 10^5 \text{ ions} - m^{-4} \quad ,$$

where the initial altitude is taken as the top of the exchange layer, which is assumed to have an average value of two kilometers.

Electrical conductivity of the fair weather atmosphere was calculated using the resulting ionic concentration distribution and the ionic mobilities described by Equations 4.2 and 4.3. Thus the expression for conductivity,

$$\sigma = q(\mu_+ + \mu_-)n = 2.357q\mu_+ n \qquad (6.10.1)$$

was evaluated, and the results for both sets of initial conditions shown in Figure 30.

The atmospheric electric field distribution was then calculated using these conductivity values and the constant conduction current density J_{c_0}, that is

$$E(Z) = \frac{J_{c_0}}{\sigma(Z)} \quad , \qquad (6.11)$$

where

$$J_{c_0} = \sigma_0 E_0 \quad .$$

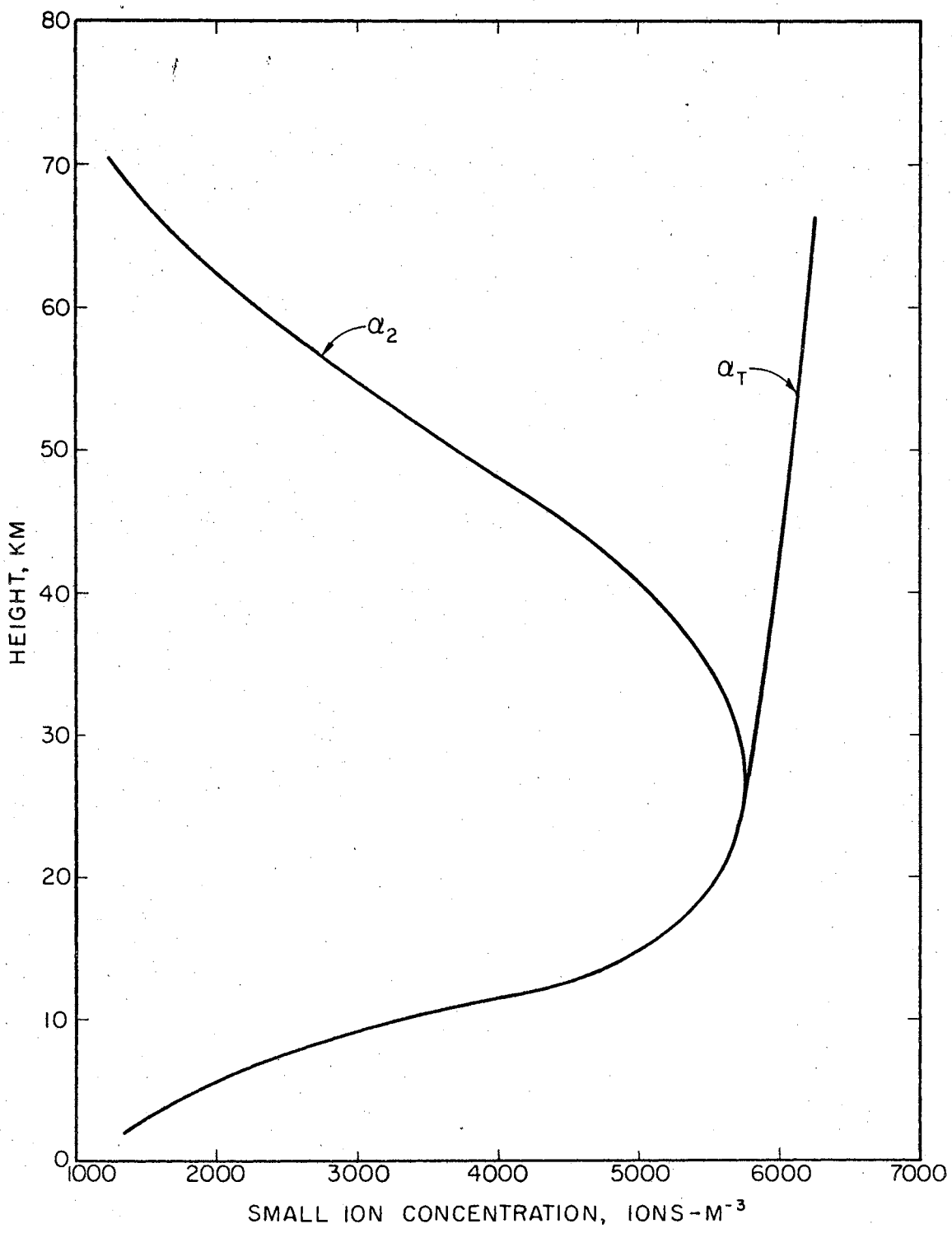

Figure 29. Theoretical Small Ion Concentrations

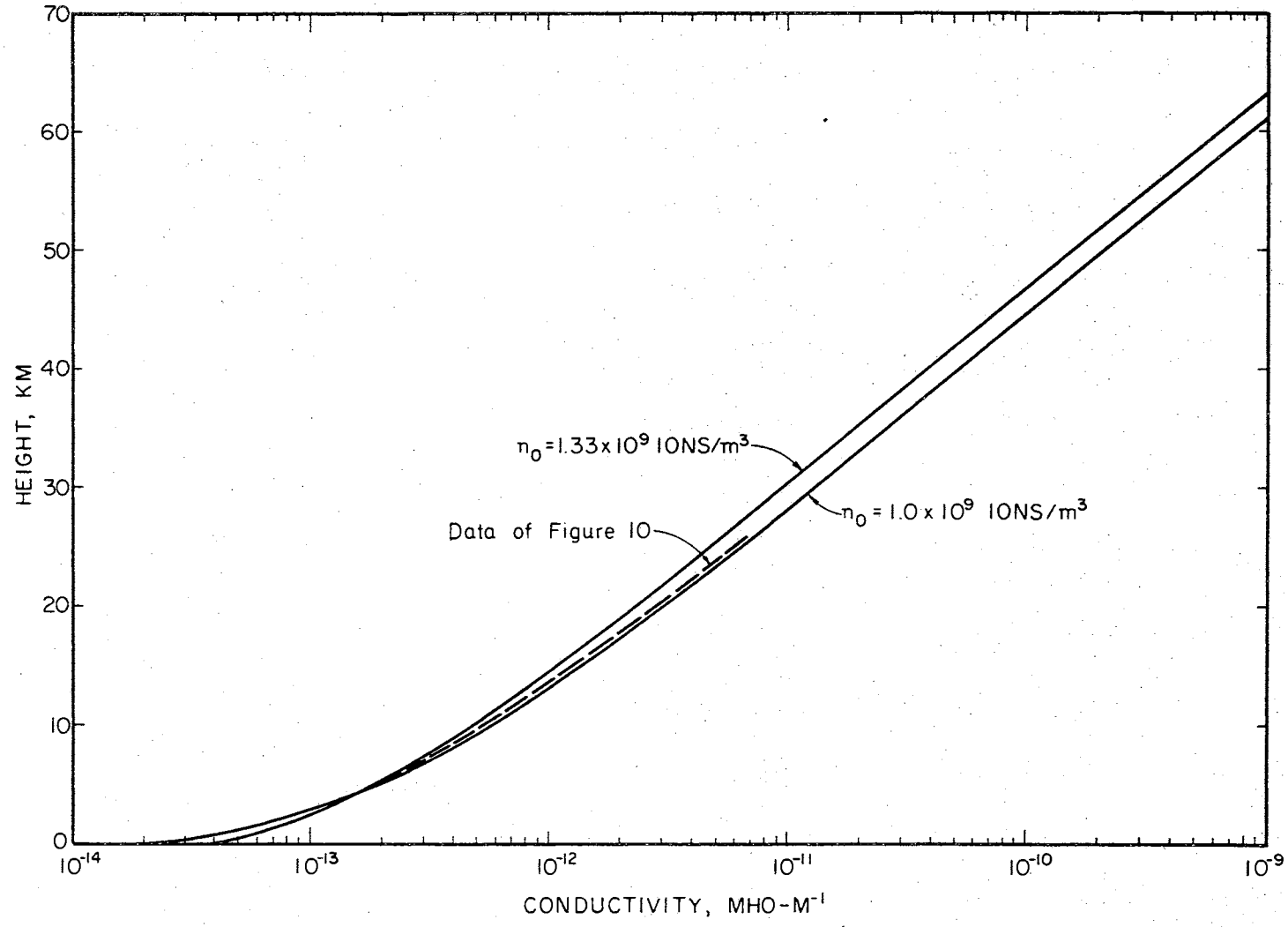

Figure 30. Theoretical Conductivity

Now σ_0 can be calculated from the initial ionic concentration and the initial mobilities. As for the initial electric field, two different values were used in obtaining solutions. Stergis' data shown in Figure 9 indicates that at two kilometers, the electric field is -70 volts/meter, and Von Schweidler's analytic expression given in Chapter III gives that at this same altitude, the electric field is -25 volts/meter. The results of electric field calculations using these initial conditions and both conductivity expressions in Equation 6.11 are shown in Figures 31 and 32. A comparison of the data in Figures 31 and 32 with data in Figure 9 shows a very close agreement.

Space charge density, ρ, can be found using the preceding results. For

$$E = \frac{J_{c_0}}{q(\mu_+ + \mu_-)n} = \frac{J_{c_0}}{2.357qn\mu_+}$$

then

$$\frac{dE}{dZ} = \frac{-2.357\, J_{c_0}\, q[\mu_+ \frac{dn}{dZ} + \frac{ndu_+}{dZ}]}{[2.357q\mu_+ n]^2} \quad . \qquad (6.12)$$

From Equation 4.2 it can be seen that

$$\frac{d\mu_+}{dZ} = 1.4 \times 10^{-4}\, \mu_+ \qquad \text{(Z in meters)},$$

and from Equation 6.9,

$$\frac{dn}{dZ} = \frac{J_{D_0}}{0.357qd_+} \quad .$$

Using these results in Equation 6.12,

$$\frac{dE}{dZ} = \frac{-J_{c_0}\left[\frac{J_{D_0}}{0.357qd_+} + 1.4 \times 10^{-4} n\right]}{2.357q\mu_+ n^2} \quad .$$

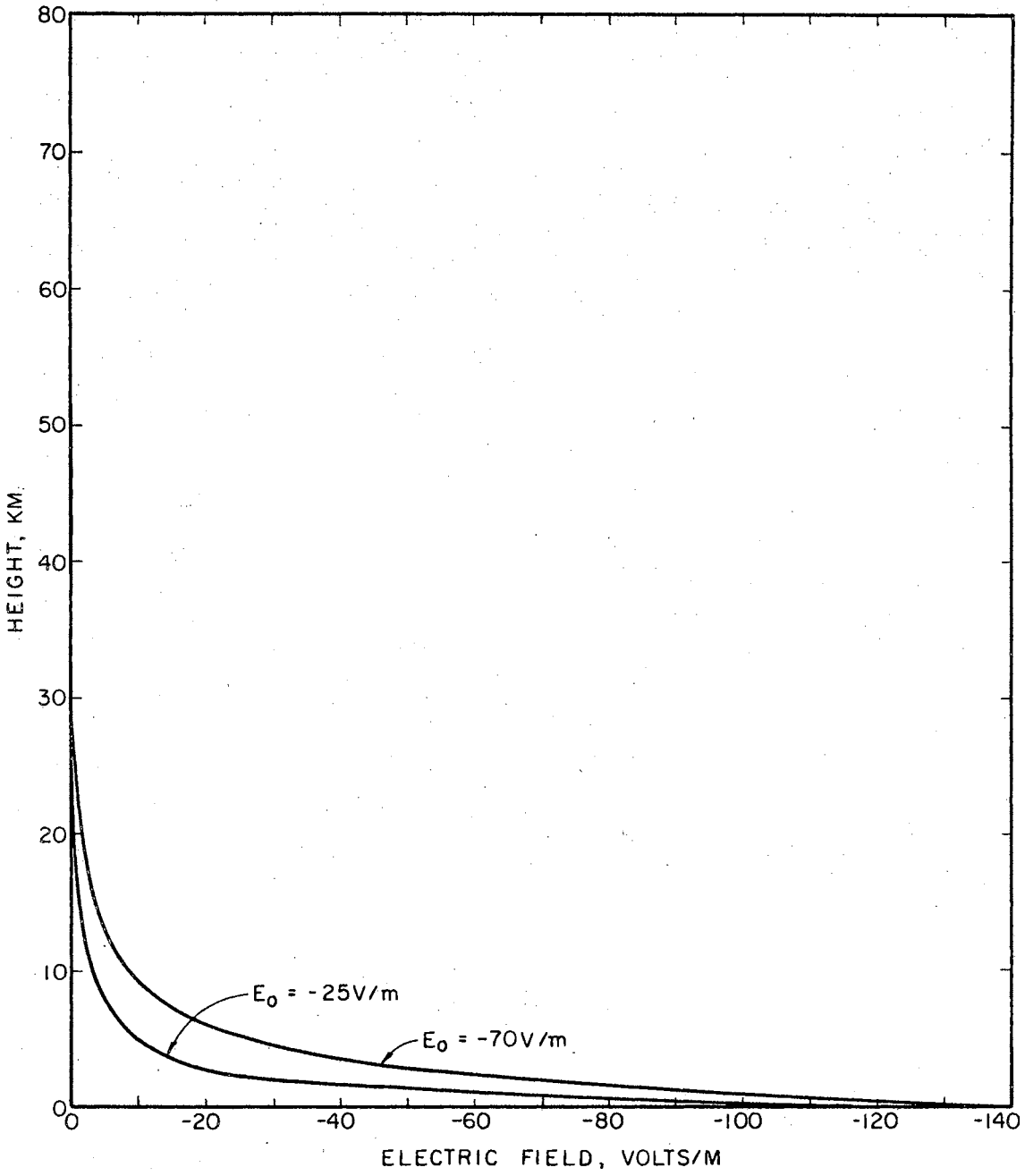

Figure 31. Theoretical Electric Field

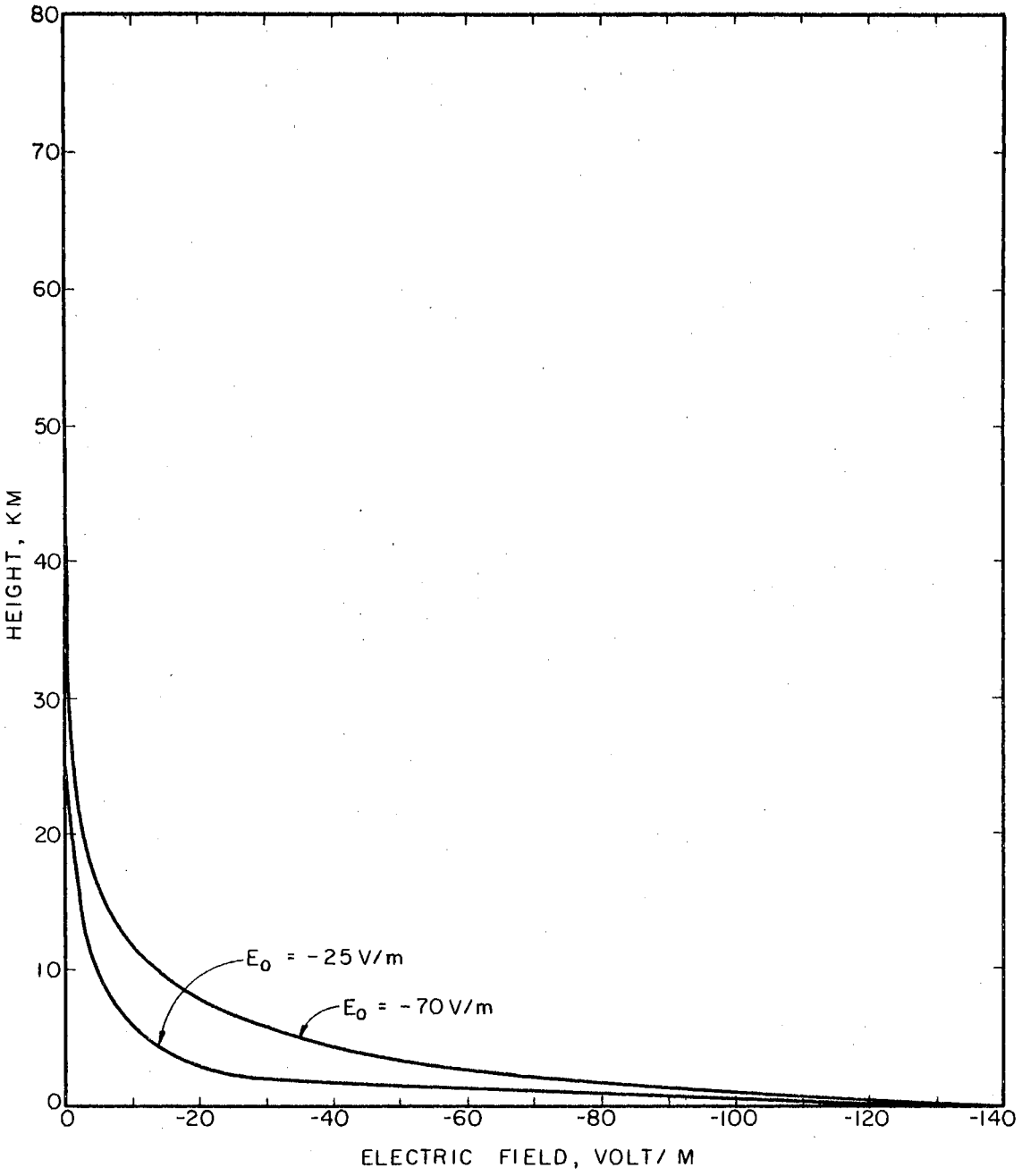

Figure 32. Theoretical Electric Field

Then

$$\rho = \varepsilon_0 \frac{dE}{dZ} = \frac{-\varepsilon_0 J_{c_0} \left[\frac{J_{D_0}}{0.357 q d_+} + 1.4 \times 10^{-4} n\right]}{2.357 q \mu_+ n^2} \quad . \tag{6.13}$$

Equation 6.13 was evaluated using the previously determined initial conditions and ionic concentrations. The results are shown in Figure 33, where it can be seen that the space charge density decreases with altitude as was predicted in Chapter V.

Calculation of ρ in the above manner avoids the possibility of errors which would be introduced using Poisson's equation where two large, nearly equal numbers would have to be subtracted, i.e., where

$$\rho = \varepsilon_0 \frac{dE}{dZ} = q(n_+ - n_-) \quad . \tag{6.14}$$

Thus the electric field data shown in Figure 31 and 32 could have been numerically differentiated and the negative small ion density found from the expression

$$n_- = n_+ - \frac{\varepsilon_0}{q} \frac{dE}{dZ} \quad , \tag{6.15}$$

and then ρ calculated according to Equation 6.14. But as stated, Equation 6.15 would introduce errors because of the subtraction of two nearly equal numbers.

The potential difference between the earth and the upper atmosphere, ϕ_{E-A}, was determined by numerically integrating the electric field distributions of Figures 31 and 32. The earth was taken as being at zero potential, so that

$$\phi_{E-A} = -\int_{Z_0}^{Z} E(p)dp \quad .$$

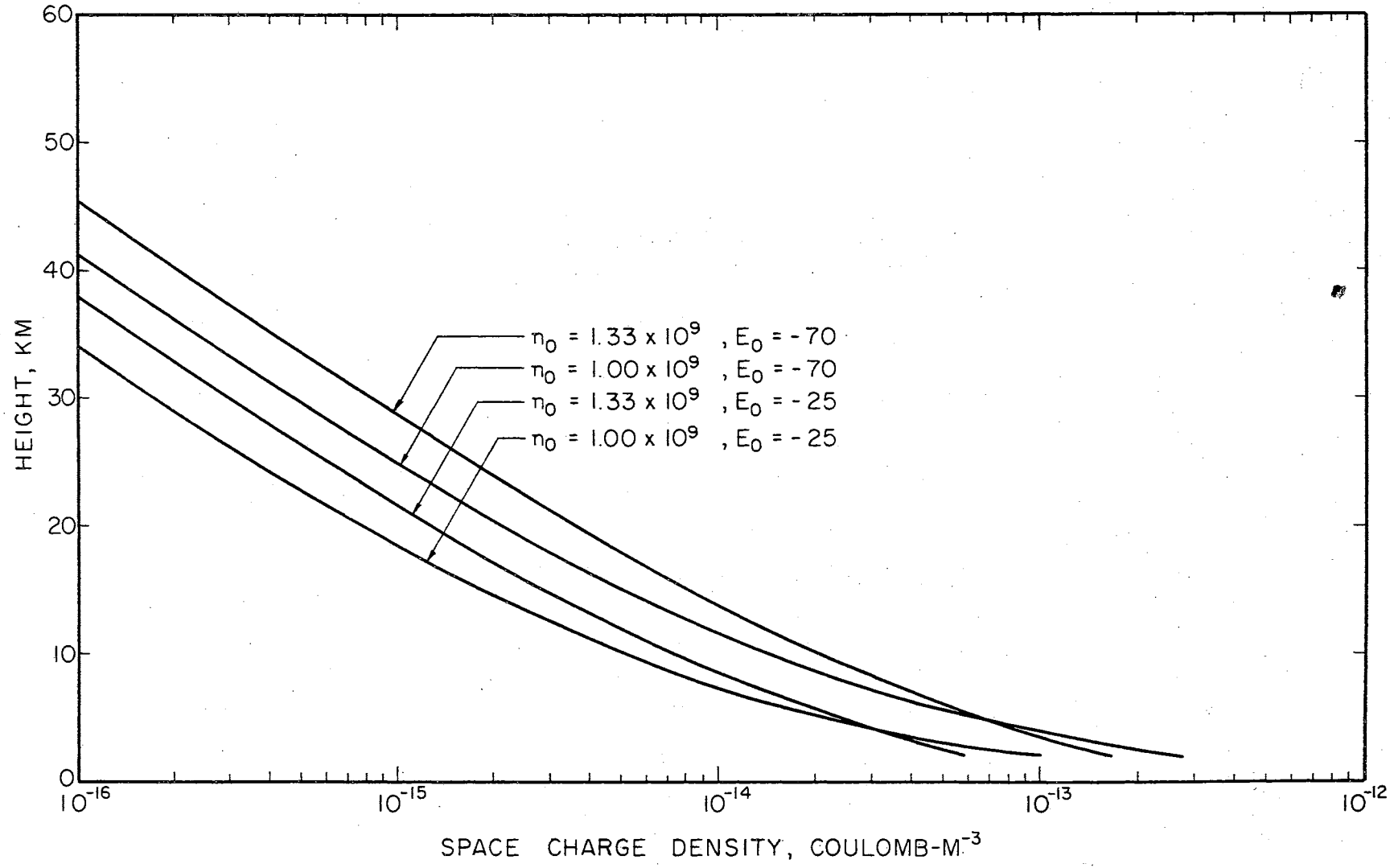

Figure 33. Theoretical Space Charge Density

Figure 34 shows the resulting potential curves for two different sets of initial conditions used in this analysis. The potential has reached a limiting value at around fifteen kilometers and remains at this value for all greater altitudes. The values obtained for ϕ_{E-A} are seen to be in close agreement with estimates based on electric field measurements.

To summarize the above analysis, measurements indicate that above the exchange layer, there exists a constant conduction current - at least up to the highest altitudes measured. It has been assumed that this situation obtains throughout the atmosphere. Then according to the atmospheric model, there will also be a constant diffusion current. Using this fact and the analytic expression for ionic mobilities and diffusivities, small ion concentration, and conductivity were determined. From Ohm's law and the existence of a constant conduction current, the electric field expression, and the potential difference between the earth and upper atmosphere was defined by numerical integration of the electric field. Necessary initial conditions were determined from the best available information. An obvious shortcoming in the choice of initial conditions is that the measurements of ionic concentrations and electric field from which these initial values were obtained were made at different times and at different geopgraphic locations. It would be highly desirable if simultaneous measurements of these variables, both as a function of altitude, could be made so that more satsifactory initial conditions could be determined, and also to allow a comparison of the preceding theoretical results with concurrent data. The sensitivity of the results as a function of initial conditions can clearly be seen from Figure 28, where a relatively small change in $(\frac{dn}{dZ})_0$ made a significant difference in the theoretical ion concentrations.

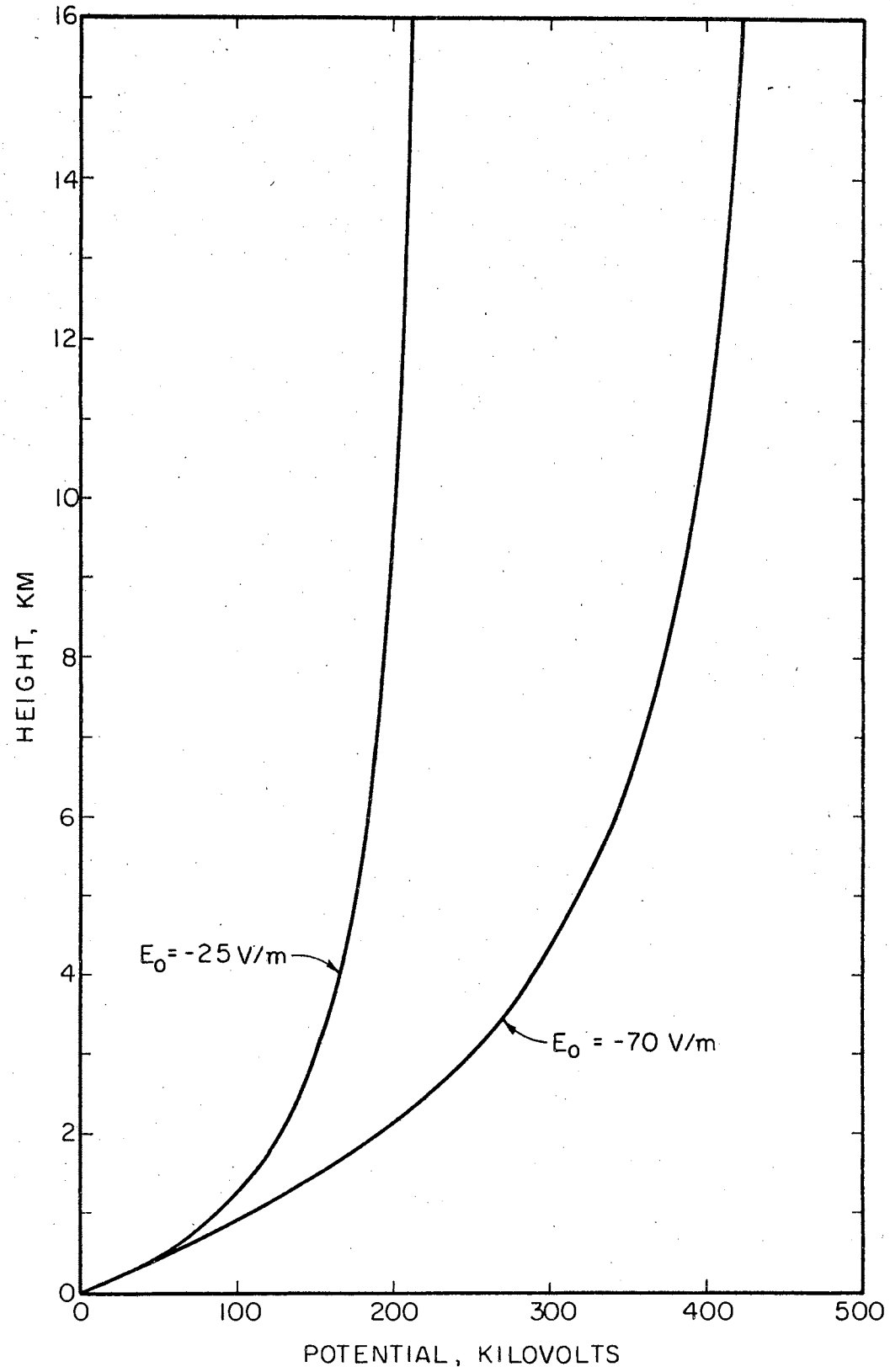

Figure 34. Atmospheric Potential

The preceding solution can be formulated for numerical solution. The polar current densities are given by

$$j_+ = q[\mu_+ n_+ E - d_+ \frac{dn_+}{dZ}]$$

$$j_- = q[\mu_- n_- E + d_+ \frac{dn_-}{dZ}] \quad .$$

Rearranging these two equations and adding yields

$$[(\mu_+ n_+ + \mu_- n_-) E + \frac{d}{dZ}(n_- - n_+)] = \frac{j_-}{qd_-} + \frac{j_+}{qd_+} \quad .$$

Using the Poisson equation to substitute for the difference in ion concentrations, and also the fact

$$\mu_- = 1.357\mu_+$$

gives

$$qd_+[2.357\mu_+ nE - \frac{\varepsilon_0}{q}\frac{d^2E}{dZ^2}] = (\frac{j_-}{1.357} + j_+) \quad . \qquad (6.16)$$

On differentiation,

$$q\frac{d}{dZ}\left|d_+[J_{c_0} - \frac{\varepsilon_0}{q}\frac{d^2E}{dZ^2}]\right| = \frac{1}{1.357}\frac{dj_-}{dZ} - \frac{dj_+}{dZ} \quad . \qquad (6.17)$$

But from the generalized continuity equations,

$$\frac{d}{dZ}(j_-) = (q_-)(g - \alpha n^2) = -q(g - \alpha n^2)$$

$$\frac{d}{dZ}(j_+) = (q_+)(g - \alpha n^2) = q(g - \alpha n^2) \quad ,$$

and from the conduction current expression,

$$n = \frac{J_{c_0}}{2.357_4 E\mu_+} \quad ,$$

so that Equation 6.17 becomes

$$\frac{d}{dZ}\left(d_+[J_{c_0} - \frac{\varepsilon_0}{q}\frac{d^2E}{dZ^2}]\right) = \frac{0.357}{1.357}[g - \alpha(\frac{J_{c_0}}{2.357\mu_+ qE})^2] \quad . \qquad (6.18)$$

This expression contains only the one unknown, E, and is amenable to numerical solution since the subtraction of like numbers is avoided. On solution, n could be found from the expression for drift current density. However, the use of Theorem 2 provides a simpler approach to the solution so that numerical integration will not be carried out. This type of numerical formulation therefore avoids the difficulties described in Section 6.3.

6.6 Analysis of the Model for Total Current Density Independent of Altitude. The assumption of time equilibrium of ionic concentrations implies altitude independence of the total atmospheric current density. Atmospheric space charge density where large ion and electron densities are negligible is

$$\rho = q(n_+ - n_-) \quad .$$

Then

$$\frac{\partial \rho}{\partial t} = q(\frac{\partial n_+}{\partial t} - \frac{\partial n_-}{\partial t}) \quad .$$

But time equilibrium requires

$$\frac{\partial n_+}{\partial t} = \frac{\partial n_-}{\partial t} = 0 \quad ,$$

so that

$$\frac{\partial \rho}{\partial t} = 0 \quad .$$

The continuity equation of electrical charge is:

$$\overline{\nabla} \cdot \overline{J}_T + \frac{\partial \rho}{\partial t} = 0 \quad .$$

Hence

$$\overline{\nabla} \cdot \overline{J}_T \approx \frac{dJ_T}{dZ} = 0 \quad ,$$

which implies the total current density, J_T, is independent of altitude. Or

$$q[d_- n_-' - d_+ n_+'] + q[\mu_+ n_+ + \mu_- n_-]E = J_T \qquad (6.19)$$

is constant.

Under the same assumptions made in the preceding section regarding mobility and diffusivity ratios and the near equality of small ion concentrations, Equation 6.19 becomes

$$0.357 d_+ \frac{dn}{dZ} + 2.357 \mu_+ nE = \frac{J_T}{q} \quad ,$$

which can be put into the form

$$\frac{dn}{dZ} + \frac{2.357\mu_+}{0.357 d_+} nE = \frac{J_T}{0.357 q d_+} \quad . \qquad (6.20)$$

Ionic concentrations will be determined from this equation using the electric field measurements described in Equations 3.5, 3.6 and 3.7.

If the mobility and diffusivity are written as

$$\mu_+ = \mu_0 e^{\mu_1 Z}$$

and

$$d_+ = d_0 e^{d_1 Z} \quad ,$$

where the numbers μ_0, d_0, μ_1 and d_1 are given in Chapter IV. Then

Equation 6.20 becomes

$$\frac{dn}{dZ} + C_1 e^{(\mu_1 - d_1)Z} nE = C_2 e^{-d_1 Z} , \qquad (6.21)$$

where

$$C_1 = \frac{2.357\mu_0}{0.357d_0}$$

and

$$C_2 = \frac{J_T}{0.357qd_0} .$$

Equation 6.21 is of the form of Bernoulli's equation and can be solved by using the integrating factor,

$$I.F. = \exp[C_1 \int e^{(\mu_1 - d_1)p} E(p)dp] .$$

The electric field will have the general form

$$E = E_0 e^{E_1 Z} ,$$

so that if

$$b_1 = \mu_1 + E_1 - d_1 ,$$

and

$$C_3 = E_0 C_1$$

then the integrating factor becomes

$$I.F. = \exp[C_3 \int e^{b_1 p} dp] = \exp[\frac{C_3}{b_1} e^{b_1 Z}] .$$

Multiplying both sides of Equation 6.21 by the integrating factor gives the result

$$\frac{d}{dZ}[(I_oF_o)n] = C_2(I_oF_o)\, e^{-d_1Z} \quad ,$$

so that

$$n = (I_oF_o)^{-1}\left[C_2 \int (I_oF_o)\, e^{-d_1Z}\, dZ + K\right] \quad , \qquad (6.22)$$

where

$$K = (n_0)\, \exp\left[\frac{C_3}{b_1} e^{b_1Z_0}\right] \quad .$$

Because of the complexity of the integrand in Equation 6.22, numerical integration is required to obtain a solution. However, a simpler expression for n can be found. For when the total constant current density, J_T, of Equation 6.19 is determined from available measured data, there arises the conclusion that

$$J_T = J_{c_0} + J_{D_0} \approx J_{c_0} \quad ,$$

i.e., the total current is principally conduction current. Consequently, Equation 6.19 can be written

$$J_T \approx J_{c_0} = q(\mu_+ n_+ + \mu_- n_-)E \quad ,$$

which becomes

$$2.357\mu_+ nE = \frac{J_{c_0}}{q} \quad ,$$

or

$$n = \frac{J_{c_0}}{2.357q\mu_+ E} \quad .$$

Using the initial conditions from Section 6.4, J_{c_0} is determined, and then using Stergis' measured electric field and the mobility

expression given in Equation 4.2, the ionic concentration can be calculated. The result is shown in Figure 35. Comparing this result with Figure 28 for the same initial conditions shows a very close agreement in the theoretical ion concentrations. Consequently, the conductivity and space charge density derivable from the data of Figure 35 would be similar to those shown in Figures 30 and 33. The significant difference between the solution of Section 6.5 and the present analysis is that in the former treatment, as a consequence of Theorem 2, only the initial electric field and ion concentration need be known in order to solve for the desired electrical properties, while in the present case, the initial ion concentration and the entire electric field must be known in order to find the remaining variables.

6.7 Analysis of the Atmospheric Model for a Constant Polar Conductivity Ratio. In Section 5.3 it was pointed out that in regions of negligible pollution, the ratio of polar conductivities apparently attains a nearly constant value equal to the mobility ratio. Thus

$$\frac{\sigma_-}{\sigma_+} = \frac{q\mu_- n_-}{q\mu_+ n_+} = \frac{\mu_- n_-}{\mu_+ n_+} = C \quad ,$$

or

$$\mu_- n_- = C\mu_+ n_+ \quad . \tag{6.24}$$

From the last statement it can be shown that

$$d_- \frac{dn_-}{dZ} = C\, d_+ \frac{dn_+}{dZ} \quad .$$

Since from Equation 6.24

$$n_- = C \frac{\mu_+}{\mu_-} n_+ = C_2\, n_+ \quad ,$$

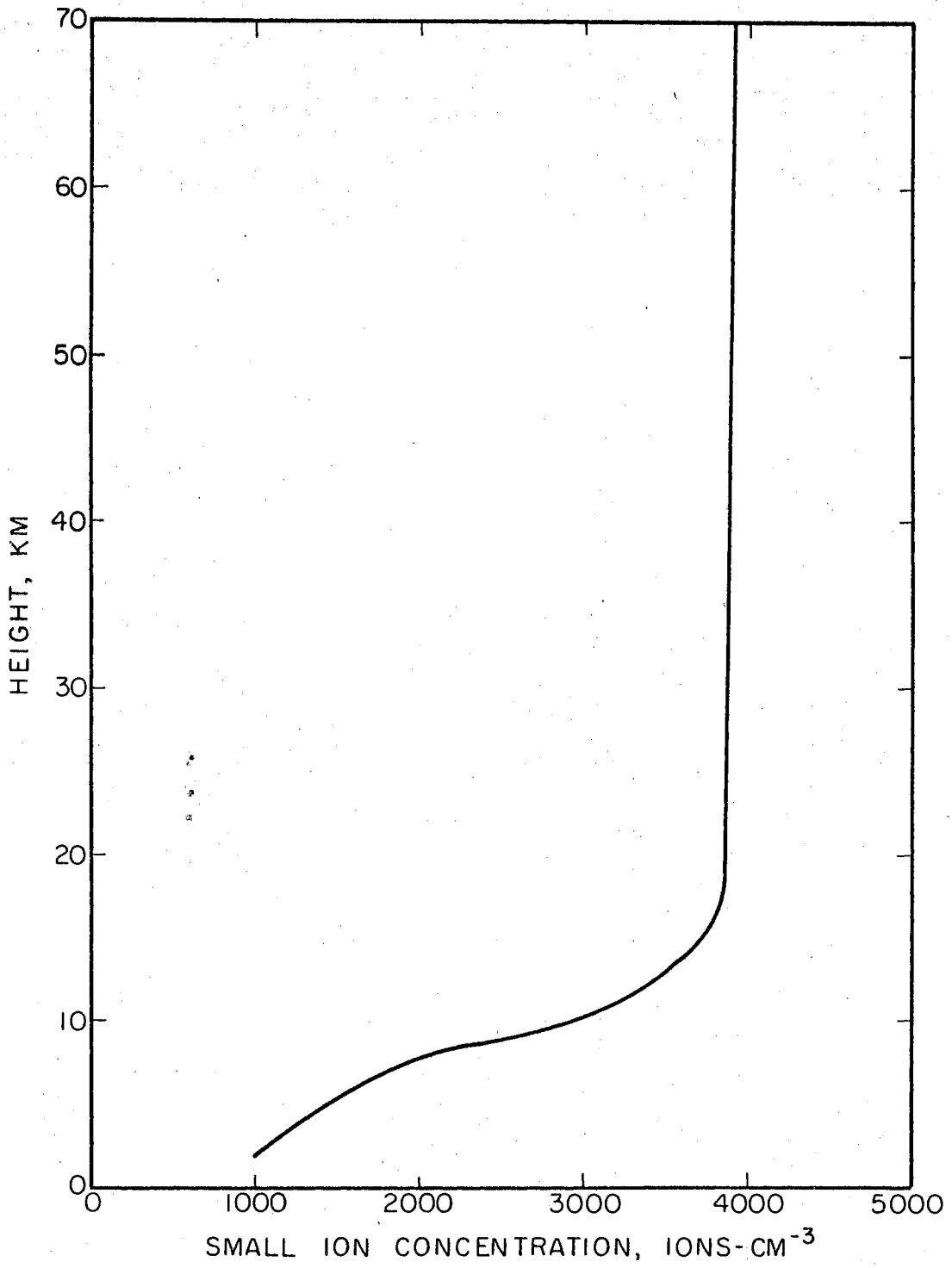

Figure 35. Theoretical Small Ion Concentration

then

$$\frac{dn_-}{dZ} = C_2 \frac{dn_+}{dZ} = C \frac{\mu_+}{\mu_-} \frac{dn_+}{dZ} \quad ,$$

which gives

$$\mu_- \frac{dn}{dZ} = C \mu_+ \frac{dn_+}{dZ} \quad .$$

Multiplying by the factor $\frac{kT}{q}$

$$\frac{kT}{q} \mu_- \frac{dn_-}{dZ} = C \frac{kT}{q} \mu_+ \frac{dn_+}{dZ} \quad ,$$

which is equivalent to the desired result, namely

$$d_- \frac{dn_-}{dZ} = C d_+ \frac{dn_+}{dZ} \quad . \qquad (6.25)$$

Now rewriting Equations 6.4 and 6.5 using the relations given in Equations 6.24 and 6.25,

$$\frac{d}{dZ}\left[C d_+ \frac{dn_+}{dZ}\right] + \frac{d}{dZ}\left[C \mu_+ n_+ E\right] + g - \alpha n_+ n_- = 0$$

$$\frac{d}{dZ}\left[d_+ \frac{dn_+}{dZ}\right] - \frac{d}{dZ}\left[\mu_+ n_+ E\right] + g - \alpha n_+ n_- = 0 \quad .$$

Dividing the first of these equations by C and then subtracting the two shows that

$$\frac{d}{dZ}(\mu_+ n_+ E) + \left(\frac{1 - C}{2C}\right)(g - \alpha n_+ n_-) = 0 \quad . \qquad (6.26)$$

As before, let

$$n_+ \approx n_- = n$$

$$E = E_0 e^{E_1 Z}$$

$$\mu_+ = \mu_0 e^{\mu_1 Z} \quad ,$$

and let

$$K = \frac{1 - C}{2C} \quad .$$

From the discussion in Chapter IV regarding generation and recombination rates, g and α in Equation 6.26 will be written

$$g = g_0 e^{g_1 Z}$$

$$\alpha = \alpha_0 e^{\alpha_1 Z} \quad .$$

Following these substitutions, Equation 6.26 assumes the form

$$\frac{d}{dZ}(\mu_0 E_0 e^{(\mu_1 + E_1)Z} n) + K(g_0 e^{g_1 Z} - \alpha_0 e^{\alpha_1 Z} n^2) = 0 \quad . \quad (6.27)$$

Performing the indicated differentiation and solving for $\frac{dn}{dZ}$,

$$\frac{dn}{dZ} = f(n,Z) = \frac{K}{\mu_0 E_0} e^{-(\mu_1 + E_1)Z} (\alpha_0 e^{\alpha_1 Z} n^2 - g_0 e^{g_1 Z}) - (\mu_1 + E_1)n \quad .$$

The function $f(n,Z)$ can be shown to have continuous first order partial derivatives $\frac{\partial f}{\partial Z}$ and $\frac{\partial f}{\partial n}$, and therefore satisfies a Lipschitz condition for all Z and n of interest. Then according to the Uniqueness and Existence Theorem[1], Equation 6.27 possesses a unique solution.

Similar to the situation encountered in Section 6.6, Equation 6.27 contains two unknowns, the electric field and the ionic concentration. On the strength of available measurements and previous analysis, the electric field is assumed to be of exponential form. E_0, the initial electric field, will be determined as before, that is from measured data.

---

[1]For a detailed treatment of the uniqueness and existence theorem for first-order ordinary differential equations see "Ordinary Differential Equations" G. Birkhoft and G. Rota, Ginn and Co., Boston, 1962.

The value of the exponent E_1 will be found from the solution of Equation 6.27.

If the electric field was assumed to be known as in the previous section, a numerical integration could be used to find the ionic concentration, but an analytic solution will be shown to yield not only n, but E_1 as well.

Although Equation 6.27 is obviously nonlinear, the form of the equation and the fact that the various coefficients are exponential indicates that the solution might also be exponential in form. Therefore, just as is done in the solution of linear differential equations, an exponential solution will be assumed, and if this trial solution can be made to satisfy the equation, then by the uniqueness theorem it will be the desired solution.

To this end, let

$$n = n_0 e^{n_1 Z} \quad ,$$

where n_0 will be a known initial condition, and n_1 remains to be determined. Equation 6.27 now becomes

$$\frac{d}{dZ}\left(\mu_0 E_0 n_0 e^{(\mu_1 + E_1 + n_1)Z}\right) + K\left(g_0 e^{g_1 Z} - \alpha_0 n^2 e^{(\alpha_1 + 2n_1)Z}\right) = 0$$

or

$$\mu_0 E_0 n_0 (\mu_1 + E_1 + n_1) e^{(\mu_1 + E_1 + n_1)Z} + K g_0 e^{g_1 Z} - K \alpha_0 n_0^2 e^{(\alpha_1 + 2n_1)Z} = 0. \quad (6.28)$$

With the two parameters E_1 and n_1 yet unknown, there are two nontrivial ways in which Equation 6.28 can be satisfied. The first requires

$$\mu_1 + E_1 + n_1 = \alpha_1 + 2n_1 = g_1 \quad ,$$

and

$$\mu_0 n_0 E_0 + K g_0 - k \alpha_0 n_0^2 = 0 \quad .$$

From these equations,

$$n_1 = \frac{g_1 - \alpha_1}{2} \tag{6.29}$$

and

$$E_1 = g_1 - \mu_1 - n_1 \quad . \tag{6.30}$$

While the second requires

$$\alpha_1 + 2n_1 = g_1$$

$$\mu_1 + E_1 + n_1 = 0$$

and

$$g_0 - \alpha_0 n_0^2 = 0 \quad ,$$

so that

$$n_1 = \frac{g_1 - \alpha_1}{2} \tag{6.31}$$

and

$$E_1 = -(\mu_1 + n_1) \quad . \tag{6.32}$$

Using the values for g_1, μ_1, and α_1 given in Chapter IV for both forms of the recombination coefficient, n_1 and E_1 can be determined. Evaluating Equation 6.30 gave an electric field expression not consistent with measured results in that E_1 increased with altitude instead of decreased as measurements indicate the case to be. As for example in the

data of Figure 9. Equation 6.32 on the other hand gave an electric field exponent which was in good agreement with experimentally determined values. Specifically, using the Thomson recombination coefficient showed E_1 to be -2.6×10^{-4} meters^{-1} up to thirteen kilometers, and -1.4×10^{-4} meters^{-1} above this height. These values are seen to compare favorably with those in Equations 3.2 through 3.7 which describe results of electric field measurements.

Taking E_1 to be defined by Equation 6.32, then n_1 is given by Equation 6.31, and

$$n_o = \left[\frac{g_0}{\alpha_0}\right]^{\frac{1}{2}} \quad . \tag{6.33}$$

The fact that there were two ways to satisfy Equation 6.28 does not violate the uniqueness theorem. In fact, Equations 6.29 and 6.31 show that in either case the functional form of n is the same. It is the added parameter E_1 which is adjusted to conform with experimental results.

Two facts are implicit in Equations 6.31, 6.32 and 6.33. The first is that the positive conduction flux is constant. This is seen by referring to Equation 6.28 where if as in Equation 6.32

$$E_1 + \mu_1 + n_1 = 0 \quad ,$$

then

$$\frac{d}{dZ}\left[\mu_+ n_+ E\right] = 0 \quad .$$

Also, since

$$\mu_- n_- = C\, \mu_+ n_+$$

$$\frac{d}{dZ}\left[\mu_- n_- E\right] = 0 \quad .$$

The conclusion is then that

$$\frac{d}{dZ}[(\mu_+ n_+ + \mu_- n_-)E] = 0$$

or

$$\frac{d}{dZ}\left[\frac{j_c}{q}\right] = 0 \quad ,$$

which implies the conduction current density in constant. Alternatively, since

$$J_c = q(\mu_+ n_+ + \mu_- n_-)E \tilde{\sim} 2.357q\mu_+ nE$$
$$= 2.357q\mu_0 n_0 E_0 e^{(\mu_1+E_1+n_1)Z} \quad ,$$

and

$$\mu_1 + E_1 + n_1 = 0 \quad ,$$

then

$$J_c = 2.357q\mu_0 n_0 E_0$$

which is independent of Z.

Then according to the theorems of Section 6.4, the diffusion current density is also constant, and the solution for this case is discussed in Section 6.5. The second implication is the fact that the generation and recombination rates are equal. This is evident from Equations 6.31 and 6.33 because

$$n = n_0 e^{n_1 Z} = \left[\frac{g_0}{\alpha_0}\right]^{\frac{1}{2}} e^{\frac{g_1 - \alpha_1}{2} Z}$$

implies that

$$n = \left[\frac{g_0 e^{g_1 Z}}{\alpha_0 e^{\alpha_1 Z}}\right]^{\frac{1}{2}} = \left[\frac{g(Z)}{\alpha(Z)}\right]^{\frac{1}{2}} \qquad (6.34)$$

Now squaring and rearranging this last equation gives the result

$$g = \alpha n^2 \quad ,$$

i.e., the generation and recombination rates are equal.

The ionic concentration specified by Equation 6.34 using both α_T and α_2 is shown in Figure 29.

The conclusion can then be drawn that a constant polar conductivity ratio implies a constant conduction current density and that ion generation and recombination rates are equal. It can also be concluded that a knowledge of the generation and recombination coefficient functions, and the mobility function is sufficient to define the electric field and ion concentration distributions, from which any other desired atmospheric electrical property can be derived.

Considering the conclusion of Theorem 2, it can also be stated that the premise on which the present solution is based, namely that of a constant polar conductivity ratio, also implies an altitude independent diffusion current density. Section 6.5 treated in detail the solution for the latter implication, and consequently the ion concentrations found there - Figure 28 - would be expected to agree with Equation 6.34. In comparing these two solutions, Figures 28 and 29, it is seen that the general forms are similar when α_T is used in Equation 6.34, but that the α_T concentration of Figure 29 is approximately twice that of Figure 28 for similar initial conditions. The probable source of this disagreement is in the initial conditions on which Figure 28 is based. In fact, it

was pointed out at the time that the solution was critically dependent on the choice of initial conditions, and since the available data was at best difficult to interpret from the standpoint of determining initial conditions, there was considerable chance for error in determining $(\frac{dn}{dZ})_0$ on which the solution of Section 6.5 was based. But since either supposition, constant conduction current or constant conductivity ratio, implies a constant diffusion current, the solutions should agree, and do in form, with the difference in magnitudes likely due to the unavailability of data from which initial conditions can accurately be obtained.

6.8 Cosmic Ray Intensity Determined From Atmospheric Electricity Measurements. An outcome of the preceding solutions is the possibility of determining cosmic ray intensity from measurements of certain atmospheric electrical properties. For example, since the best available evidence indicates both a constant conduction current density and a constant conductivity ratio in the unpolluted atmosphere - both of which according to the model imply a constant diffusion current - measurements of initial ionic concentration and electric field should be sufficient to define the cosmic ionization function. Thus as shown in Section 6.5, a knowledge of the initial derivative of the ionic concentration and the diffusivity expression defined the ionic concentration distribution, and a knowledge of the initial ion concentration, and the initial electric field defined the electric field distribution. Then from Section 6.7 where

$$n(Z) = [\frac{g_0}{\alpha_0}]^{\frac{1}{2}} e^{(\frac{g_1 - \alpha_1}{2})Z}$$

and

$$E(Z) = E_0 e^{-(\mu_1 - \frac{g_1}{2} + \frac{\alpha_1}{2})Z}$$

it can be seen that once n(Z) and E(Z) are known, g_0 and g_1 can be determined. This will suffice to define the cosmic ray ion generation rate, without the necessity of direct measurements.

6.9 Summary. The original atmospheric model was simplified using known atmospheric properties. Implications of the model were presented in the form of a set of theorems, some of which proved useful in subsequent analysis. Solutions were obtained under three conditions, total conduction current constant, total current constant, and polar conductivity ratio constant. The solutions agreed in functional form, but some discrepancy existed in the magnitudes of some of the calculated variables.

The reason for this discrepancy is thought to be the unavailability of data from which the required initial conditions can be obtained with the necessary accuracy. An experimental measurement program could possibly resolve the discrepancy. As a consequence of the analysis, a simplified method of determining cosmic ray intensity within the atmosphere is proposed.

CHAPTER VII

ELECTRICAL THUNDERSTORM MODEL

7.1 Introduction. Since in fair weather areas, there is apparently a constant conduction current flowing from the high atmosphere to the earth, in order to maintain the earth's negative charge, current must be flowing away from the earth in non-fair weather, that is, thunderstorm areas. Indeed, measurements made above thunderstorms show a conduction current flowing upward toward the ionosphere (Gish and Wait, 1950 and Stergis et al., 1957). Thus a thunderstorm is envisioned as a generator maintaining the electrical balance of the earth-atmosphere system, the positive generator pole being at the top of the cell and its negative pole at the bottom.

As was mentioned in Chapter I, electric field measurements made in the vicinity of thunderstorms indicate that typically the upper portion of the cell is positively charged, the lower portion negatively charged, with the possibility of an additional small positive charge in the lower part of the cell. If the lower positive charge is neglected, and the remaining upper and lower charges assumed to be point charges, then a dipole or bipolar cloud model is obtained. The estimated magnitudes of these charges for "typical" storms vary over a wide range of values. Gish and Wait (1950) propose 39 coulombs for both upper and lower charges, while Kasemir (1965) quotes +60 coulombs for the upper charge and -340 coulombs for the lower. If the third charge is included, then a

tripolar model can be formulated.

In this chapter, an electrical model will be examined to determine the behavior of atmospheric electrical properties both near and far removed from the storm. This model will be general in that the effect of any number of charge centers at arbitrary locations can be considered. The variation of conductivity with height will also be included in the storm model.

7.2 Formulation of Thunderstorm Model. Three assumptions previously discussed will be incorporated in the model. These are: 1) Steady-state conditions obtain, 2) conductivity variations in the horizontal directions are negligible and 3) atmospheric conductivity varies exponentially with height according to the expression:

$$\sigma = \sigma_0 e^{aZ}. \tag{7.1}$$

Under these assumptions,

$$\overline{\nabla} \times \overline{E} = -\frac{\partial \overline{B}}{\partial t} = 0 \tag{7.2}$$

$$\overline{\nabla} \cdot \overline{E} = \rho/\varepsilon \tag{7.3}$$

$$\overline{\nabla} \cdot \overline{J}_T = \overline{\nabla} \cdot (\overline{J}_c + \overline{J}') = -\frac{\partial \rho}{\partial t} = 0. \tag{7.4}$$

and

$$\overline{J}_c = \sigma \overline{E}. \tag{7.5}$$

Where $\overline{J}_c$ denotes conduction current obeying Ohm's law, and $\overline{J}'$ denotes any other currents in the cell. For example, the charge separation process in a thunderstorm can be considered a convection current in which positive charge is carried to the top of the cell. Thus the region of

the positive charge is a source of conduction current, and a sink for the convection current, with the roles reversed for the negative charged region.

From Equation 7.2, the electric field can be taken as the negative gradient of a scalar potential function, i.e.,

$$\overline{E} = - \overline{\nabla} V. \tag{7.6}$$

Using Equations 7.5 and 7.6 in 7.4 gives

$$\overline{\nabla} \cdot (\overline{J}_c + \overline{J}') = \overline{\nabla} \cdot (-\sigma \overline{\nabla} V + \overline{J}') = 0$$

or

$$\sigma \nabla^2 V + \overline{\nabla}\sigma \cdot \overline{\nabla} V = \overline{\nabla} \cdot \overline{J}'.$$

Considering Equation 7.1,

$$\sigma \nabla^2 V + a \sigma \frac{\partial V}{\partial Z} = \overline{\nabla} \cdot \overline{J}',$$

or

$$\nabla^2 V + a \frac{\partial V}{\partial Z} = \frac{\overline{\nabla} \cdot \overline{J}'}{\sigma}. \tag{7.7}$$

The storm charges will be considered as point charges so that in cylindrical coordinates,

$$\overline{\nabla} \cdot \overline{J}' = - \frac{q_i \sigma}{\varepsilon_0 r} \delta(r - r_i) \, \delta(Z - Z_i) \, \delta(\phi - \phi_i).$$

This result follows from Poisson's equation where

$$\nabla^2 V = - \frac{\rho_T}{\varepsilon_0} = \frac{\overline{\nabla} \cdot \overline{J}'}{\sigma} - a \frac{\partial V}{\partial Z}.$$

Now if the ith charge is assumed to be a source of $\overline{J}'$ (sink of $\overline{J}_c$), then

at the given charge,

$$\frac{\bar{\nabla} \cdot \bar{J}'}{\sigma} = -\frac{\rho_i}{\varepsilon_c} = -\frac{q_i}{\varepsilon_0 r}\,\delta(r - r_i)\,\delta(Z - Z_i)\,\delta(\phi - \phi_i).$$

It can also be seen from this discussion that because of the varying conductivity there is an added space charge density term, a $(\partial V/\partial Z)$, in Poisson's equation. Then Equation 7.7 becomes

$$\nabla^2 V + a\frac{\partial V}{\partial Z} = -\frac{q_i}{\varepsilon_0 r}\,\delta(r - r_i)\,\delta(Z - Z_i)\,\delta(\phi - \phi_i).$$

Summing over all charges present gives the differential equation describing the electric potential in the atmosphere due to the charges present in the thunderstorm,

$$\nabla^2 V + a\frac{\partial V}{\partial Z} = -\sum_{i=1}^{p}\frac{q_i}{\varepsilon_0 r}\,\delta(r - r_i)\,\delta(Z - Z_i)\,\delta(\phi - \phi_i). \qquad (7.8)$$

The situation for two charges (p = 2) is shown in Figure 36, where the earth's surface is considered to be a conducting surface at zero potential, and the ionoshpere at height h is another conducting layer at potential V_0.

7.3 Solution of Thunderstorm Model. The detailed solution of Equation 7.8 subject to the boundary conditions of Figure 36 is shown in Appendix C. The potential function is

$$V(r,\phi,Z) = V_0\left[\frac{1 - e^{-aZ}}{1 - e^{-ah}}\right] + \sum_{i=1}^{p}\frac{q_i e^{-\frac{a}{2}(Z-Z_i)}}{\varepsilon_0 \pi h}\sum_{k=-\infty}^{\infty} e^{ik(\phi-\phi_i)}\sum_{n=1}^{\infty} I_k(m_n r_i)\,K_k(m_n r)\,\sin\frac{n\pi Z}{h}\,\sin\frac{n\pi Z_i}{h}. \qquad (7.9)$$

If all charges are situated on the Z axis, as for example, in the bipolar

model where p = 2, the solution is shown in Equation C.18. There

$$V(r,Z) = V_0\left[\frac{1 - e^{-aZ}}{1 - e^{-ah}}\right] + \sum_{i=1}^{p} \frac{q_i e^{-\frac{a}{2}(Z-Z_i)}}{\varepsilon_0 \pi h} \sum_{n=1}^{\infty} K_0(m_n r) \sin\frac{n\pi Z}{h} \sin\frac{n\pi Z_i}{h} \tag{7.10}$$

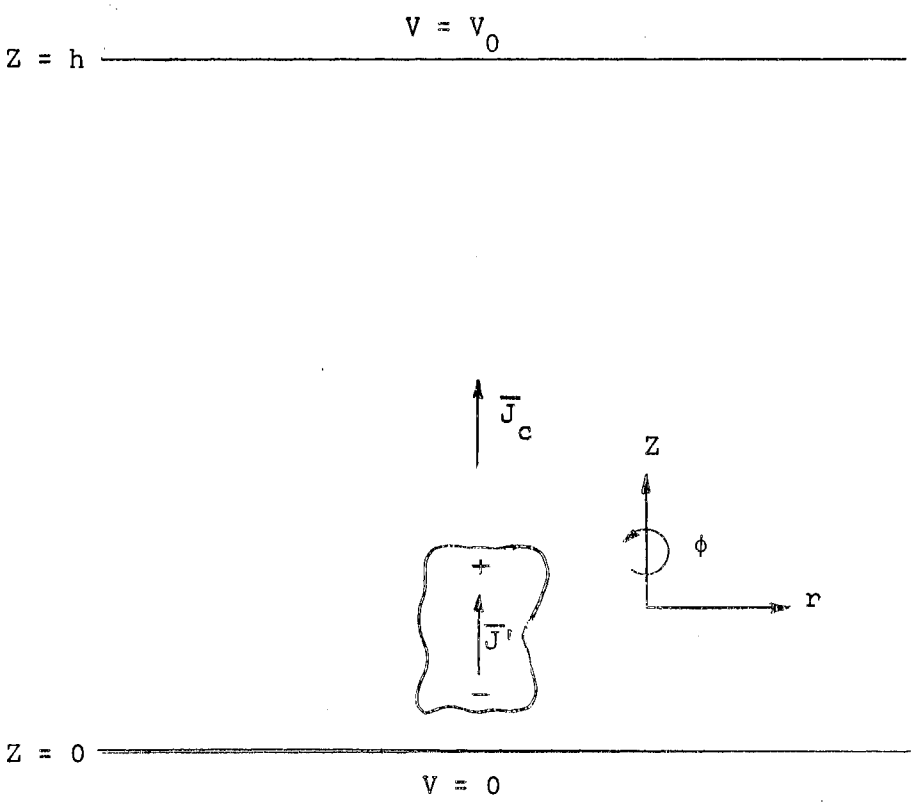

Figure 36. Bipolar Thunderstorm Model

A result similar to Equation 7.10 was obtained by Holzer and Saxon (1952) for the case of one charge on the axis. The electric field components can be derived from these potential functions using Equations 7.6. Thus

$$E_r = -\frac{\partial V}{\partial r}$$

and

$$E_Z = - \frac{\partial V}{\partial Z}$$

The resulting expressions using Equation 7.10 (p = 2) are given in Equations C.21 and C.22, and show that as $r \to \infty$,

$$E_r \to 0$$

$$E_Z = - \frac{aV_0 \, e^{-aZ}}{1 - e^{-ah}} ,$$

so that in fair weather areas, the electric field behaves as determined in Chapter VI.

Assuming the charge magnitudes and locations are known, then the preceding potential functions can be used to solve for other electrical quantities. For example, the conduction current density is given by

$$\overline{J}_c = \sigma \overline{E} = - \sigma \, \overline{\nabla} \, V, \qquad (7.11)$$

and the total current above the storm at any given height Z_1 can be obtained by integrating Equation 7.11. Thus

$$I = \int_{r=0}^{r_1} \int_{\phi=0}^{2\pi} J_c(r,\phi,Z_1) \, r dr d\phi \, .$$

where it is assumed the cell is cylindrical with radius r_1. The total space charge density can also be determined from the relation

$$\rho_T = - \varepsilon_0 \nabla^2 V,$$

which far removed from the storm activity is

$$\rho_T = \frac{a^2 \varepsilon_0 V_0 e^{-aZ}}{1 - e^{-ah}} .$$

This behavior is also consistent with the results of Chapter VI.

7.4 Conclusions. The theory that thunderstorms serve as generators for the global atmospheric electricity system is the most widely accepted. However, just as in the fair weather situation, experimental results in thunderstorm regions are sketchy and contradictory. For example, the conductivity within a thunderstorm is an unknown quantity, although Kasemir (1965) theorizes a value of about one-third that of the fair weather conductivity. The magnitudes of the charge centers within the cell are also a subject of controversy as pointed out in Section 7.1. Nevertheless, the foregoing analysis provides results which are consistent with the results of fair weather atmospheric analysis.

CHAPTER VIII

SUMMARY AND CONCLUSIONS

8.1 Summary. An analysis of the electrical properties of the atmosphere was made using a model consisting of the generalized continuity equations and Poisson's equation. In particular, charge transport and equilibrium were investigated using this model in the light of certain observed features of atmospheric electricity. Desired results were theoretical predictions of ionic concentrations, electric field distributions, conduction and diffusion currents, and space charge density.

In Chapter II, the form of the model was derived from basic physical laws and from known geophysical data. It was shown that gravitational and magnetic forces could be neglected in the model.

Chapters III and IV were concerned with determining the functional form of the ionic mobilities, diffusivities, and recombination and generation rates which appeared in the model.

The effect that uncertainties and discrepancies in measured characteristics of the atmosphere would have on an analysis of the model is discussed in Chapter V. The most generally accepted features were selected as a basis of comparison for the theoretical results. Analysis of the model was carried out in Chapter VI. Solutions were obtained under three assumptions made as a consequence of the discussion in Chapter V.

Chapter VII presented a general model of a thunderstorm cell. This

model was more comprehensive than previous models in that any arbitrary location of charge centers in the cell could be included in evaluating the electric potential function.

8.2 Conclusions. On the basis of analysis of the model it can be concluded that small ion concentrations increase with height up through the stratosphere and then remain essentially constant throughout the remainder of the atmosphere. Also, the electric field decreases monotonically with height, which agrees with measured data. Diffusion currents appear to be negligible in comparison with conduction currents. Using the atmospheric model, it is possible to predict the electrical properties of the atmosphere as a function of height on the basis of temperature and pressure soundings, and as a function of the measured electric field and small ion concentrations at the top of the exchange layer. These same measurements can also be used to determine cosmic ray intensity as a function of height by using the atmospheric model.

8.3 Recommendations for Further Study. The most interesting and fruitful extension of this thesis would be a program of experimental measurements to determine correlations between the theoretical predictions and measured results when the necessary measurements were made at the same time and location. This could resolve the uncertainties in the previous results which arose because the initial conditions used in the analysis were taken from data measured at different geographic locations and during different phases of the solar cycle.

A second extension would be to supplement the model with an additional continuity equation describing the concentration of electrons. Such a model would be significant in the higher atmosphere where the electron mean lifetime is greater. In this case the model would assume

the form,

$$\frac{\partial n_e}{\partial t} = \bar{\nabla} \cdot [d_e \bar{\nabla} n_e + \mu_e n_e \bar{E}] + g - \alpha_1 n_e - \alpha_2 n_e n_+ + \alpha_3 n_-$$

$$\frac{\partial n_-}{\partial t} = \bar{\nabla} \cdot [d_- \bar{\nabla} n_- + \mu_- n_- \bar{E}] + \alpha_1 n_e - \alpha_3 n_- - \alpha_4 n_+ n_-$$

$$\frac{\partial n_+}{\partial t} = \bar{\nabla} \cdot [d_+ \bar{\nabla} n_+ - \mu_+ n_+ \bar{E}] + g - \alpha_2 n_+ n_e - \alpha_4 n_+ n_-$$

and

$$\bar{\nabla} \cdot \bar{E} = \frac{q}{\varepsilon_0} (n_+ - n_- - n_e).$$

The functional form of the various attachment, detachment, and recombination coefficients would have to be determined as well as the electron mobility and diffusivity to enable solution of this model.

BIBLIOGRAPHY

Banerji, S. K. and S. R. Lele. "Electric Charges of Rain Drops." Proceedings National Institute of Science, India, Vol. 18 (1952), 93-124.

Boudreaux, F. J. "A Study of the Quasi-Static Electric Fields of Severe Thunderstorms." (unpub. Ph.D. thesis, Oklahoma State University, 1959).

Bowen, I. S., R. A. Millikan, and H. V. Neher. "New Light on the Nature and Origin of the Incoming Cosmic Rays." Physical Review, Vol. 53 (1938), 855-861.

Bricard, J. "Action of Radioactivity and of Pollution Upon Parameters of Atmospheric Electricity." Problems of Atmospheric and Space Electricity. Ed. S. C. Coroniti. Amsterdam: Elsevier Publishing Co., 1965, 82.

Chalmers, J. A. Atmospheric Electricity. London: Pergamon Press, 1957.

Chalmers, J. A. "Charge Generation Outside Thunderstorms." Problems of Atmospheric and Space Electricity. Ed. S. C. Coroniti. Amsterdam: Elsevier Publishing Co., 1965, 167.

Clark, J. F. "The Fair Weather Atmospheric Electric Potential and its Gradient." Recent Advances in Atmospheric Electricity. Ed. L. G. Smith. Oxford: Pergamon Press, 1958, 61.

Cole, R. K. and J. T. Pierce. "Electrification in the Earth's Atmosphere for Altitudes Between 0 and 100 Kilometers." Journal of Geophysical Research, Vol. 70 (1965), 2735-2749.

Curtis, H. O. and M. C. Hyland. "Aircraft Measurements of the Ratio of Negative to Positive Conductivity." Recent Advances in Atmospheric Electricity. Ed. L. G. Smith. Oxford: Pergamon Press, 1958, 111.

Forbush, S. E. "World-Wide Cosmic Ray Variations, 1937-1952." Journal of Geophysical Research, Vol. 59 (1954), 525.

Gish, O. H. and K. L. Sherman. "Electrical Conductivity of Air to an Altitude of 22 km." National Geographic Society Stratosphere Series, Vol. 2 (1936), 94-116.

Gish, O. H. "Evaluation and Interpretation of the Columnar Resistance of the Atmosphere." Terrestrial Magnetism and Atmospheric Electricity, Vol. 49 (1944), 150-168.

Gish, O. H. and G. R. Wait. "Thunderstorms and the Earth's General Electrification." Journal of Geophysical Research. Vol. 55 (1950), 437-484.

Hatakeyama, H. "Atmospheric Electricity Research in the Far East." Problems in Atmospheric and Space Electricity. Ed. S. C. Coroniti. Amsterdam: Elsevier Publishing Co., 1965, 11.

Hess, V. F. and G. A. O'Donnell. "On the Rate of Ion Production." Journal of Geophysical Research, Vol. 56 (1951), 557-562.

Holzer, R. E. and D. S. Saxon. "Distribution of Electrical Conduction Currents in the Vicinity of Thunderstorms." Journal of Geophysical Research, Vol. 57 (1952), 207-216.

Israël, H. "Bemerkung zum Energie-Umsatz im Gewitter." Geofisica Pura Applications, Vol. 24 (1953), 3-11.

Kasemir, H. W. "The Thundercloud." Problems in Atmospheric Electricity. Ed. S. C. Coroniti. Amsterdam: Elsevier Publishing Co., 1965, 215.

Koenigsfeld, L. "Investigations of the Potential Gradient at the Earth's Ground Surface and Within the Free Atmosphere." Thunderstorm Electricity. Ed. H. Byers. Chicago: University of Chicago Press, 1953, 24.

Kraakevik, J. H. "Electrical Conduction and Convection Currents in the Troposphere." Recent Advances in Atmospheric Electricity. Ed. L. G. Smith. Oxford: Pergamon Press, 1958, 75.

Kroening, J. L. "Ion Density Measurements in the Stratosphere." Journal of Geophysical Research, Vol. 65 (1960), 145-151.

Law, J. "The Ionization of the Atmosphere Near the Ground in Fair Weather." Quarterly Journal Royal Meteorological Society, Vol. 89 (1963), 107-121.

Loeb, L. B. Fundamental Processes of Electrical Discharge in Gases. New York: J. Wiley and Sons, 1939.

Mühleisen, R. "Report on Atmospheric Electricity in Central Europe 1959-1962." Problems of Atmospheric and Space Electricity. Ed. S. C. Coroniti. Amsterdam: Elsevier Publishing Co., 1965, 25.

Neher, H. V., V. Z. Peterson, and E. A. Stern. "Fluctuations and Latitude Effect of Cosmic Rays at High Altitudes and Latitudes." Physical Review, Vol. 90 (1953), 655-674.

Neher, H. V., and H. Anderson. "Cosmic Ray Changes From 1954 to 1957." Physical Review, Vol. 109 (1958), 608.

Paltridge, G. W. "Experimental Measurements of the Small-Ion Density and Electrical Conductivity of the Stratosphere." Journal of Geophysical Research, Vol. 70 (1965), 2751-2761.

Phillips, B. B. et al. "An Experimental Analysis of the Effect of Air Pollution on the Conductivity and Ion Balance of the Atmosphere." Journal of Geophysical Research, Vol. 60 (1955), 289-296.

Sagalyn, R. C. and G. A. Faucher. "Aircraft Investigation of the Large Ion Content and Conductivity of the Atmosphere and Their Relation to Meteorological Factors." Journal of Atmospheric and Terrestrial Physics, Vol. 5 (1954), 253-272.

Sagalyn, R. C. and G. A. Faucher. "Space and Time Variations of Charged Nucleii and Electrical Conductivity of the Atmosphere." Quarterly Journal Royal Meteorological Society, Vol. 82 (1956), 428-445.

Sagalyn, R. C. "The Production and Removal of Small Ions and Charged Nucleii Over the Atlantic Ocean." Recent Advances in Atmsopheric Electricity. Ed. L. G. Smith. Oxford: Pergamon Press, 1958, 21.

Sayers, J. "Ionic Recombination in Air." Proceedings of the Royal Society of London, Vol. A169 (1938), 83.

Schonland, B. F. J. "The Interchange of Electricity Between Thunderclouds and the Earth." Proceedings of the Royal Society, Vol. 118 (1928), 252-262.

Schonland, B. F. J. Atmospheric Electricity. London: Metheun's Monographs on Physical Subjects, 1953.

Stergis, C. G. et al. "Conductivity Measurements in the Stratosphere." Journal of Atmospheric and Terrestrial Physics, Vol. 6 (1955), 233-242.

Stergis, C. G., G. C. Rein, and T. Kangas. "Electric Field Measurements in the Stratosphere." Journal of Atmospheric and Terrestrial Physics, Vol. 11 (1957), 77-82.

Stott, D. and W. C. A. Hutchinson. "The Electrification of Freezing Water Drops." Quarterly Journal Royal Meteorological Society, Vol. 91 (1965), 80-86.

Whipple, E. C. "Electricity in the Terrestrial Atmosphere Above the Exchange Layer." Problems of Atmospheric and Space Electricity. Ed. S. C. Coroniti. Amsterdam: Elsevier Publishing Co., 1965, 123.

Wilson, C. T. R. "Investigation on Lightning Discharges and on the Electric Field of Thunderstorms." Philosophical Transactiors Royal Society, Vol. 221 (1920), 73-115.

Woessner, R. H., W. E. Cobb, and R. Gunn. "Simultaneous Measurements of the Positive and Negative Light Ion Conductivities to 26 Kilometers." Journal of Geophysical Research, Vol. 63 (1958), 171-180.

Workman, E. J. and S. E. Reynolds. "Electrical Activity as Related to Thunderstorm Cell Growth." Bulletin American Meteorological Society, Vol. 30 (1949), 142-144.

Wormell, T. W. "Currents Carried by Point Discharge Beneath Thunderclouds and Showers." Proceedings of the Royal Society, Vol. 115 (1927), 443-455.

Wormell, T. W. "The Effects of Thunderstorms and Lightning Discharges on the Earth's Electric Field." Philosophical Transactions of the Royal Society, Vol. 238 (1939), 249-303.

Von Schweidler, E. Einführung in die Geophysik. Berlin: Springer, 1929.

APPENDIX A

THOMSON RECOMBINATION COEFFICIENT

A.1 Introduction. The Thomson recombination coefficient, α_T, which was used during analysis of the atmospheric model is derived in this Appendix[1]. α_T has been shown to apply for electron attaching gases, for example O_2, for pressures of 10^{-2} mm Hg to 760 mm Hg (Sayers, 1938).

A.2 Derivation of α_T. Consider two oppositely charged ions in the atmosphere separated by a distance r. The coulomb potential energy is

$$E = \frac{q^2}{4\pi\epsilon_0 r},$$

and assuming a Maxwell-Boltzman phase space distribution the average molecular kinetic energy is

$$K.E. = \frac{3}{2} kT$$

where k is Boltzman's constant and T is the absolute temperature. When the ions are within that distance d of each other where the two energies are equal, they are said to be within the sphere of active attraction. Thus d is defined by

$$\frac{3}{2} kT = \frac{q^2}{4\pi\epsilon_0 d}.$$

Thomson's theory states that even if the two ions are within d of

---

[1]The Thomson recombination theory is discussed in detail by Leonard B. Loeb, "Basic Processes of Gaseous Electronics", University of California Press, Berkeley, 1955, Chapter VI.

each other, recombination is not certain because the ions may possess sufficient energy to escape from the sphere of attraction. However, if either or both of the ions experience a kinetic collision with a neutral molecule while within this sphere then enough energy is lost in the collision so that recombination will occur.

Assume the ion densities are n_+ and n_- ions/cc, and the ions move with average thermal velocities v_+ and v_-. Then the ions move relative to each other with a random Maxwellian velocity of $[v_+^2 + v_-^2]^{1/2}$. Now assume further that ions of one polarity (positive say) are fixed in position, then a moving negative ion sweeps out an attractive volume of $\pi\, d^2[v_+^2 + v_-^2]^{1/2}$ cm^3 $-sec^{-1}$-ion^{-1} during which recombinations possibly occur. So that if recombination is proportional to the ion densities, the rate of change of ion density due to recombination is then

$$\frac{dn_+}{dt} = \varepsilon\, \pi\, d^2[v_+^2 + v_-^2]^{1/2}\, n_+ n_- = \alpha_T\, n_+ n_- \,, \qquad (A.1)$$

where ε is a probability function accounting for the probability of ion-molecule collisions.

Geometrically, consider the sphere of radius d centered about a fixed positive ion in Figure 37. The negative ion travels the path A-B. The probability that the negative ion escapes a molecular impact is given by the survival equatio e^{-x/L_-}, where L_- is the mean free path of the negative ion. The area of the annular ring is seen to be $2\pi d^2 \sin\phi d\phi$, and the area of the base of a hemisphere is πd^2, therefore the relative area is

$$\frac{2\pi d^2 \sin\phi d\phi}{\pi d^2} = 2 \sin\phi d\phi,$$

which is the probability of a path length 2d cos ϕ at the angle ϕ.

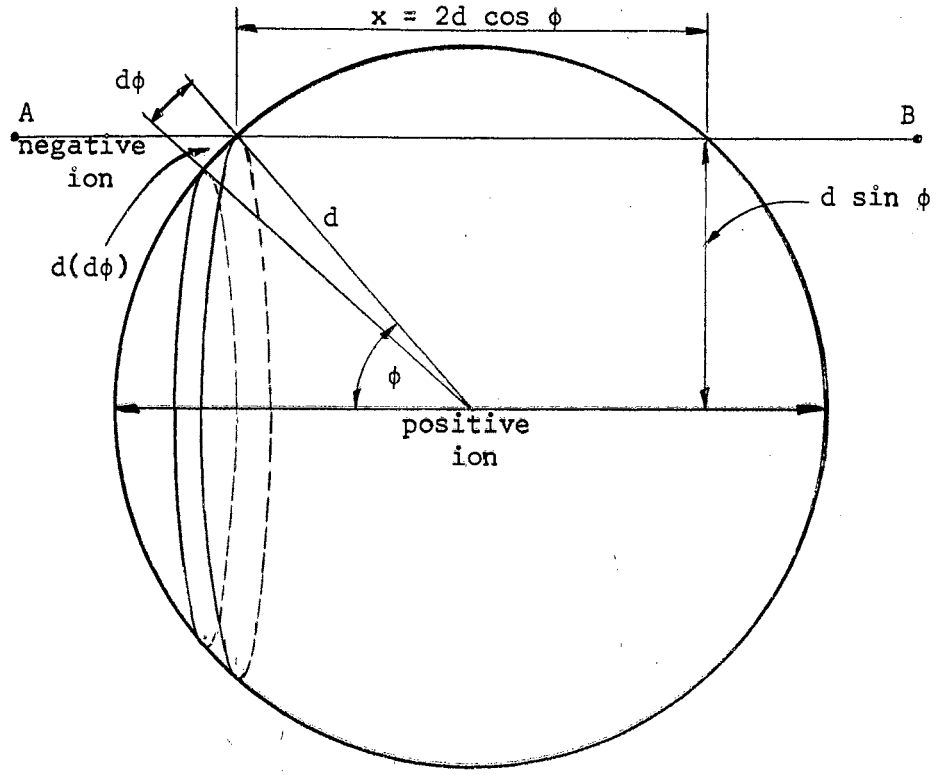

Figure 37. Sphere of Attraction

Then 2 sin ϕ cos $\phi d\phi$ gives the relative area perpendicular to the direction of travel, so that the probability of escaping a collision for any ϕ from 0 to $\pi/2$ is

$$I_- = \int_0^{\frac{\pi}{2}} e^{-\frac{2d\cos\phi}{L_-}} \sin\phi\cos\phi d\phi = \frac{2L_-^2}{4d^2}\left[1 - e^{-\frac{2d}{L_-}}\left(1 + \frac{2d}{L_-}\right)\right].$$

Then the probability of a negative ion-molecule collision and hence recombination is

$$P_- = 1 - I_-,$$

and the probability of a positive ion-molecule collision

$$P_+ = 1 - I_+,$$

where I_+ is obtained from I_- by replacing L_- with L_+. Finally the probability of either or both ions experiencing a collision is the logical union of P_+ and P_-, or

$$\varepsilon = P_+ \cup P_- = P_+ + P_- - P_+P_-.$$

If

$$v_+ = v_- = v$$

and

$$\frac{L_+ + L_-}{2} = L,$$

then α_T becomes

$$\alpha_T = (2)^{1/2}\ \pi v d^2\ (2P - P^2), \qquad (A.2)$$

where

$$P = [1 - \frac{L^2}{2d^2}\ (1 - e^{-\frac{2d}{L}}\ (\frac{2d}{L} + 1))].$$

Let

$$y = \frac{2d}{L}.$$

then

$$P(y) = [1 - \frac{2}{y^2}\ (1 - e^{-y}\ (y + 1))]$$

and

$$f(y) = 2P - P^2 = 1 - \frac{4}{y^4}\ [1 - e^{-y}\ (y + 1)]^2. \qquad (A.3)$$

Evaluating d gives

$$d = \frac{q^2}{4\pi\varepsilon_0(\frac{3}{2}kT)} = 4.05 \times 10^{-8} \left(\frac{273}{T}\right) \text{ meters} \qquad (A.4)$$

Loeb (1939) states that in air,

$$L \tilde{=} \frac{1 \times 10^{-5}}{3} \frac{760}{P}. \qquad (A.5)$$

And

$$v \tilde{=} 1.7 \times 10^{5} \left(\frac{2\ T}{273\ M}\right)^{\frac{1}{2}},$$

where M is the molecular weight. Thus

$$y = \frac{2d}{L} = 2.43 \left(\frac{273}{T}\right)^2 \left(\frac{P}{760}\right), \qquad (A.6)$$

and α_T becomes

$$\alpha_T \tilde{=} 1.73 \times 10^{-5} \left(\frac{273}{T}\right)^{\frac{3}{2}} \left(\frac{1}{M}\right)^{\frac{1}{2}} f(y). \qquad (A.7)$$

From experimental data at 293°K and 760 mm Hg, α_T is 1.6×10^{-6} cm^3 $-sec^{-1}$ $-ion^{-1}$. Evaluating y and f(y) under these conditions gives the value of $(\frac{1}{M})^{1/2}$, so that finally,

$$\alpha_T = 1.93 \times 10^{-6} \left(\frac{273}{T}\right)^{\frac{3}{2}} f(y),$$

where f(y) and y are given by Equations A.3 and A.6 respectively.

APPENDIX B

SAMPLE COMPUTER PROGRAMS

Sample listings of some of the computer programs used in the derivation and analysis of the atmospheric model are shown in the following tables.

Table VII shows the program used in Chapter IV to calculate mobilities, diffusivities and recombination coefficients. The input data consisted of altitude, temperature and pressure and initial (STP) ion mobilities. Temperature and pressure data was taken from "U. S. Standard Atmosphere, 1962" and its 1966 supplement. Double precision was used in the recombination coefficient calculations to reduce round off and truncation errors. Mobility and diffusivity calculations were not as critical and were made in single precision.

The programs used to implement the analysis of Section 6.5 are shown in Tables VIII and IX.

The program of Table VIII calculates ion concentration, electric field, conductivities and space charge density. Mobilities and diffusivities are determined using the relations given in Chapter IV. The input data is also shown in the listing. The electric field thus calculated is then integrated by the program shown in Table IX to determine the electric potential as a function of height.

TABLE VII

PROGRAM TO CALCULATE MODEL PARAMETERS

```
C      PROGRAM TO CALCULATE IONIC MOBILITIES, DIFFUSION COEFFICIENTS, AND
C      THOMSON RECOMBINATION COEFFICIENT FOR ALTITUDES TO 70KM. REQUIRED
C      INPUTS ARE ALTITUDE, PRESSURE, TEMPERATURE AND MOBILITIES FOR
C      POSITIVE AND NEGATIVE IONS AT STP.
       DOUBLE PRECISION X1,S,Y,ALPHA
1      WRITE(6,100)
C
C      READ INITIAL IONIC MOBILITIES.
C
2      READ(5,101)UP0,UN0
3      WRITE(6,102)UP0
4      WRITE(6,103)UN0
5      WRITE(6,104)
C
C      READ ALTITUDE, TEMPERATURE AND PRESSURE.
C
6      READ(5,105)Z,T,P
C
C      TEST FOR END OF DATA.
C
       IF(Z.GT.70.0)CALL EXIT
C
C      CALCULATE THOMSON RECOMBINATION COEFFICIENT.
C
       X1=2.43*((273.0/T)**2.0)*(P/760.0)
       S=1.0-(2.0/(X1**2.0))*(1.0-(DEXP(-X1))*(X1+1.0))
       Y=2.0*S-(S*S)
       ALPHA=(1.93E-06)*((273.0/T)**1.5)*Y
C
C      CALCULATE ION MOBILITIES.
C
       UP=UP0*(760.0/P)*(T/273.0)
       UN=UN0*(760.0/P)*(T/273.0)
C
C      USING EINSTEIN RELATION FOR CALCULATING DIFFUSION COEFFICIENTS.
C
       DP=(((1.38E-23)*T)/1.602E-19)*UP
       DN=(((1.38E-23)*T)/1.602E-19)*UN
       WRITE(6,106)Z,UP,UN,X1,Y,ALPHA,DP,DN
       GO TO 6
100    FORMAT(1X,104HTHOMSON RECOMBINATION COEFFICIENT AND POSITIVE AND N
      1EGATIVE SMALL ION MOBILITIES FOR ALTITUDES TO 70 KM.)
101    FORMAT(2F10.5)
102    FORMAT(1H0,3X,41HPOS ION MOBILITY AT STP(SQ CM/VOLT-SEC)=    ,E9.4)
103    FORMAT(4X,41HNEG ION MOBILITY AT STP(SQ CM/VOLT-SEC)=    ,E9.4)
104    FORMAT(1H0,1X,129H    Z(KM)        UP(SQ CM/VOLT-SEC)  UN(SQ CM/VOL
      1T-SEC)    X          F(X)       ALPHA(CC/ION-SEC)        DP(SQ CM/SEC)
      1  DN(SQ CM/SEC))
105    FORMAT(3F10.5)
106    FORMAT(3E16.4,3D16.4,2E16.4)
       END
$ENTRY
$IBSYS
```

TABLE VIII

PROGRAM FOR MODEL SOLUTION

```
$ID         A-0001 ED SHREVE                        4367-51001
$JOB                ED SHREVE                       4367-51001
$IBJOB NAMEPR  MAP
$IBFTC DCKNAM
C     PROGRAM TO CALCULATE IONIC CONCENTRATION AND ELECTRIC FIELD
C     ASSUMING CONSTANT CONDUCTION CURRENT IMPLIES CONSTANT DIFFUSION
C     CURRENT.
C
C     READ INITIAL CONDITIONS.
C
1     READ(5,1000) CPZ,CPPZ,EZERO,ZZERO,CDZ,CCZ
      WRITE(6,1001)
      CDZERO=CDZ*1.0E-19
      CCZERO=CCZ*1.0E-12
      ZMAX=7.0E+04
      DZ=5.0E+02
      CK=1.602E-19
      U1=1.4E-04
      UZERO=1.4E-04
      C1=1.357
      Z=ZZERO
C
C     Z=ALTITUDE.
C     DZ=ALTITUDE INCREMENT.
C     CK=ELECTRONIC CHARGE.
C     U1=MOBILITY EXPONENT.
C     UZERO=INITIAL POSITIVE ION MOBILITY.
C
      CPZERO=CPZ*1.0E+09
      CPMZRO=CPPZ*1.0E+05
      WRITE(6,1003) CPZERO
      WRITE(6,1004) CPMZRO
      WRITE(6,1005) CDZERO
      WRITE(6,1006) CCZERO
C
C     CPZERO=INITIAL ION CONCENTRATION.
C     CPMZRO=INITIAL DERIVATIVE OF ION CONCENTRATION.
C     CDZERO=INITIAL DIFFUSION CURRENT DENSITY.
C     CCZERO=INITIAL DRIFT CURRENT DENSITY.
C
C     TEST FOR END OF DATA.
C
      IF(CPZERO.EQ.0.0) CALL EXIT
C
C     PARAMETERS FOR DIFFUSION COEFFICIENT CALCULATIONS.
C
      D11=0.916E-04
      D1ZERO=3.6E-06
      D12=1.534E-04
      D2ZERO=1.939E-06
      D13=1.17E-04
      D3ZERO=1.2006E-05
      X1=(1.0/(D1ZERO*D11))*(EXP(-D11*ZZERO)-EXP(-D11*1.0E+04))
      X2=(1.0/(D2ZERO*D12))*(EXP(-D12*1.0E+04)-EXP(-D12*5.0E+04))
C
C     CALCULATE MOBILITIES.
C
2     UPOS=UZERO*EXP(U1*Z)
      UNEG=C1*UPOS
C
C     CALCULATE DIFFUSION COEFFICIENTS AND ION CONCENTRATION.
C
      IF(Z.GT.1.0E+04) GO TO 3
      DCP=D1ZERO*EXP(D11*Z)
      DCN=C1*DCP
      CP=CPZERO+(CDZERO/(CK*(C1-1.0)*D1ZERO*D11))*(EXP(-D11*ZZERO)-EXP(-
     1D11*Z))
      GO TO 6
3     IF(Z.GT.5.0E+04) GO TO 4
      DCP=D2ZERO*EXP(D12*Z)
      DCN=C1*DCP
      CP=CPZERO+(CDZERO/(CK*(C1-1.0)))*(X1+(1.0/(D2ZERO*D12))*(EXP(-D12*
     11.0E+04)-EXP(-D12*Z)))
      GO TO 6
4     DCP=D3ZERO*EXP(D13*Z)
      DCN=C1*DCP
      CP=CPZERO+(CDZERO/(CK*(C1-1.0)))*(X1+X2+(1.0/(D3ZERO*D13))*(EXP(-D
     113*5.0E+04)-EXP(-D13*Z)))
C
C     CONVERT ALTITUDE FROM METERS TO KILOMETERS FOR PRINTOUT.
C
6     Z1=Z*1.0E-03
C
C     CALCULATE ELECTRIC FIELD.
C
      EF=CCZERO/(CP*(C1+1.0)*UPOS*CK)
C
C     CALCULATE TOTAL AND POLAR CONDUCTIVITIES.
C
      SIGMAP=CK*UPOS*CP
      SIGMAN=CK*UNEG*CP
      SIGTOT=SIGMAP+SIGMAN
C
C     CALCULATE SPACE CHARGE DENSITY.
C
      RH1=((-CCZERO)*((CDZERO/((C1-1.0)*CK*DCP))+(1.4E-04)*CP))/((C1+1.0
     1)*CK*UPOS*CP*CP)
      RHO=RH1*8.854E-12
      WRITE(6,1002)Z1,CP,EF,DCP,DCN,UPOS,UNEG,SIGMAP,SIGMAN,SIGTOT,RHO
      Z=Z+DZ
      IF(Z.LE.ZMAX) GO TO 2
      GO TO 1
1000  FORMAT(6F12.6)
1001  FORMAT(1X,125HZ(KM) CP(IONS/QM) EF(V/M)   DPOS(SQM/SEC)DNEG(SQM/SE
     1) UP(SQM/V-S)UN(SQM/V-S) SIGP(MHO/M) SIGN(MHO/M) SIGT(MHO/M) RHO(C
     2OUL/QM))
1002  FORMAT(F5.1,10E12.6)
1003  FORMAT(1X,18HCPZERO(IONS/M**3)= ,E15.8)
1004  FORMAT(1X,18HCPMZRO(IONS/M**4)= ,E15.8)
1005  FORMAT(1X,18HCDZERO(AMPS/M**2)= ,E15.8)
1006  FORMAT(1X,18HCCZERO(AMPS/M**2)= ,E15.8)
      END
$ENTRY
1.0         3.0         -70.0       2000.0      .757        -4.9
1.0         3.0         -25.0       2000.0      .757        -1.75
1.329       1.7         -70.0       2000.0      .42         -6.51
1.329       1.7         -25.0       2000.0      .42         -2.325
0.0         3.0         -70.0       2000.0      .757        -4.9
$IBSYS
```

TABLE IX

PROGRAM TO CALCULATE ATMOSPHERIC POTENTIAL

```
$ID          A-0001 ED SHREVE                          4367-51001
$JOB                ED SHREVE                          4367-51001
$IBJOB NAMEPR  MAP
$IBFTC DCKNAM
C      PROGRAM TO INTEGRATE ELECTRIC FIELD TO OBTAIN IONOSPHERIC
C      POTENTIAL
       DOUBLE PRECISION Y,Z,H,HT,SUM1,SUM2,AUX,AUX1,AUX2
       DIMENSION ZZ(200),Y(200),Z(200),XEF(200),XZ(200),EF(200)
C
C      READ INITIAL CONDITIONS.
C
10     READ(5,1000) H,NDIM,EZERO,CPZERO
       WRITE(6,1001) EZERO
       WRITE(6,1002) CPZERO
C
C      H=INTEGRATION STEP SIZE.
C      NDIM=NUMBER OF DATA CARDS.
C      EZERO=INITIAL ELECTRIC FIELD.
C      CPZERO=INITIAL ION CONCENTRATION.
C
C      TEST FOR END OF DATA.
C
       IF(H.EQ.0.0) CALL EXIT
       WRITE(6,1003)
C
C      READ ALTITUDE AND ELECTRIC FIELD DATA CARDS.
C
       DO 1 I=1,NDIM
1      READ(5,1004) ZZ(I),EF(I)
C
C      CHANGE SIGN OF ELECTRIC FIELD.
C
       DO 2 I=1,NDIM
2      Y(I)=-EF(I)
C
C      CALL INTEGRATION SUBROUTINE.
C
       CALL DQSF(H,Y,Z,NDIM)
C
C      PRINT OUT ALTITUDE, ELECTRIC FIELD AND POTENTIAL.
C
       DO 3 I=1,NDIM
3      WRITE(6,1005) ZZ(I),EF(I),Z(I)
       GO TO 10
1000   FORMAT(F8.4,I4,2F8.4)
1001   FORMAT(1X,11HEZERO(V/M)=,E15.8)
1002   FORMAT(1X,30HCPZERO((IONS/M**3)*(10.E-09))= ,E15.8)
1003   FORMAT(1X,36H  Z(KM)     EF(V/M)      ATMPOT(VOLTS))
1004   FORMAT(F8.2,15X,E15.8)
1005   FORMAT(F8.2,2E15.8)
       END
$ENTRY
$IBSYS
```

APPENDIX C

SOLUTION OF THUNDERSTORM MODEL

C.1 Problem Definition. The simplest case will be examined first and the result extended to the general case of Chapter VII. Thus, the electric potential inside a grounded cylindrical box when point charges are located on the cylinder's axis (Z axis) is desired. The cylinder is defined by

$$0 \leq Z \leq h$$

and

$$r = b \quad .$$

Also, the conductivity of the cylinder varies with height according to the expression

$$\sigma = \sigma_0 e^{aZ} \quad .$$

As shown in Chapter VII the equation for the electric potential is

$$\nabla^2 V + a \frac{\partial V}{\partial Z} = \sum_{i=1}^{p} \frac{q_i}{\epsilon_0} \frac{\delta(r)\, \delta(Z - Z_i)}{2\pi r} = - \sum_{i=1}^{p} \frac{\rho_i}{\epsilon_0} \quad . \qquad (C.1)$$

Where p is the number of point charges, and q_i is located at the point

$$\overline{r_i} = (r_i, \phi_i, Z_i) = (0, 0, Z_i) \quad .$$

From symmetry it is seen that the potential is independent of the

azimuthal angle. V is also subject to the boundary conditions.

$$V(r,0) = V(r,h) = V(b,Z) = 0 \quad . \tag{C.2}$$

In Equation C.1, impulse functions are used to denote the charge location in cylindrical coordinates, so that integrating the charge density over the volume of a small cylinder centered at the ith charge should yield, q_i, i.e.,

$$\int\int\int \rho_i \, dV = \int_{\phi=0}^{2\pi} d\phi \int_{Z=Z_i-\varepsilon}^{Z_i+\varepsilon} \int_{r=0}^{\varepsilon} q_i \frac{\delta(r)\delta(Z - Z_i)rdrdZ}{2\pi r} = q_i$$

where the known integral properties of the impulse function,

$$\int_{C-\varepsilon}^{C+\varepsilon} \delta(x - C)dx = 1$$

have been used.

The solution will be obtained for only one charge and then superposition will allow extension to any number of charges on the axis. Superposition will again be used to solve the problem if one end of the cylinder is at a potential V_0. Finally, to form the thunderstorm model, the radius b will be allowed to increase to give the potential at large distances from the thunderstorm. This solution will then be generalized to include the case where the charges are not on the axis. The method of solution will be to construct a Green's function from the eigenvalues of the differential operator of Equation C.1 subject to the boundary conditions of Equation C.2.

C.2 Solution for one Charge on the Axis. For one charge, Equation C.1 becomes

$$L(V) = \frac{-q_1 \, \delta(r) \, \delta(Z - Z_1)}{2\pi\varepsilon_0 r} \quad , \tag{C.3}$$

Where L is the operator

$$\nabla^2 + a \frac{\partial}{\partial V} = \frac{1}{r} \frac{\partial}{\partial r} \left(r \frac{\partial}{\partial r}\right) + \frac{\partial^2}{\partial Z^2} + a \frac{\partial}{\partial Z} \quad .$$

In order to find the eigenvalues and eigenfunctions of L subject to C.2, consider the homogeneous equation

$$\frac{1}{r} \frac{\partial}{\partial r} \left(r \frac{\partial V}{\partial r}\right) + \frac{\partial^2 V}{\partial Z^2} + a \frac{\partial V}{\partial Z} = 0 \quad . \qquad (C.4)$$

Assume a product solution of the form

$$V(r,Z) = R(r)\, Q(Z) \quad ,$$

and using the standard separation of variables technique, Equation C.4 gives

$$\frac{1}{Q} \frac{d^2Q}{dZ^2} + \frac{a}{Q} \frac{dQ}{dZ} = - \frac{1}{rR} \frac{d}{dr} \left(r \frac{dR}{dr}\right) = - m^2 \quad ,$$

where m is a separation constant. Then

$$\frac{d^2Q}{dZ^2} + a \frac{dQ}{dZ} + m^2 Q = 0$$

which has the general solution

$$Q(Z) = e^{-\frac{aZ}{2}} \left[A \cos\left(m^2 - \frac{a^2}{4}\right)^{\frac{1}{2}} Z + V \sin\left(m^2 - \frac{a^2}{4}\right)^{\frac{1}{2}} Z\right] \qquad (C.5)$$

For the radial dependence,

$$\frac{1}{rR} \left(r \frac{d^2R}{dr^2} + \frac{dR}{dr}\right) - m^2 = 0 \quad ,$$

or

$$\frac{d^2R}{dr^2} + \frac{1}{r} \frac{dR}{dr} - m^2 R = 0 \quad .$$

This is the modified Bessel equation with the solution in terms of

modified Bessel functions of zero order,

$$R(r) = C_1 I_0(mr) + D_1 K_0(mr) \quad . \tag{C.6}$$

The product solution is

$$V(r,Z) = e^{-\frac{aZ}{2}} \left[A \cos\left(m^2 - \frac{a^2}{4}\right)^{\frac{1}{2}} Z + B \sin\left(m^2 - \frac{a^2}{4}\right)^{\frac{1}{2}} Z\right] \cdot$$

$$\left[C_1 I_0(mr) + D_1 K_0(mr)\right]$$

From Equation C.2,

$$V(r,0) = A\left[C_1 I_0(mr) + D_1 K_0(mr)\right] = 0 \quad ,$$

which implies A = 0. Also

$$V(r,h) = e^{-\frac{ah}{2}} \left[\sin\left(m^2 - \frac{a^2}{4}\right)^{\frac{1}{2}} h\right] \left[CI_0(mr) + DK_0(mr)\right] = 0 \quad .$$

Then

$$\sin\left(m^2 - \frac{a^2}{4}\right)^{\frac{1}{2}} h = n\pi, \qquad n = 1, 2, \ldots \quad .$$

From this relation the eigenvalues, m_n, are found to be

$$m_n^2 = \frac{n^2\pi^2}{h^2} + \frac{a^2}{4} \quad , \tag{C.7}$$

so that the solution becomes

$$V_n(r,Z) = e^{-\frac{aZ}{2}} \sin\frac{n\pi Z}{h} \left[C_n I_0(m_n r) + D_n K_0(m_n n)\right] \quad .$$

Now from Green's function theory[1] the Green's function for the given

---

[1] A detailed treatment of Green's function expansions is given in Chapter III of "Classical Electrodynamics" by J. D. Jackson, John Wiley & Sons, New York, 1962.

differential equation and boundary conditions can be expressed as an expansion using the above eigenfunctions. Since by definition, the Green's function is the potential due to a unit point charge, then finding the Green's function and multiplying by q_i will give the desired potential. Consequently, solutions of the form

$$V(r,Z) = \sum_{n=1}^{\infty} e^{-\frac{aZ}{2}} R_n(r) \sin \frac{n\pi Z}{h} \qquad (C.8)$$

are to be determined, where

$$R_n(r) = A_n I_0(m_n r) + B_n K_0(m_n r) \quad .$$

From the boundary condition

$$R_n(b) = A_n I_0(m_n b) + B_n K_0(m_n b) = 0 \ ,$$

$$B_n = - A_n \frac{I_0(m_n b)}{K_0(m_n b)} \ ,$$

so that

$$R_n(r) = A_n [I_0(m_n r) - \frac{I_0(m_n b)}{K_0(m_n b)} K_0(m_n r)] \quad . \qquad (C.9)$$

Inserting C.8 into the nonhomogeneous Equation C.3 gives

$$\sum_{n=1}^{\infty} e^{-\frac{aZ}{2}} \sin \frac{n\pi z}{h} \frac{1}{r} \frac{d}{dr} (r \frac{dR_n}{dr}) + \sum_{n=1}^{\infty} R_n(r) \frac{d^2}{dZ^2} e^{-\frac{aZ}{2}} \sin \frac{n\pi Z}{h}$$

$$+ a \sum_{n=1}^{\infty} R_n(r) \frac{d}{dZ} e^{-\frac{aZ}{2}} \sin \frac{n\pi Z}{h} = - \frac{q_1 \, \delta(r) \, \delta(Z - Z_1)}{2\pi\epsilon_0 r} \quad .$$

Performing the differentiation and collecting terms using Equation C.7 gives

$$\sum_{n=1}^{\infty} \left[\frac{1}{r}\frac{d}{dr}\left(r\frac{dR}{dr}\right) \sin\frac{n\pi Z}{h} - R_n m_n^2 \sin\frac{n\pi Z}{h}\right] = \frac{-q_1\,\delta(r)\,\delta(Z - Z_1)e^{\frac{aZ}{2}}}{2\pi\varepsilon_0 r} \quad . \tag{C.10}$$

Multiplying both sides of Equation C.10 by $\frac{2}{h}\sin\frac{p\pi Z}{h}$ and integrating from 0 to h gives

$$\frac{1}{r}\frac{d}{dr}\left(r\frac{dR_n}{dr}\right) - m_n^2 R_n = \frac{-q_1\,\delta(r)e^{aZ_1}}{\pi r\varepsilon_0 h}\sin\frac{n\pi Z_1}{h} \quad . \tag{C.11}$$

This result follows from the orthonormal properties of the sine function and the sifting property of the delta function, i.e.,

$$\frac{2}{h}\int_0^h \sin\frac{n\pi Z}{h}\sin\frac{p\pi Z}{h}\,dZ = \delta_{np} = \begin{cases} 1, & n = p \\ 0, & n \neq p \end{cases}$$

and

$$\int_{Z_1-\varepsilon}^{Z_1+\varepsilon} f(Z)\,\delta(Z - Z_1)\,dZ = f(Z_1) \quad .$$

Now multiplying Equation C.11 by r and integrating r from 0 to ε gives

$$\int_0^{\varepsilon}\frac{d}{dr}\left(r\frac{dR_n}{dr}\right)dr - \int_0^{\varepsilon} m_n^2\, r\, R_n\,dr = \frac{-q_1 e^{aZ_1}}{\pi\varepsilon_0 h}\sin\frac{n\pi Z_1}{h}\int_0^{\varepsilon}\delta(r)dr \quad .$$

The limit as ε approaches zero then gives

$$\lim_{\varepsilon\to 0} r\frac{dR_n}{dr}\Big|_0^{\varepsilon} - \lim_{\varepsilon\to 0}\int_0^{\varepsilon} m_n^2 r R_n\,dr = \frac{-q_1 e^{aZ_1}}{\pi\varepsilon_0 h}\sin\frac{n\pi Z_1}{h} \quad .$$

The second term vanishes since rR_n is a continuous function, so that

$$\lim_{\varepsilon\to 0} r\frac{dR_n}{dr}\Big|_0^{\varepsilon} = \frac{-q_1 e^{aZ_1}}{\pi\varepsilon_0 h}\sin\frac{n\pi Z_1}{h} \quad ,$$

or

$$\lim_{\varepsilon\to 0}\left[rm_n A_n \frac{d}{d(rm_n)}\left(I_0(m_n r) - \frac{I_0(m_n b)}{K_0(m_n b)} K_0(m_n r)\right)\right]_0^{\varepsilon} = \frac{-q_1 e^{\frac{aZ_1}{}}}{\pi\varepsilon_0 h} \sin\frac{n\pi Z_1}{h} \quad . \tag{C.12}$$

Using the known Bessel function identities

$$\frac{d}{dx} K_m(x) = \frac{mK_m(x)}{x} - K_{m+1}(x) \quad ,$$

and

$$\frac{d}{dx} I_m(x) = \frac{mI_m(x)}{x} + I_{m+1}(x) \quad ,$$

Equation C.12 ($m = 0$, $x = m_n r$) becomes

$$\lim_{\varepsilon\to 0}\left[m_n r A_n\left(I_1(m_n r) + \left(\frac{I_0(m_n b)}{K_0(m_n b)}\right) K_1(m_n r)\right)\right]_{\varepsilon} = \frac{-q_1 e^{\frac{aZ_1}{2}}}{\pi\varepsilon_0 h} \sin\frac{n\pi Z_1}{h}$$

or

$$\lim_{\varepsilon\to 0}\left[m_n A_n \varepsilon\left(I_1(m_n\varepsilon) + \left(\frac{I_0(m_n b)}{K_0(m_n b)}\right) K_1(m_n\varepsilon)\right)\right] = \frac{-q_1 e^{\frac{aZ_1}{2}}}{\pi\varepsilon_0 h} \sin\frac{n\pi Z_1}{h} \quad . \tag{C.13}$$

For small arguments,

$$I_k(x) \sim \frac{1}{2^k k!} x^k$$

and

$$K_k(x) \sim \frac{2^{k-1}(k-1)!}{x^k} \quad ,$$

so that

$$\lim_{\varepsilon\to 0} A_n\left[\frac{(m_n\varepsilon)^2}{2} + \frac{I_0(m_n b)}{K_0(m_n b)} \frac{m_n\varepsilon}{m_n\varepsilon}\right] = A_n \frac{I_0(m_n b)}{K_0(m_n b)} \quad .$$

Then from Equation C.13,

$$A_n = -\frac{K_0(m_n b)\, q_1 e^{\frac{aZ_1}{2}}}{I_0(m_n b)\, \varepsilon_0 \pi h} \sin\frac{n\pi Z_1}{h} \quad .$$

Using this result for A_n in Equation C.9 and then putting C.9 into C.8 gives as the desired potential:

$$V(r,Z) = \frac{q_1 e^{-\frac{a}{2}(Z-Z_1)}}{\varepsilon_0 \pi h} \sum_{n=1}^{\infty} \left[\frac{I_0(m_n b)\, K_0(m_n r) - K_0(m_n b)\, I_0(m_n r)}{I_0(m_n b)} \right.$$

$$\left. \sin \frac{n\pi Z}{h} \sin \frac{n\pi Z_1}{h} \right] \quad . \qquad \text{(C.14)}$$

For q_1 a unit charge, C.14 is the Green's function for the operator in Equation C.3 subject to the given boundary equations. In the limit as $b \to \infty$, Equation C.14 becomes

$$V(r,Z) = \frac{q_1 e^{-\frac{a}{2}(Z-Z_1)}}{\varepsilon_0 \pi h} \sum_{n=1}^{\infty} K_0(m_n r) \sin \frac{n\pi Z}{h} \sin \frac{n\pi Z_1}{h} \quad , \qquad \text{(C.15)}$$

because

$$\lim_{x \to \infty} K_0(x) = 0 \quad .$$

C.3 Solution for an Arbitrary Number of Charges on the Axis. For more than one charge on the axis, the potential function is a superposition of solutions of the form given in Equation C.15, i.e.,

$$V(r,Z) = \sum_{i=1}^{p} \frac{q_i e^{-\frac{a}{2}(Z-Z_i)}}{\varepsilon_0 \pi h} \sum_{n=1}^{\infty} K_0(m_n r) \sin \frac{n\pi Z}{h} \sin \frac{n\pi Z_i}{h} \qquad \text{(C.16)}$$

Now consider this cylinder of large radius with no charges present. If the top is at a potential V_0 and the bottom at zero potential, then the potential within the cylinder is a function only of Z so that Equation C.3 is

$$\frac{d^2V}{dZ^2} + a \frac{dV}{dZ} = 0 \quad .$$

The solution is

$$V(Z) = C_1 + C_2 e^{-aZ} \quad ,$$

which after evaluating the integration constants becomes

$$V(Z) = V_0 \frac{1 - e^{-aZ}}{1 - e^{-ah}} \quad . \qquad (C.17)$$

This result can be added to Equation C.16 to give the complete solution for the potential due to the charges in a thunderstorm and due to the ionospheric potential V_0, i.e.,

$$V(r,Z) = V_0 \left[\frac{1 - e^{-aZ}}{1 - e^{-ah}}\right] + \sum_{i=1}^{p} \frac{q_i e^{-\frac{a}{2}(Z-Z_i)}}{\varepsilon_0 \pi h} \sum_{n=1}^{\infty} K_0(m_n r) \sin \frac{n\pi Z}{h} \sin \frac{n\pi Z_i}{h} \qquad (C.18)$$

C.4 Solution Assuming the Ionospheric Height Approaches Infinity.

In the case of the limiting transition $h \to \infty$, Equation C.18 assumes a more simple form. Under this assumption, the contribution due to the ionospheric potential becomes

$$\lim_{h\to\infty} V_0 \left[\frac{1 - e^{-aZ}}{1 - e^{-ah}}\right] = V_0(1 - e^{-aZ}) \quad .$$

Now consider the inner sum of Equation C.18

$$V_i = \frac{q_i}{\varepsilon_0 \pi h} \sum_{n=1}^{\infty} K_0(m_n r) \sin \frac{n\pi Z}{h} \sin \frac{n\pi Z_i}{h} \quad .$$

Then if

$$\mu_n = \frac{n\pi}{h} \quad ,$$

$$V_i = \frac{q_i}{\varepsilon_0 \pi^2} \sum_{n=1}^{\infty} K_0(m_n r) \sin \mu_n Z \sin \mu_n Z_i \, \Delta \mu_n \quad .$$

So that in the limit,

$$V_i \to \frac{q_i}{\varepsilon_0 \pi^2} \int_0^\infty K_0(mr) \sin \mu Z \sin \mu Z_i \, d\mu$$

$$= \frac{q_i}{2\pi^2 \varepsilon_0} \int_0^\infty K_0\left[\left(\mu^2 + \frac{a^2}{4}\right)^{\frac{1}{2}} r\right] \left[\cos \mu(Z - Z_i) - \cos \mu(Z + Z_i)\right] d\mu \, .$$

Using the known Bessel function identity

$$\int_0^\infty K_0\left[\left(\mu^2 + \frac{a^2}{4}\right)^{\frac{1}{2}} r\right] \cos \mu(Z - Z_i) d\mu = \frac{\pi \, e^{-\frac{a}{2}\left(r^2 + (Z-Z_i)^2\right)^{\frac{1}{2}}}}{2\left(r^2 + (Z-Z_i)^2\right)^{\frac{1}{2}}} \, ,$$

gives

$$V_i = \frac{q_i}{4\pi\varepsilon_0} \left\{ \frac{e^{-\frac{a}{2}\left(r^2 + (Z-Z_i)^2\right)^{\frac{1}{2}}}}{\left(r^2 + (Z-Z_i)^2\right)^{\frac{1}{2}}} - \frac{e^{-\frac{a}{2}\left(r^2 + (Z+Z_i)^2\right)^{\frac{1}{2}}}}{\left(r^2 + (Z+Z_i)^2\right)^{\frac{1}{2}}} \right\} \, .$$

Then for $h \to \infty$, Equation C.18 becomes

$$V(r,Z) = V_0(1 - e^{-aZ}) + \sum_{i=1}^{P} \frac{q_i e^{-\frac{a}{2}(Z-Z_i)}}{4\pi\varepsilon_0} \left\{ \frac{e^{-\frac{a}{2}\left(r^2 + (Z-Z_i)^2\right)^{\frac{1}{2}}}}{\left(r^2 + (Z-Z_i)^2\right)^{\frac{1}{2}}} - \frac{e^{-\frac{a}{2}\left(r^2 + (Z+Z_i)^2\right)^{\frac{1}{2}}}}{\left(r^2 + (Z+Z_i)^2\right)^{\frac{1}{2}}} \right\} \tag{C.19}$$

for the potential in the atmosphere due to the ionospheric potential and charges on the thunderstorm axis.

C.5 Solution for Charges not on the Axis. Assume q_i is located at the point

$$\vec{r}_i = (r_i, \phi_i, Z_i)$$

then azimuthal symmetry no longer obtains and the operator L becomes

$$L = \frac{1}{r}\frac{\partial}{\partial r}\left(r\frac{\partial}{\partial r}\right) + \frac{1}{r^2}\frac{\partial^2}{\partial \phi^2} + \frac{\partial^2}{\partial Z^2} + a\frac{\partial}{\partial Z} \quad .$$

Then proceeding just as in Section C.2 gives, instead of Equation C.18,

$$V(r,\phi,Z) = V_0\left[\frac{1 - e^{-aZ}}{1 - e^{-ah}}\right] + \sum_{i=1}^{p}\frac{q_i e^{-\frac{a}{2}(Z-Z_i)}}{\varepsilon_0 \pi h}\sum_{k=-\infty}^{\infty} e^{ik(\phi-\phi_i)}\sum_{n=1}^{\infty}\left[I_k(m_n r_i)\, K_k(m_n r)\sin\frac{n\pi Z}{h}\sin\frac{n\pi Z_i}{h}\right] \qquad (C.20)$$

where it is required that

$$r > r_i \qquad \text{for all } i \quad .$$

C.6 Electric Field Derivations. The electric field will be determined for the two cases described by Equations C.18 and C.19 using the fact that under static conditions

$$\bar{E} = -\bar{\nabla} V \quad .$$

In cylindrical coordinates, assuming azimuthal symmetry,

$$\bar{E} = (E_r, E_Z) = -\left[\frac{\partial V}{\partial r}\bar{a}_r + \frac{\partial V}{\partial Z}\bar{a}_Z\right] \quad ,$$

where $\bar{a}_r$ and $\bar{a}_Z$ are unit vectors in the r and Z directions respectively.

From Equation C.18, where due to the nature of the functions involved, it is assumed term-by-term differentiation is permitted,

$$E_r = -\sum_{i=1}^{p}\frac{q_i e^{-\frac{a}{2}(Z-Z_i)}}{\varepsilon_0 \pi h}\sum_{n=1}^{\infty} m_n K_1(m_n r)\sin\frac{n\pi Z}{h}\sin\frac{n\pi Z_i}{h} \qquad (C.21)$$

and

$$E_Z = - \frac{aV_0 e^{-aZ}}{1-e^{-ah}} - \frac{1}{\varepsilon_0 \pi h} \sum_{i=1}^{p} q_i e^{-\frac{a}{2}(Z-Z_i)} [(\sum_{n=1}^{\infty} \frac{n\pi}{h} K_0(m_n r) \cos \frac{n\pi Z}{h} \sin \frac{n\pi Z_i}{h})$$

$$- \frac{a}{2} (\sum_{n=1}^{\infty} K_0(m_n r) \sin \frac{n\pi Z}{h} \sin \frac{n\pi Z_i}{h})] \quad . \qquad (C.22)$$

As $r \to \infty$, the field components become

$$E_r \to 0$$

$$E_Z = - \frac{aV_0 e^{-aZ}}{1-e^{-ah}}$$

which follows because

$$\lim_{x \to \infty} K_k(x) = 0 \quad .$$

Thus at large distances from thunderstorm activity, the electric field is vertical, negative, and decreases exponentially with height.

From Equation C.19,

$$E_r = \frac{1}{4\pi\varepsilon_0} \sum_{i=1}^{p} q_i e^{-\frac{a}{2}(Z-Z_i)} \left[\frac{r}{R_1^2} e^{-\frac{a}{2}R_1} (\frac{a}{2} + \frac{1}{R_1}) - \frac{r}{R_2^2} e^{-\frac{a}{2}R_2} (\frac{a}{2} + \frac{1}{R_2}) \right] \qquad (C.23)$$

and

$$E_Z = - aV_0 e^{-aZ} + \frac{1}{4\pi\varepsilon_0} \sum_{i=1}^{p} q_i e^{-\frac{a}{2}(Z-Z_i)} \left[\frac{(Z-Z_i)}{R_1^2} e^{-\frac{a}{2}R_1} (\frac{a}{2} + \frac{1}{R_1}) \right.$$

$$\left. - (\frac{Z-Z_i}{R_2^2}) e^{-\frac{aR_2}{2}} (\frac{a}{2} + \frac{1}{R_2}) + \frac{a}{2} (\frac{e^{-\frac{a}{2}R_1}}{R_1} - \frac{e^{-\frac{a}{2}R_2}}{R_2}) \right] \qquad (C.24)$$

where

$$R_1 = (r^2 + (Z - Z_i)^2)^{\frac{1}{2}}$$

and

$$R_2 = (r^2 + (Z + Z_i)^2)^{\frac{1}{2}} \quad .$$

Again letting $r \to \infty$, results in

$$E_r = 0$$

and

$$E_Z = - aV_0 e^{-aZ} \quad ,$$

with the same conclusion as before regarding the electric field far removed from thunderstorm activity.

VITA

Edward Lyle Shreve

Candidate for the Degree of

Doctor of Philosophy

Thesis: AN ANALYSIS OF CHARGE TRANSPORT AND EQUILIBRIUM IN THE GLOBAL ATMOSPHERE

Major Field: Electrical Engineering

Biographical:

Personal Data: Born on October 21, 1934, in Oklahoma City, Oklahoma, the son of Everett L. and Jessie F. Shreve.

Education: Attended primary and secondary schools in Oklahoma City, Oklahoma, and graduated from Capitol Hill High School in May, 1953; received the Bachelor of Science degree in Electrical Engineering from the University of Oklahoma in June, 1962; received the Master of Science degree in Electrical Engineering from New Mexico State University in June, 1964; completed requirements for the Doctor of Philosophy degree at Oklahoma State University in May, 1969.

Professional Experience: Electronics Technician, U. S. Navy from November, 1953 to September, 1957; employed by Western Electric, Oklahoma City, Oklahoma during Summer, 1961; employed by Bell Telephone Laboratories, White Sands Missile Range, New Mexico as a member of the technical staff from February, 1962 to January, 1966; employed by the School of Electrical Engineering, Oklahoma State University as a graduate research and teaching assistant from January, 1966 to September, 1968.

Professional Organizations: Member of Eta Kappa Nu, Tau Beta Pi, Pi Mu Epsilon, Phi Eta Sigma, and the Institute of Electrical and Electronic Engineers.